INFLUENCE OF EXTRACELLULAR FACTORS ON p53-MEDIATED DNA DAMAGE RESPONSES

Thesis submitted for the degree of

Doctor of Philosophy

at the University of Leicester

by

Samantha Carrera

Department of Biochemistry

University of Leicester

September 2012

Abstract

Influence of extracellular factors on p53-mediated DNA damage responses

Samantha Carrera

Cells have evolved sophisticated mechanisms to maintain genomic stability after cellular stress. Activation of DNA damage response pathways, and most importantly p53, leads to adaptive responses that can be influenced by different extracellular factors. The aim of this project was to study how extracellular factors modulate p53 cell-fate decisions after DNA damage, with particular interest in oxygen tensions and vitamin A metabolites. First, we focused on how physiological oxygen tensions (5% O_2) may influence cellular responses to genotoxic stress. We showed that normal and cancer cells cultured at 5% O_2 had a reduction in p53-mediated apoptosis after exposure to different genotoxic stresses. This was not due to a decrease p53 protein levels or its transactivation activity, and the oxidative damage caused by DNA damaging agents was not affected by oxygen tensions. We also found a p53-independent activation of MAPK at 5% O_2, which when inhibited restored levels of p53-induced apoptosis. HIF-1α, a transcription factor induced at lower O_2 concentrations, was present and active at 5% O_2. However, this did not affect MAPK activation and HIF-1α was not involved in the resistance to apoptosis under these conditions, although MAPK was necessary for HIF-1α expression and activation. We next explored the effect of the vitamin A (retinol) pathway on the cellular responses to DNA damage. We showed that Stra6, a retinol-inducible gene, is upregulated by p53 after DNA damage. While overexpression of Stra6 sensitized cells to p53-induced apoptosis independently of the retinoic acid signalling, its inhibition resulted in decreased apoptosis after DNA damage and less induction of oxidative stress. This shows that both oxygen tensions and vitamin A metabolites, through Stra6, are potent modulators of the p53 responses to DNA damage

Acknowledgements

First, I wish to thank my supervisor Dr Salvador Macip for giving me the opportunity to do my PhD in his group. It has been a great experience being the first member of his lab and I was able to learn so many valuable things that will be useful for my future career. He gave me the space to be independent and at the same time was there whenever I needed him. Many thanks to Jesvin Samuel who arrived to complement our small research group; it was nice to having someone to discuss the projects in the lab with. Also appreciate the valuable comments on my research, his ideas and support but most importantly his friendship.

I want to thank Dr Nick Barlev for his valuable comments and observations as part of my thesis committee. Special thanks to Dr Shaun Cowley, not only for being part of my thesis committee and for his questions that make me think more about my research project, but also for his support and insights during the time we shared in the lab. Many thanks to Dr Kayoko Tanaka for listening, giving me advice and also being an inspiration. I would like to thank Dr Oliver Dovey, Dr Charles Foster, Bipin Patel, Dr Neil Bates, Emma Kelsall, Monsterrat Aguilar and Nicola Portolano for sharing the lab and writing up area with me, for the endless talks and the great company.

I also want to thank my Mum, Dad and the rest of my family for their love and support and even with the great distance that separates us they have been with me every step of the way. Many thanks to Dr Ursula Flores Perez for her friendship and support, for the laughs and the cries.

Finally, but most importantly, I want to thank Rob for his love and for his immense support. Also, for helping me go through the craziness of the writing-up period.

Table of contents

List of figures

List of tables

Abbreviations

APAF-1	Apoptotic protease activating factor 1
APL	Acute promyelocytic leukaemia
ATP	adenosine triphosphate
ATRA	all-trans retinoic acid
BAD	Bcl-2-associated death promoter
BAK	Bcl-2 antagonistic/killer
BAX	Bcl-2-associated X protein
Bcl-2	B-cell lymphoma 2
Bcl-xL	B-cell lymphoma-extra large
BSA	bovine serum albumin
CAD	C-terminal transactivation domain
CBP	CREB-binding protein
CDK	cyclin-dependent kinase
cDNA	complimentary deoxyribonucleic acid
ChIP	chromatin immunoprecipitation
$CoCl_2$	Cobalt chloride
CODDD	C-terminal oxygen-dependent degradation domain
DAPI	4,6-diamidino-2-phenylindole
DBD	DNA-binding domain
ddH_2O	double distilled H_2O

DEPC	diethylpyrocarbonate
DFX	deferoxamine
DISC	death-inducing signalling complex
DMEM	Dulbecco's Modified Eagle Medium
DMSO	dimethyl sulfoxide
DNA	deoxyribonucleic acid
dNTP	deoxyribonucleic triphosphate
EDTA	ethylenediaminetetraacetic acid
EGF	epidermal growth factor
EPAS1	endothelial PAS domain protein 1
EPO	erythropoietin
ERK	extracellular signal-regulated kinases
FACS	fluorescence-activated cell sorting
FBS	Foetal bovine serum
FIH	factor inhibiting HIF-1
FITC	Fluorescein isothiocyanate
Fpg	formamidopyrimidine DNA-glycosylase
GAPDH	glyceraldehyde 3-phosphate dehydrogenase
Glut-1	glucose transporter 1
GTP	Guanosine triphosphate
H_2O_2	hydrogen peroxide
HBP1	HMG-box transcription factor 1
HIF	hypoxia inducible factor

HIPK2	Homeodomain-interacting protein kinase 2
hMSC	human mesenchymal stem cells
HRE	hypoxia responsive elements
IGF-1	insulin-like growth factor 1
IMS	intermembrane space
IPAS	inhibitory PAS domain protein
JAK2	Janus kinase 2
JNK	Jun amino-terminal kinases
Km	Michaelis constant
MAPK	mitogen-activated protein kinase
MEF	mouse embryonic fibroblast
MOMP	Mitochondrial outer-membrane permeabilization
MPK	MAPK phosphatases
N-CoR	nuclear receptor co-repressor 1
NODDD	N-terminal oxygen-dependent degradation domain
PBS	phosphate buffered saline
PFA	paraformaldehyde
PGK1	phosphoglycerate kinase 1
PHD	prolyl hydroxylase domain
PI	propidium iodide
PI3K	phosphoinositide 3-kinase
PS	phosphatidylserine
PUMA	p53 upregulated modulator of apoptosis

pVHL	von-Hippel-Lindau protein
qPCR	quantitative polymerase chain reaction
qRT-PCR	quantitative reverse transcription polymerase chain reaction
RA	retinoic acid
RAR	retinoic acid receptor
RARE	retinoic acid response element
RBP	retinol-binding protein
RNA	ribonucleic acid
ROS	reactive oxygen species
RXR	retinoid X receptor
RXRE	retinoid X response element
SDS	sodium dodecyl sulphate
SDS-PAGE	sodium dodecyl sulphate polyacrilamide gel electrophoresis
shRNA	short hairpin RNA
siRNA	small interfering RNA
SMAC	second mitochondria-derived activator of caspase
SMRT	silencing mediator for retinoid or thyroid-hormone receptors
STAT5	signal transducer and activator of transcription 5
STRA6	Stimulated by retinoic acid gene 6
TTR	transporter of thyroxin and retinol
UV	ultraviolet
VEGF	vascular endothelial growth factor
wt	wild-type

XIAP	X-linked inhibitor of apoptosis

Chapter 1. Introduction

There are many different types of cellular stress, such as DNA damage, genotoxicity, heat shock, metabolic changes, oncogene activation, oxidative stress, hypoxia and loss of cell-cell contact. Cells are constantly subjected to these stresses and they have evolved sophisticated mechanisms of DNA repair that allow the maintenance of genomic stability. DNA damage response pathways – like the p53 pathway – are activated in the cell in response to these stresses and this leads to adaptive responses. These pathways induce cell-cycle arrest, which allows the DNA to be repaired, and cells to survive, or apoptosis when the damage is too extensive to be repaired. Also, the adaptive responses to cellular stress include growth arrest, senescence, autophagy and activation of pro-survival pathways. Cells that lack, or have aberrations in the DNA damage response pathways, display genome instability and aberrant DNA replication that results in an increased rate of mutations; this can lead to tumour development. Extracellular factors, like oxygen and nutrients, can be responsible for altering the DNA damage response in normal and cancer cells. The understanding of how extracellular factors influence the way cells respond to damage can lead to the design of better strategies for cancer prevention and therapy. Here, we will focus on characterizing how two independent factors, oxygen tension and vitamin A metabolites, through induction of Stra6, can modulate p53-mediated responses to DNA damage.

1.1 DNA damage responses through p53

p53 is an essential cell cycle regulator and it is well known that its loss of function is one of the most important steps in carcinogenesis (Meek, 2009). The p53 pathway responds to a wide variety of stress signals, including different types of DNA damage, genotoxic damage, oncogene activation, and hypoxia, to mention a few (Vousden & Prives, 2009). In general, these signals induce p53 by stabilizing the protein, leading to an increase in its cellular accumulation. p53 activation leads to three main functional responses: apoptosis, senescence or cell-cycle arrest. Besides these responses, p53 is also able to alter other cellular processes like autophagy and regulation of signal transduction pathways, among others (Feng et al., 2005; Tasdemir et al., 2008).

1.1.1 The biology of p53

p53 is a tumour suppressor protein that mainly acts as a transcription factor to activate a wide variety of genes. The human p53 protein is composed by 393 amino acids and is constituted of five distinct structural and functional domains (Cho et al., 1994). The transactivation domain is localized in the N-terminal region of the protein. This domain is important for the activation of p53-inducible genes; it does so by interacting with the transcriptional co-activators p300 and CBP. This domain is also important for the regulation of p53 stability, as MDM2 interacts with p53 in this region (Figure 1.1). The DNA-binding domain is localized in the central part of the protein and it is the portion that binds to the p53-responsive elements of p53 target genes, most of

the mutations found in human cancer are located in this region (Greenblatt et al., 1994; Olivier et al., 2010). Between the transactivation and DNA-binding domains there is a domain rich in prolines; this region contributes to the functional activities of p53 and especially to its ability to induce apoptosis. Also, this region is involved on the negative regulation of transcription and is important for the interaction with signal transduction pathways (Prives & Hall, 1999). The tetramerization domain is localized after the DNA binding domain, this region is essential for the interaction with other p53 proteins to form dimers and tetramers. Binding of p53 to DNA is optimal when the protein is in its tetrameric form. The last domain is localized in the C-terminal part of the protein and is the regulatory domain. This region is rich in basic amino acids and it is subjected to several post-translational modifications that are essential for the regulation of p53 activity.

Figure 1.1 Diagram of p53. The protein has five distinct structural domains (from N-terminal to C-terminal): a transactivation domain that is important for activating p53 target genes; a proline-rich domain that contributes to the functional activity of the protein; a central domain that is essential for DNA binding; an oligomerization domain that allows the interaction with other p53 proteins; and a C-terminal regulatory domain where post-translational modifications allows the regulation of p53's functions.

The functions of p53 are regulated by several mechanisms, one of the most important and effective of which is the regulation of protein stability. Regardless of the type of stress by which p53 is induced, the crucial event in the induction of the pathway is the uncoupling of p53 from its key negative regulators: MDM2 and MDM4. MDM2 is an E3 ubiquitin ligase that catalyses the ubiquitination of p53 and this leads to its degradation (Haupt et al., 1997; Kubbutat et al., 1997; Honda & Yasuda, 2000). It has been shown that DNA damage signalling destabilizes MDM2, this leads to accumulation of active p53 (Stommel & Wahl, 2004). p53 transcriptionally regulates MDM2 which creates a negative feedback loop, when p53 is activated this increases the levels of MDM2 and in turn keeps p53 levels low under normal growth and development (Vousden, 2000).

1.1.2 p53 and the induction of apoptosis

One of p53 functions is as transcription factor that regulates the expression of target genes that contain p53-binding sites in their regulatory regions (Riley et al., 2008). Once p53 is stabilized and accumulates; in the nucleus, it targets a number of pro-apoptotic genes – like BAX and PUMA – and promotes their transcription to induce cell death. In a recent review, a list of 129 p53 transcriptionally regulated genes is mentioned, but there is the possibility that many more exist (Riley et al., 2008).

p53 also possesses biological activities beyond its role as a transcription factor (Green & Kroemer, 2009) and increasing evidence suggests that p53 cytoplasmic functions are

as important for the induction of apoptosis (Mihara et al., 2003). It has been shown that p53 mutants that lack part of the DNA-binding domain (DBD) are able to activate apoptosis. Induction of apoptosis by this mutant p53 is slower than apoptosis induced by wild-type p53 (Haupt et al., 1995). Also, Kakudo, *et al.* (2005) showed that overexpression of a variety of p53 mutant proteins with defects for transactivation functions can efficiently induce apoptosis in human cells. After initiation of apoptosis, a fraction of wt-p53 translocates to the mitochondria, where it binds to Bcl-2 and Bcl-xL (Mihara et al., 2003). It may be the case that transcription-dependent and transcription-independent functions of p53 are necessary to promote apoptosis and avoid tumorigenesis (Vousden & Prives, 2009).

p53 is an important tumour suppressor because of its ability to inhibit cell proliferation by blocking cell cycle progression and promoting apoptotic cell death. Another way in which p53 can inhibit tumour growth is by inducing senescence, a permanent growth arrest phenotype with specific morphologic and metabolic changes (Campisi, 2003).

The outcome of the p53 response to cellular stress is determined by the type and intensity of the stress, as well as the cell type and the genetic background. Also, the crosstalk between the p53 and other pathways such as pro-survival and proliferation pathways can be determinant to the fate of cell, making the difference between survival and death (Meek, 2009). There are many extracellular elements – like oxygen availability, nutrients and growth factors, among others – that can affect the way the

cells respond to DNA damage. These factors can determine which way the balance is going to tilt and affect the cell death or survival after DNA damage.

1.2 Apoptosis

Apoptosis is a genetically controlled process of cell death that is involved in normal development and helps maintain homeostasis by killing damaged, superfluous or potentially dangerous cells. This process is essential for multicellular organisms and defects on the control of apoptosis can lead to the development several pathologies, including cancer (Gewirtz et al., 2007).

The apoptotic machinery can be divided into two classes of components: sensors and effectors. The sensors are responsible for monitoring the extracellular and intracellular environment for conditions of normality and abnormality that influence whether the cell shall live or die. The sensors include the members of the BH3-only protein family like BID, BAD, BIM, NOXA and PUMA, among others. Each of them is activated by a specific cell damage and are translocated to the mitochondria to promote apoptosis. The effectors, like BAX and BAK, are then modified and activated to initiate apoptosis (Gewirtz et al., 2007).

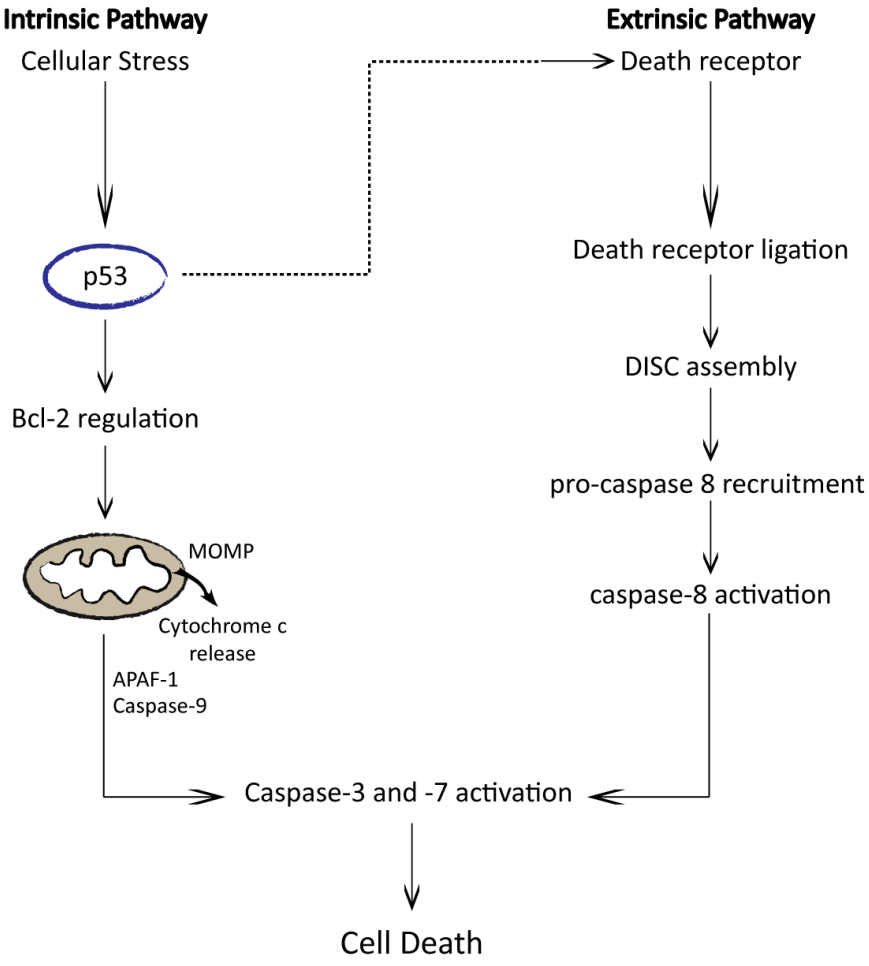

Figure 1.2 Intrinsic and extrinsic pathways of apoptosis. Figure shows a comparison between the intrinsic and the extrinsic pathway of apoptosis. p53 has been shown to induce the transcription of the death receptor FAS and TRAIL **(Müller et al., 1998; Liu et al., 2004)**.

In vertebrate cells, the two main apoptotic pathways are the intrinsic and the extrinsic pathways (Figure 1.2). The intrinsic pathway is activated in response to stresses, like DNA damage and hypoxia. Cells that have engaged in p53-dependent apoptosis typically follow the intrinsic cell death pathway. The intrinsic pathway of apoptosis involves the transcriptional and post-translational regulation of B-cell lymphoma 2 (Bcl-2) proteins that directly impact on the mitochondria. Genes encoding the Bcl-2

protein family members are transcriptionally regulated by p53 and also it has been shown that p53 can also interact with Bcl-2 and Bcl-xL (Mihara et al., 2003).

Mitochondrial outer-membrane permeabilization (MOMP) occurs through the action of pro-apoptotic domain members of the BCL-2 family such as Bcl-2-associated X protein (BAX) and Bcl-2 antagonistic/killer (BAK). Activation of either BAX or BAK is necessary for MOMP (Wei, 2001). MOMP leads to the release of pro-apoptotic proteins from the intermembrane space (IMS) and this is crucial for activation of the initiator caspases. One of these proteins is cytochrome c, which when released from the IMS binds to apoptotic protease activating factor 1 (APAF1) and results in the formation of the apoptosome. The apoptosome is a capsase initiator complex that recruits and activates procaspase-9, which then activates executioner caspases-3 and -7 (Reviewed in Chipuk & Green, 2006) (Tait & Green, 2010). Other proteins released from the IMS are second mitochondria-derived activator of caspase (SMAC; also known as DIABLO) and OMI (also known as HTRA2), which block the inhibition of caspase activity by X-linked inhibitor of apoptosis (XIAP) (Potts et al., 2003).

In the extrinsic pathway, extracellular ligands stimulate death-receptor oligomerization and death-inducing signalling complex (DISC) assembly, which is responsible for the induction of apoptosis by activating caspase-8 and -10. Active caspase-8 directly cleaves and activates the executioner caspases. p53 has been shown to contribute to

the activation of the extrinsic pathway. Death-receptors for both TRAIL and FasL have been identify as p53 target genes (Müller et al., 1998; Liu et al., 2004).

The ultimate effectors of apoptosis include an array of intracellular proteases named caspases. Both the intrinsic and extrinsic pathways converge on activating the executioner caspases, caspase-3 and caspase-7 (Figure 1.2). Caspases are a family of cysteine proteases that orchestrate the dismantling and clearance of the apoptotic cell. Besides their role in apoptosis, some members of the caspase family have functions in processes such as cytokine maturation, inflammation and differentiation (Murray et al., 2008). The apoptotic caspases can be divided in two groups: initiator caspases (caspase-2, -8, -9, and -10) and effector caspases (caspase-3, -6 and -7). All of the apoptotic pathways lead to the activation of the major effector caspases, caspase-3, caspase-6 and caspase-7, and these enzymes carry out much of the proteolysis that is seen during the demolition phase of apoptosis (Olsson & Zhivotovsky, 2011). After activation, caspases cleave hundreds of proteins and also many of the major constituents of the cytoskeleton; this probably contributes to the rounding and retraction of the cell that is seen in the early stages of apoptosis (Tait & Green, 2010).

If caspase activity is inhibited by reduction of APAF1 expression or up-regulation of XIAP, proliferating cells can recover from MOMP. This can have important implications for tumour development and cancer therapy because tumour cells often display defects in caspase activation (Tait & Green, 2010).

1.3 MAPK

The apoptotic signalling pathway is not the only one determining the fate of cells after stress. There are also survival pathways that are activated in response to a wide variety of environmental stimuli and convert these signals into cellular responses. For example, the Mitogen-activated protein kinase (MAPK) pathways have been shown to be induced after DNA damage (Lee et al., 2000). MAPK also regulate a wide variety of cellular activities like gene expression, cell cycle, cellular metabolism, motility, survival, apoptosis, and differentiation. MAPKs consist of three sequential kinase levels in which MAPK is activated upon phosphorylation by MAPKK, which is in turn activated when phosphorylated by MAPKKK (Figure 1.3). Six different groups of MAPK pathways have been characterized so far in mammals and each of them are activated by distinct sets of factors allowing a coordinated response to multiple stimuli. These groups are: the extracellular signal-regulated kinases (ERK) 1/2, ERK 3/4, ERK5, ERK7/8, the Jun amino-terminal kinases (JNK 1-3) and the p38 kinases (p38α, β, γ and δ) (Dhillon et al., 2007). The most studied pathway is the ERK1/2, and in this thesis we will be referring to this pathway as MAPK.

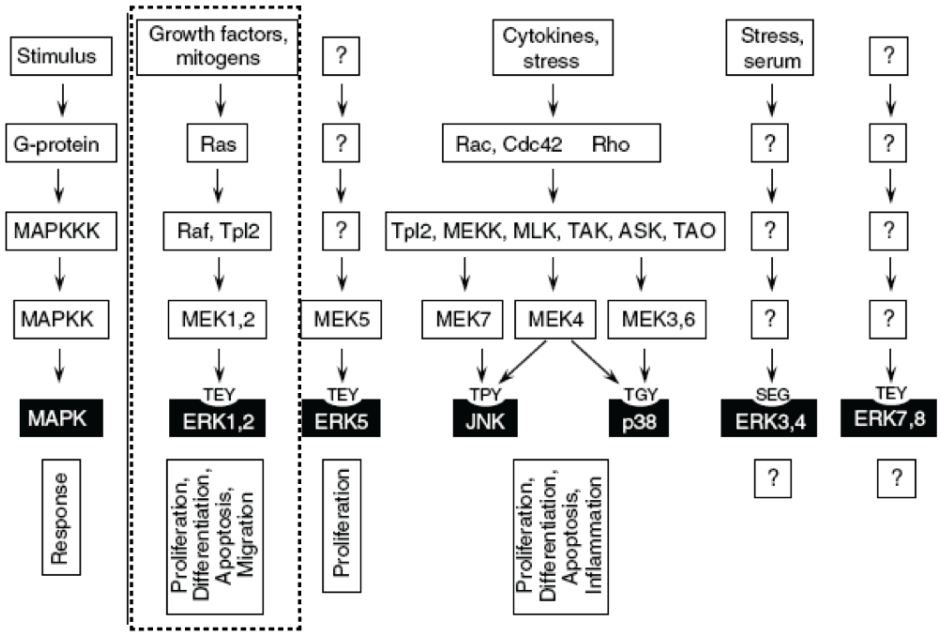

Figure 1.3 Schematic representation of the MAPK pathways. MAPK pathways are activated by extracellular stimuli that are sensed by a G-protein, which activates MAPKKK by phosphorylation. MAPKKK, in turn, activates MAPKK that activates MAPK. This signalling cascade then leads to adaptive responses. The six mammalian MAPK pathways are represented in the figure; the dashed box highlights the ERK1/2 pathway. Adapted from Dhillon, *et al.* 2007.

The JNKs are strongly activated in response to cytokines, UV radiation, and DNA damaging agents. Mammalian JNKs are encoded by three distinct genes: *JNK1*, *JNK2* and *JNK3*. JNK activation needs phosphorylation within a conserved Thr-Pro-Tyr motif. Following activation JNKs may be relocated to the nucleus. A wide range of proteins – predominantly transcription factors and nuclear hormone receptors – have been demonstrated to be substrates of JNK (Krishna & Narang, 2008). Like the JNKs, the mammalian p38s are also activated by environmental stresses and inflammatory cytokines and are inconsistently activated by insulin growth factors (Héron-Milhavet et al., 2001). It also plays a role in the regulation of apoptosis, cell cycle progression, growth and differentiation. A link between p38 and cell cycle control has been

proposed through regulation of substrates like HMG-box protein 1 (HBP1) (Xiu et al., 2003) and p21 (Kim et al., 2002). Activation of p38 was observed in cells undergoing apoptosis induced by a variety of agents (Dhillon et al., 2007).

The MAPK signalling cascade is usually initiated by the activation of cell surface receptors. Ligand-mediated phosphorylation of specific tyrosine residues mediates the activation of receptor tyrosine kinases, which triggers the loading of GTP to the Ras GTPase. Ras then recruits Raf kinase to the plasma membrane for activation. Raf in turn phosphorylates and activates the downstream kinases MEK 1 and 2 (Dhillon et al., 2007). These kinases phosphorylate ERK 1/2 in a conserved Thr-Pro-Tyr motif; activated ERKs phosphorylate a large number of substrates, including a series of transcription factors like c-Fos (Murphy et al., 2002), p53 (Milne et al., 1994), and c-Jun (Morton et al., 2003)(Reviewed in Krishna & Narang, 2008). The inactivation of ERKs is mainly mediated by removal of phosphates from either one, or both of the regulatory Thr or Tyr residues of the protein. The MAPK phosphatases (MPKs) are a family of dual-specificity protein phosphatases, which can dephosphorylate both residues and subsequently inactivate MAPK (Sun et al., 1993).

The MAPK pathway is deregulated in approximately one third of all human cancers (Dhillon et al., 2007). MAPK is a central regulator of cell proliferation and functions by up regulating genes involved in cell growth and down regulating anti-proliferative genes, which gives tumour cells an advantage for growth and survival. It has been

shown that sustained activation of MAPK signalling promotes the activation of genes like cyclin D1, cyclin E and other E2F genes required for cell-cycle entry and also repress the expression of genes that inhibit proliferation (Yamamoto et al., 2006). In addition to cell proliferation other components downstream of MAPK are involved in angiogenesis, cell migration, invasion and metastasis (Dhillon et al., 2007).

The effect of MAPK on survival can be explained in terms of anti-apoptotic actions. Erhardt, *et al.* (1999) have shown that induction of MAPK results in protection from apoptosis by interfering with cytosolic caspase activation following release of cytochrome c from mitochondria. The mechanism by which this occurs was proposed by Allan *et al.* (2009), where they show that MAPK directly phosphorylates Caspase-9 preventing its processing and thus its activation of Caspase-3. It has also been shown that phosphorylation of the pro-apoptotic protein BAD by MAPK suppresses its apoptotic effect (Bonni et al., 1999).

1.4 Oxygen tensions

The amount of oxygen that a cell receives is determined by its proximity to the arterial blood supply and the rates of O_2 consumption by the cell and its neighbours (Jiang et al., 1996). Hypoxia is usually defined as ≤2% O_2 and anoxia is defined as ≤0.02% O_2. Tumour mass usually grows beyond the possible sources of O_2 and cancer cells are exposed to hypoxia. Adapting to hypoxia is important for cancer cells so they are able to continue growth. Hypoxia is associated with poor treatment outcome (Hockel et al., 1996; Generali et al., 2006), suggesting that it should be considered in the development of optimum treatment strategies.

1.4.1 Physiological oxygen tensions

The physiological oxygen levels in most mammalian tissues ranges between 2-9% (10-30 μM), very different from the 20% O_2 present in the atmosphere (Braun et al., 2001). Culture of cell lines at atmospheric oxygen tensions is a common practice, but accumulating evidence suggests that culturing mammalian cells at 20% O_2 promotes DNA damage and senescence. Changes in oxygen tensions can affect the replicative lifespan of cultured cells as it has been shown that mouse embryonic fibroblasts (MEFs) (Parrinello et al., 2003) and human fibroblasts, IMR-90 (Chen et al., 1995), cultured at 3% O_2 proliferate for longer time than the ones cultured at 20% O_2. This increase in replicative lifespan was associated with increased rates of cell proliferation and increased saturation density. It has also been shown that human mesenchymal

stem cells (hMSC) have a higher growth rate when cultured at physiological oxygen tensions (3% O_2) compared to their counterparts cultured at atmospheric oxygen (20% O_2) which exhibited an increased rate of telomere shortening (Estrada et al., 2012). Oxidative stress is more likely to be present at higher oxygen concentrations. The increased proliferation seen in MEFs, as well as the smaller decline in telomere shortening rate in hMSC, at physiological oxygen tensions was due to a decrease in oxidative DNA damage and DSBs under low oxygen conditions (Parrinello et al., 2003) (Estrada et al., 2012). However, Parrinello, *et al.* (2003) were not able to see an increase in oxidative damage in human fibroblasts cultured at atmospheric oxygen tensions.

Not only non-transformed cells benefit from being cultured at physiological oxygen tension. In the case of cancer cells, Ravi *et al.* (2011) showed that ovarian cancer cells have an increase in growth and proliferation when cultured at 3% O_2 compared to atmospheric oxygen (20%) (Ravi et al., 2011).

1.4.2 Hypoxia inducible factor

Cellular responses to reduced oxygen levels are mediated by a family of hypoxia inducible transcription factors (HIF) that respond to low oxygen concentrations. HIFs are heterodimeric transcription factors consisting of an α and a β subunit (Wang et al., 1995). The α-subunit is oxygen labile but is rapidly stabilized in response to low oxygen conditions. Unlike the α-subunit, the β-subunit is constitutively expressed and

insensitive to changes in oxygen levels. HIF activity is dependent upon the availability of HIFα subunit, which is in turn regulated by oxygen levels and growth factors. Three HIFα subunits have been characterized: HIF-1α, HIF-2α (also known as endothelial PAS domain protein 1 (EPAS1)) and HIF-3α (also known as inhibitory PAS domain protein (IPAS)); HIF-1α is the most studied of them (Semenza, 1999).

1.4.3 HIF-1α regulation by hydroxylation

Under high oxygen levels, HIF-1α binds to the von-Hippel-Lindau protein (pVHL), a substrate recognition component for an E3 ubiquitin ligase complex that targets the subunit for degradation by the proteosome (Maxwell et al., 1999). The binding of HIF-1α to pVHL depends on the hydroxylation of two prolyl residues in the oxygen-dependent degradation domains (NODDD and CODDD) of HIF-1α (Figure 1.4). This hydroxylation is mediated by a family of three prolyl hydroxylase domain containing (PHD) enzymes (Epstein et al., 2001). PHD enzymes use Fe^{2+} to bind oxygen to hydroxylate both 2-oxoglutarate and the target proline residue.

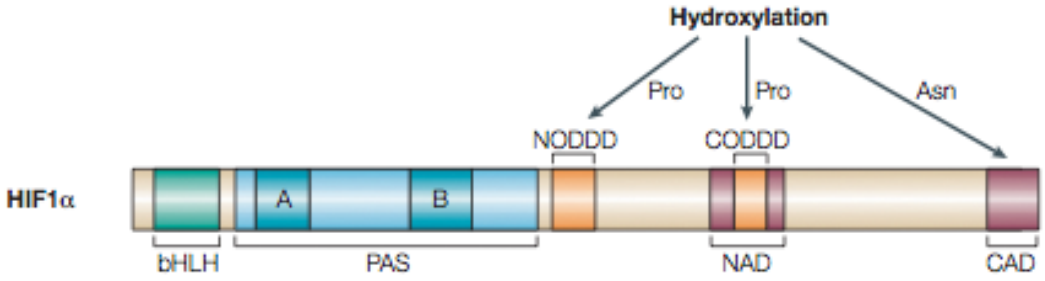

Figure 1.4 HIF-1α regulation by hydroxylation. HIF-1α domain structure showing the sites of hydroxylation. The hydroxylation of HIF-1α in the oxygen degradation domains (NODDD and CODDD) is mediated by PHD enzymes and affects HIF-1α stability by allowing recognition of the subunit by the pVHL protein. Hydroxylation of asparagine in the c-terminal transactivation domain is mediated by FIH and interferes with binding of p300 affecting HIF-1α activity. **(Schofield & Ratcliffe, 2004)**

Besides protein stability, transcriptional activation in an oxygen-dependent manner is another form of regulation of HIF-1α. Hypoxic conditions promote the interaction of HIF-1α C-terminal transactivation domain (CAD) with co-activators (Figure 1.4). Protein factor inhibiting HIF-1 (FIH) was shown to regulate HIF-1α activity by mediating the hydroxylation of an asparagine (Asn^{803}) residue in the CAD of HIF-1α preventing its association with p300 (Lando et al., 2002).

Under hypoxic conditions, hydroxylation is blocked, resulting in increased HIF-1α stability and accumulation. It has been proposed that not all HIF-1 target genes are equally sensitive to inhibition of CAD by FIH (Dayan et al., 2006). This, together with the fact that FIH and PHDs have different Km for oxygen (Koivunen et al., 2003), suggests a differential gene regulation under a range of oxygen concentrations. This supports the idea that expression of certain genes that are sensitive to CAD inhibition will only be achieved under severe hypoxia.

The persistence of basal level HIF-1α protein may be important for normal physiological functions. Physiological oxygen concentrations are below Km values of PHDs and this ensures that PHD activity is sensitive to fluctuations in O_2 concentrations. This means that a decrease in the level of O_2 will suppress the activity of PHD and trigger HIF-1α accumulation (Fong, 2009). PHDs enzymes have a high Km for oxygen, which means that the enzyme needs high O_2 concentrations in order to achieve maximum reaction velocity making it possible that the enzymes are not completely active at physiological oxygen tensions (Hirsilä et al., 2003).

1.4.4 Other factors regulating HIF-1α

In addition to changes in oxygen tensions, HIF-1α expression can also be regulated by growth factors and oncogenic signals. Various stimuli can induce HIF-1 response in normoxic conditions, these include: transition metals, nitric oxide, reactive oxygen species (ROS), growth factors, mechanical stress or oncogenic activation (Bardos & Ashcroft, 2004).

Growth factors, like EGF and insulin, increase the levels of HIF-1α by regulating the protein at a post-transcriptional level through a mechanism involving PI3K signalling (Jiang et al., 2001; Zhong et al., 2000). It has been suggested that PI3K/Akt signalling pathway is necessary for HIF-1α stabilization (Chen et al., 2001; Zundel et al., 2000), but there was no evidence of direct interaction or phosphorylation of HIF-1α by Akt.

Another growth factor, IGF-1, is also able induce HIF-1α expression and activity by a mechanism dependent on MAPK and PI3K signalling pathways (Fukuda et al., 2002).

1.4.5 HIF-1 regulation of transcription

HIF-1 functions as a DNA-binding transcription factor and activates 100-200 genes that promote adaptation and survival under low O_2 concentrations (Manalo et al., 2005). HIF-1 binds to specific sequences within target genes, the consensus binding site 5'-RCGTG-3' known as hypoxia responsive elements (HREs). The binding of p300 is believed to be necessary for the binding of HIF-1 to HREs, but it has been shown that some target genes does not require the activation of the CAD for expression (Koivunen et al., 2003).

Genes under the control of HIF-1 include those involved in vasodilatation like iNOS (Palmer et al., 1998), in angiogenesis like vascular endothelial growth factor (VEGF) (Carmeliet et al., 1998), in enhanced blood oxygenation like erythropoietin (EPO) gene (Jiang et al., 1996a), and also genes encoding glycolytic enzymes like phosphoglycerate kinase 1 (PGK1) (Carmeliet et al., 1998). The activation of these genes by HIF-1 can have major implications for growing tumours, because they can lead to survival and proliferation by mediating angiogenesis and promoting an aggressive tumour phenotype.

A growing body of evidence suggests that HIF-1α is an important contributor to tumour progression (Hockel et al., 1996) and metastasis (Liao et al., 2007; Hiraga et al., 2007). Many of the signalling pathways that are deregulated in cancer – like MAPK and PI3K – promote HIF-1 activity (Richard et al., 1999; Sutton et al., 2007; Minet et al., 2000). It has been shown that HIF-1α is overexpressed in a variety of cancers and its expression is associated with poor prognosis (Zhong et al., 1999). Expression of HIF-1α can give tumours a survival advantage as the cellular responses enhanced by HIF-1 – like glucose metabolism and angiogenesis – have key roles in cancer biology.

1.4.6 HIF-1 and survivial

Some signalling pathways are activated in response to a reduction in oxygen levels and this can influence cell growth and survival in response to DNA damage. It has been shown that the PI3K/Akt (Walsh et al., 2009), MAPK (Conrad et al., 1999; Minet et al., 2000) and p38 (Khandrika et al., 2009) pathways are activated at low oxygen concentrations. The activation of pro-survival pathways during hypoxia can have major implications for the activity of HIF-1.

As mentioned earlier, MAPK pathways coordinate a series of cellular activities like gene expression, cell cycle, cellular metabolism, motility, survival, apoptosis, and differentiation. Many of these pathways are altered in cancer, and some of them are important in the regulation of HIF-1α accumulation and activity, which can benefit tumour growth. This can provide cancer cells with a distinct advantage for survival and

proliferation and the activation of HIF-1 can be advantageous because of its role in promoting angiogenesis and enhanced expression of glycolytic enzymes.

Richard *et al.* (1999) showed that HIF-1α could be phosphorylated *in vivo* by MAPK, although this phosphorylation did not appear to be implicated in the stabilization of the protein. The authors showed that phosphorylation of HIF-1α by MAPK effectively promotes the transcriptional activity of HIF-1. It is thought that MAPK promotes HIF-1α transactivation activity by facilitating the interaction between p300 and the CAD domain of HIF-1α (Sang et al., 2003). In accordance to this, Sutton *et al.* (2007) showed that overexpression of MAPK enhances HIF-1 activity without affecting HIF-1α expression in response to hypoxia and growth factors. The inhibition of MAPK resulted in a 50% reduction of HIF-1 activity, but they observed that MAPK pathway was not involved in the accumulation of HIF-1α protein and that it is not required for binding to HIF-1β.

Most studies regarding the MAPK pathway and HIF-1α have been performed by examining downstream components of the pathway. However, in a paper by Kikuchi *et al.* (2009), they studied the effect of activating mutations in KRAS and BRAF in the expression of HIF-1α. They found that the expression of the mutated KRAS (V12) and BRAF (V600E) proteins enhanced the expression of HIF-1α during hypoxia. Enhanced HIF-1α was not due to an increase in the levels of the mRNA or an effect on the protein stability. Their data suggest that activating mutations in *Kras* play an important role in

enhancing the hypoxic induction of HIF-1α by regulating its translation through the PI3K pathway (Kikuchi et al., 2009).

PI3K/Akt signalling cascade is one of the major survival pathways in the cell and it has been shown to be activated during hypoxia. Walsh *et al.* (2009) showed that Akt phosphorylation increases when normal prostate cells are exposed to hypoxia and that this inhibited apoptosis. The inhibition of Akt resulted in re-sensitisation of hypoxic cells to apoptosis (Walsh et al., 2009). Another study showed that up-regulation of the PI3K pathway can lead to an increase in HIF-1α expression and binding activity under non-hypoxic conditions, leading to an increase in its transactivation activity (Zhong et al., 2000).

1.4.7 HIF-1 and Apoptosis

Hypoxia induces accumulation of the p53 tumour suppressor protein and this is associated with increased apoptosis (Graeber et al., 1994; Alarcón et al., 1999). Loss of p53 reduces hypoxia-induced cell death, which is beneficial for tumour growth. It has been proposed that in hypoxic tumours there is a selective pressure towards the loss of p53 (Graeber et al., 1994). It has been suggested that the accumulation of p53 during hypoxia is due to a down-regulation of MDM2 (Alarcón et al., 1999; Koumenis et al., 2001). The authors found that the levels of MDM2 decrease during hypoxia and that these translated into less degradation of p53, promoting accumulation of the protein. In contrast, another report shows that hypoxia up-regulates MDM2

independently of p53 and this leads to a decrease in the levels of p53 (Zhang & Hill, 2004). It has been shown that p53 acts mainly as a repressor under hypoxic conditions by binding to the co-repressor mSin3A (Hammond et al., 2006).

The relationship between HIF-1α and p53 has been explored but there is still controversy in the field as to the exact nature of this relationship. Some evidence suggests that HIF-1α is linked to p53 accumulation under hypoxic conditions. An *et al.* (1998), established that HIF-1α is responsible for the stabilization of the p53 protein during hypoxia and that this probably occurs via a direct association between the two proteins. On the other hand, it has been suggested that overexpression of HIF-1α leads to a decrease in p53 apoptotic activity (Nardinocchi et al., 2011). The authors found that HIF-1α induced down-regulation of HIPK2, impairing the phosphorylation of p53 Ser46 and thus interfering with p53 apoptotic functions. There also have been observations suggesting that p53 inhibits HIF-1 transactivation functions, with p53 binding to p300 being necessary for this inhibition (Blagosklonny et al., 1998). Another mechanism has been proposed for the inhibition of HIF-1 by p53: Ravi et al. (2000) found that the presence of p53 reduces the levels of HIF-1α protein during hypoxia and thus interferes with HIF-1 activity. Increased levels of HIF-1α protein but not in mRNA could be observed in p53 -/- cells suggesting a protein regulation. Authors showed that p53 limits the expression of HIF-1α during hypoxia by promoting its ubiquitination and proteosomal degradation (Ravi et al., 2000).

1.5 Retinoic acid pathway

Vitamin A (Retinol) is an essential vitamin and cannot be synthesized in animals. It is absorbed from the diet and it is essential for diverse biological functions like embryonic development, vision, immune function and normal cell proliferation and differentiation (Duester, 2008). Vitamin A is the precursor for the generation of critical metabolites like retinoic acid (RA) (Chambon, 1996).

Retinoids are compounds that are chemically related to vitamin A. They are important for a diverse group of functions in the cells and are essential in embryonic development. The physiological actions of *all-trans* RA (ATRA) are mediated primarily by heterodimerization of two different classes of nuclear receptors: retinoic acid receptors (RARs) and retinoid X receptors (RXRs) (Petkovich et al., 1987; Giguere et al., 1987). RXRs and RARs are members of a family of intracellular or nuclear receptors that function as a ligand-dependent transcription factors (Chambon, 1996). Multiple isotypes (α, β and γ) of both RARs and RXRs have been identified.

The RARs interact with different co-activator and co-repressor proteins to regulate transcription. RAR/RXR complexes act as transcriptional repressors in the absence of ligand by binding to co-repressor complexes that contain N-CoR or SMRT, plus additional proteins (Perissi et al., 1999). The binding of a ligand, such as RA, alters the heterodimer interaction with these co-repressor proteins and allows the interaction

with co-activator proteins (Heery et al., 1997). RAR/RXR complexes also recruit ATP-dependent chromatin remodelling complexes and these actions result in transcriptional activation in the presence of RA (Tang & Gudas, 2011).

The receptor heterodimers bind to DNA-response elements termed retinoic acid-response elements (RAREs). RAREs consist of direct repeats of a consensus half-site sequence separately most commonly by five or two nucleotides (DR5 or DR2). RXREs are most commonly separated by one nucleotide (DR1) (Balmer & Blomhoff, 2005). Upon binding they recruit co-activators and lead to transcription activation of retinoic acid-regulated genes (Heery et al., 1997).

1.5.1 Retinol binding protein

Although retinol can diffuse through membranes, it rarely exists in its free form. In the blood, the main carrier for retinol is serum retinol-binding protein (RBP4). The plasma retinol-RBP4 concentration is strictly maintained at 2μM despite variations on the daily intake of vitamin A. RBP4 is synthesized primarily in the liver where it requires binding of retinol to trigger its secretion. It has been shown that RBP4 is bound to the transporter of thyroxin and retinol (TTR) when circulating in the blood (Naylor & Newcomer, 1999). *In vitro*, one tetramer of TTR can bind two molecules of RBP4; however, the complex isolated from the serum is composed of TTR and RBP in a 1:1 molar stoichiometry. This interaction appears to be necessary to prevent extensive loss of RBP4 through glomerular filtration in the kidneys. RBP4 knockout mice are

viable and fertile, but exhibit impaired retinal function. Normal vision can be restored in these mice if they are supplemented with vitamin A (Quadro et al., 1999).

An elevation in the serum levels of RBP4 in an insulin resistance mouse model and patients with type 2 diabetes, suggests a possible role of this protein in insulin resistance. This was confirmed by injection of mice with RBP4, which caused insulin resistance and glucose intolerance. This suggests a possible alternative role of RBP4 in insulin resistance (Yang et al., 2005).

1.5.2 Stra6

Stimulated by retinoic acid gene 6 (Stra6) is a cell surface receptor that mediates the intake of retinol when it is bound to RBP4 (Kawaguchi et al., 2007). In mammals, Stra6 is expressed in a variety of embryonic and adult tissues. It is highly expressed in adult kidney, trachea, breast, prostate, testis and uterus (Bouillet et al., 1997; Szeto et al., 2001). Stra6 is a RA-inducible gene and treatment with ATRA increased the levels of mRNA in a concentration dependent manner. RA induction of Stra6 is preferentially mediated by RXRα/RARγ heterodimers and it is expressed even in RARα and RXRβ null mutants (Bouillet et al., 1997).

Stra6 is a highly hydrophobic 74kDa protein that is formed by 19 distinct regions: 5 extracellular, 5 intracellular and 9 putative transmembrane (Figure 1.5) (Kawaguchi et

al., 2008). It has no homology to any protein with known function. STRA6 binds to holo-RBP4 and mediates the retinol uptake in the cell by transporting it across the plasma membrane. A large-scale mutagenesis study identified the possible sites for RBP4 binding in bovine Stra6 protein (Kawaguchi et al., 2008). Tyr^{336}, Gly^{340} and Gly^{342} were identified as RBP4 binding sites in this study. One of these mutations correlated with a polymorphism in human Stra6 (G339S) associated with pathological defects, suggesting an impaired RBP4 binding function (Pasutto et al., 2007)(Figure 1.5).

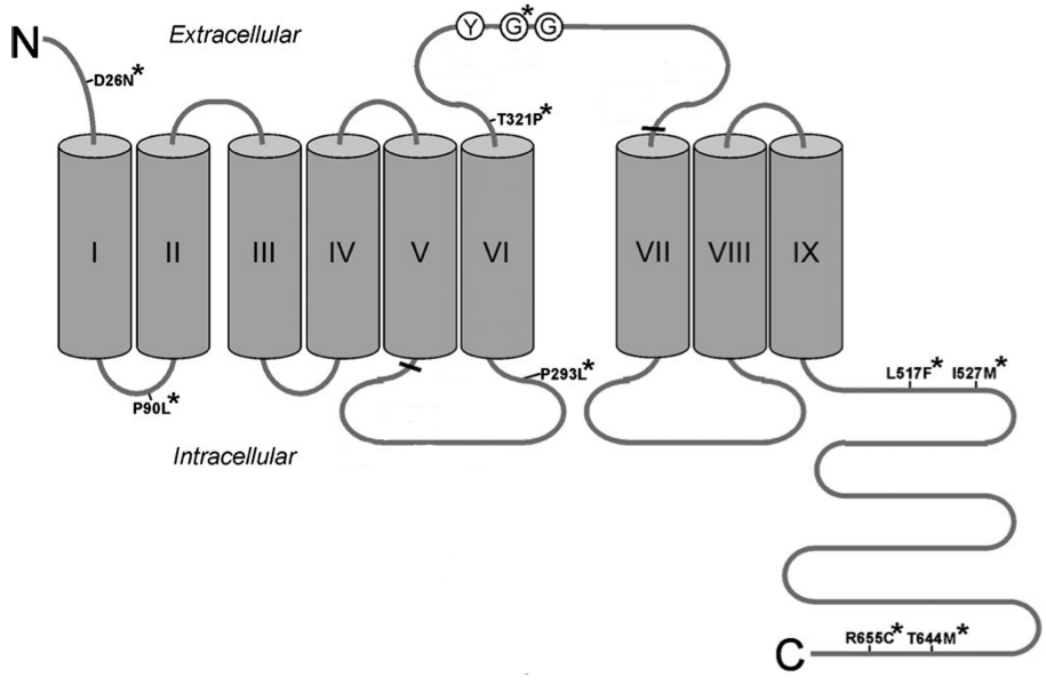

Figure 1.5 Model of Stra6 protein. Stra6 is a cell surface receptor that contains nine different transmembrane domains, showed in roman numerals. It has five extracellular domains the residues indicated in circle are believed to be essential for RBP4 binding. Five distinct intracellular domains can also be observed. The residues indicated with an asterisk are mutations associated with severe phenotypes in humans. Modified from Kawaguchi *et al.* (2008)

Mutations in Stra6 are responsible for Matthew-Wood syndrome and cause a broad spectrum of severe pathological phenotypes in humans, characterized by anophthalmia, facial dysmorphism, mental retardation, malformation of heart and lungs, among others (Pasutto et al., 2007). Stra6-deficient zebrafish embryos also develop multisystemic malformations similar to those described in humans (Isken et al., 2008).

A model has recently been proposed that considers Stra6 as a signalling molecule (Chen et al., 2012; Berry et al., 2011). The intracellular orientation of the C-terminal domain is highly conserved among human, mouse and bovine Stra6. An identified mutation in Stra6 (T664M) in the cytosolic C-terminus domain (Pasutto et al., 2007) is located within a protein sequence recognizable as a phosphotyrosine motif, a protein sequence often used by membrane signalling receptors to recruit downstream effectors. It has been shown that upon induction by holo-RBP, a transient phosphorylation of Stra6 on T^{664} can be observed (Berry et al., 2011). The authors also show that binding of Stra6 with STAT5 and JAK2 was stimulated by holo-RBP. Treatment of cells with retinol-RBP increased the phosphorylation of STAT5. Another group has correlated this alternative Stra6 functions with the activation of caspase 3 (Chen et al., 2012). The Stra6 functions as a signalling membrane receptor are independent from its function as a retinol receptor and independent of induction with RA.

1.5.3 Retinoids, Stra6 and cancer

Retinoids inhibit cell cycle progression in a variety of human cancer cells by directly or indirectly modulating cyclins, CDKs and cell cycle inhibitors. Generally, RA causes a block in the G1 phase of the cell cycle and this has inhibitory effects on cell proliferation (Sueoka et al., 1999). It does so by regulating the mRNA and protein levels of cyclins. Besides this, it also causes cell cycle arrest by increasing the expression and posttranslational stability of CDK inhibitors like p21 and p27 (Tang & Gudas, 2011). Retinoids also induce apoptosis in a variety of cancer cells, for example, in acute promyelocytic leukaemia (APL) where they induce postmaturation apoptosis. Differentiation therapy is a type of treatment that is based on the induction of differentiation in cancer cells to prevent further proliferation (Huang et al., 1988). As retinoids can induce differentiation in normal embryonic stem cells, RA is being used in combination with chemotherapy as differentiation therapy for the treatment of APL.

It is suggested that Stra6 has potential to be important in cancer. Through a screen to identify genes regulated by Wnt-1 induction, it was found that Stra6 mRNA was highly expressed (Szeto et al., 2001). Also in this study, Stra6 was found to be upregulated in human colorectal, ovarian and endometrial cancers. The authors showed that combination of ATRA and Wnt-1 overexpression increased the levels of Stra6 by 10-fold and suggested a synergistic effect between the Wnt-1 and the RA pathway to

induce Stra6 expression. In fact, they showed that Wnt-1 induction of Stra6 is mediated by RAR activity.

1.6 Aims of the project

The cellular responses to DNA damage are important for maintaining tissue integrity and preventing cancer. This process can be highly influenced by extracellular factors. The project is focused on understanding the effect of some of these elements in the responses to DNA damage after genotoxic stress, with particular interest on p53-induced apoptosis. The two factors explored in this project are physiological oxygen tensions and the vitamin A/retinoic acid pathway.

1.6.1 Hypothesis

Extracellular factors, in particular the oxygen availability and the retinoic acid pathway, have an impact on the cellular responses to DNA damaging agents in a p53-dependent manner.

1.6.2 Specific aims

- To characterize cellular responses to genotoxic stress in cells cultured at physiologic O_2 levels, specifically related to p53-induced apoptosis.
- To determine the involvement of HIF-1α in the effects of physiologic oxygen tensions on cell growth and DNA damage responses.

- To characterize the role of retinoid signalling and the stimulated by retinoic acid gene 6 (*Stra6*) receptor in p53-mediated cellular responses to genotoxic stress.

Chapter 2. Materials and Methods

2.1 Culture of cancer cell lines

Cancer cell lines from different tissues with modifications that allow us to knockdown or overexpress the proteins of interest were used to study the cellular responses to DNA damage (Table 1). Cell lines were maintained in culture using Dulbecco's Modified Eagle Medium (DMEM) (GIBCO) supplemented with 10% Foetal Bovine Serum (FBS) (GIBCO) and 50 units/ml of Penicillin-Streptomycin (GIBCO). Cells were grown in a 5% CO_2 incubator at 37 °C. For the physiological oxygen tensions part of the project, cells were cultured in a 5% CO_2 and 5% O_2 incubator at 37 °C for at least 24 hours prior to assessment.

The EJp53 cell line contains a p53 expression plasmid under the control of tetracycline and expresses the wild type p53 protein upon withdrawal of tetracycline (Sugrue et al., 1997). The culture media for this cell line was supplemented with hygromycin (100 µg/ml) and geneticin (750 µg/ml) and 1µg/ml of tetracycline for maintaining the cell line. When expression of p53 was required cells were washed twice with 1× Phosphate Buffer Saline (PBS) to remove tetracycline before splitting them.

HCT116 stably expressing a Luciferase (HCT116shLuci) or a Stra6 (HCT116shStra6) shRNA were prepared in the laboratory using shRNA HuSH plasmids from Origene, following manufacturer's protocols. The selection of stable clones was performed with 1 μg/ml puromycin. These cells were used to explore the effect of Stra6 depletion on the cellular responses to DNA damage.

Table 1. Cancer cell lines used

Name	Source	Modification
HCT116	Colorectal Carcinoma	
HCT116 p53-/-	Colorectal Carcinoma	p53 knockout by homologous recombination
HCT116shLuci	Colorectal Carcinoma	Stably transfected shRNA against Luciferase
HCT116shStra6	Colorectal Carcinoma	Stably transfected shRNA against Stra6
U2OS	Osteosarcoma	
U2OSp53-/-	Osteosarcoma	
EJp53	Bladder carcinoma	Tet-off p53 inducible system

2.1.1 Passage of cells by trypsinization

To passage a confluent 100 mm plate of cells, old medium was aspirated from the plates and they were washed once with 5 ml of sterile PBS (GIBCO) to remove any residual media. 1 ml of 0.25% Trypsin-EDTA (GIBCO) was added to each plate and they were placed in the incubator for 3 min. Cells were collected with 4 ml of media in a 15 ml falcon tube and centrifuged for 5 min at 1100 rpm. Cells were resuspended in 5 ml of media and 1 ml was plated in 100 mm plates.

2.1.2 Cell line long term storage

To store cell lines for a longer period of time, cells were frozen. Confluent 100 mm plates were used for freezing, old medium was aspirated and the cells were washed with 5 ml of 1× PBS. 1 ml of Trypsin was added and they were placed in the incubator for 3 min. The cells were collected with 4 ml of media in 15 ml tubes and centrifuged for 5 min at 1100 rpm. For each plate used, 0.9 ml of media and 0.1ml of DMSO were mixed and added to the pellet of cells. 1 ml of cells was transferred to each 1.5 ml cryovials. Controlled decrease in temperature is required to ensure survival of cells, the vials were inserted into freezing containers with isopropanol and placed at -80°C. After 24-48 hours vials were transferred to liquid nitrogen tank.

To thaw the cells when they were needed, the cryovials were incubated in a 37°C water bath for 1-2 min. Then, cells were transferred to a plate containing 9 ml of warm media. The next day media was aspirated and replaced with fresh media to allow cells to recover.

2.1.3 Cell counting

When cells needed splitting for experiments, they were counted to ensure that the same amount of cells was used for each experiment and maintain reproducibility. A Bright Line Counting Chamber with an improved Neubauer ruling pattern was used. 10 µl of cells were put into the chamber and the number of cells in $4mm^2$ was counted.

The number obtained was divided by 4 and multiply by 10^4 to obtain the number of cells per ml. The desired number of cells was plated in 60 mm, 6-well or 24-well plates.

2.1.4 Chemical treatment of cells

Doxorubicin is an anthracycline antibiotic, commonly used as a chemotherapy drug, that works by intercalating DNA and acting as a topoisomerase II inhibitor (Fornari et al., 1994). Doxorubicin Hydrochloride (Fisher Bioreagents) was used to induce DNA damage and study the effect of external factors on the cellular responses to damage. Cells were treated with doxorubicin 24 hours after splitting or 2 hours after changing the media of transfected cells. The concentration of doxorubicin used varied depending on the experiment but was kept between 0.2 μg/ml and 1 μg/ml to ensure a sufficient amount of cell death. After treatment, cells were grown for 24-48 hours before being used for the desired experiment.

To study the possible role of MAPK pathway in the responses to physiological oxygen tensions the MEK inhibitor U0126 (LC Laboratories®) was used to block the phosphorylation of ERK 1/2. Cells were treated with U0126 24 hours after splitting or 2 hours after changing the media if transfected. When doxorubicin treatment was required, cells were first treated with U0126 and 1 hour later they were treated with doxorubicin. When physiological oxygen was required, cells were placed at 5% O_2 immediately after treatment. Cells were left to grow for 18-24 hours before using them for further experiments.

YC-1 is a nitric oxide-independent activator of soluble guanylyl cyclase, and it has been found to inhibit HIF-1 *in vitro*. It is thought that YC-1 mediated reduction in HIF-1α protein levels occurs at the post-transcriptional level (Yeo et al., 2003). YC-1 was used to investigate the effect of HIF-1 inhibition on the cellular responses to DNA damage. HCT116 cells were treated with 40μM of YC-1 24 hours after splitting. When treatment with doxorubicin was needed, cells were treated first with YC-1 and 5 hours later with doxorubicin. Cells were left to grow for 18-24 hours before using them for further experiments.

Cobaltus ions and iron chelators are non-specific hydroxylase inhibitors that are used to mimic hypoxia by preventing HIF-1α hydroxylation and degradation. Co^{2+} is thought to act as a hypoxia-mimetic by displacing the essential Fe^{2+} ion in prolyl hydroxylases, causing a stabilisation of HIF-1α. For experiments investigating the role of HIF-1 on the cellular responses to DNA damage, Cobalt chloride ($CoCl_2$) and Deferoxamine (DFX) were used to simulate hypoxic conditions and activate HIF-1α. HCT116 were treated with 500μM of $CoCl_2$ or 500μM DFX for at least 16 hours prior to using them for other experiments.

All-trans retinoic acid (ATRA) is the acid form of vitamin A, and it is important for many cellular processes. As a drug, it is commonly used in chemotherapy to treat acute promyelocytic leukemia (APL). ATRA was used in this project to study the retinoic acid

pathway. Cells were treated with 2µM of ATRA 24 hours after splitting or 2 hours after changing the media if transfected. Cells were left to grow for 24-48 hours before using them for further experiments.

2.2 Plasmid and RNA transfection

2.2.1 Transformation and culture of bacterial cells

Different plasmids were used to either overexpress a desired protein or for reporter assays (Table 2). To have enough plasmids for cell transfection, plasmids were grow using competent DH5α cells. The bacteria cells were put on ice to thaw and mixed with 0.5 µg of plasmid. They were incubated on ice for 30 min and heat shocked at 42°C for 30s. After the heat shock, they were immediately placed on ice and 900 µl of LB media was added to each tube. Then, cells were left to grow for 1 hour at 37°C in the shaker. The bacterial cells were spun down and resuspended in 100 µl and plated in agar plates containing the desired antibiotic. Plates were placed in the 37°C oven overnight. The next day, a colony was picked and placed in 50 ml of TB supplemented with the desired antibiotic (100 µg/ml) and left to grow overnight in the shaker at 37°C.

Table 2. Plasmids

Name	Insert name	Vector
β-Gal	β-galactosidase	
PGK-1	Phosphoglycerate kinase 1	pGL3- promoter (Promega)
pGL2	No insert	pGL2-promoter (Promega)
Stra6	Stra6	pCMV6-XL4 (OriGene)
Stra6 Luc	Five DR1 RAREs	pGL2-basic (Promega)

The E.Z.N.A. ® Plasmid Midiprep Kit (OMEGA Bio-Tek, Inc.) was used for the isolation of plasmids from the 50 ml bacterial cultures. Bacteria were pelleted by centrifugation at 4000 rpm for 10 min; the following steps were performed according to the manufacturer. DNA was eluted in 1 ml of sterile ddH_2O and quantify using a spectrophotometer. Plasmids were stored at -20°C until further use.

2.2.2 Plasmid transfection

Transfection of plasmids was made using Lipofectamine™ 2000 (Invitrogen). Cells were split one day before transfection and were 70-80% confluent on the day of transfection. For each 60 mm plate, 0.5 ml of serum-free media were mixed with 20 µl of Lipofectamine™ 2000 in one tube and incubated at room temperature. In another tube, 8 µg of DNA plasmid were diluted in 0.5 ml of serum-free medium. After the 5 min incubation, the diluted DNA was combined with the diluted Lipofectamine™ 2000. The solution was mixed gently and incubated for 20 min at room temperature to allow the formation of the complexes. In the meantime, the medium in the cells was aspirated and changed for serum-free media. After the incubation time 1 ml of the complexes was added to each plate and the cells were placed in the incubator at 37°C. Medium was changed after 5 hours and cells were left for 18-24 hours before using them for further experiments. For transfection using other size of plates, volumes were scaled down accordingly.

2.2.3 siRNA transfection

The use of siRNA allows the down regulation of expression of specific mRNAs; siRNA against HIF-1α and MEK 1/2 were used in this project. ON-TARGETplus SMARTpool siRNA Human MAP2K2 and MAP2K1 (Thermo Scientific) were used to knock down MEK 1 and 2. HIF-1α siRNA (Santa Cruz) was used to knock down levels of HIF-1.

siRNA was transfected into HCT116 cells using Lipofectamine™ 2000. Cells were split the day before transfection and were 70%-80% confluent at the moment of transfection. For each 60mm plate, 10 µl of Lipofectamine™ 2000 were mixed with 0.5 ml of media and incubated for 5 min. In a separate tube, 100nM of the siRNA was mixed with 0.5 ml of media. After the incubation time, the diluted siRNA was mixed with the diluted Lipofectamine™ 2000 and incubated at room temperature for 20 min. During this time, the medium in the plates was aspirated and changed for serum-free media. 1 ml of the siRNA/lipofectamine complexes was added to each plate and the plates were placed in the incubator at 37°C. The medium in the plates was changed the next morning and the cells were used for experiment 18-24 hours after transfection. When using other sizes of plates, the transfection volumes were scaled down accordingly.

2.3 Colony Formation Assay

Colony formation assay is a cell survival assay that is based on the ability of a single cell to form a colony. To evaluate the capacity of cells under physiological oxygen concentrations to form colonies, HCT116 cells were split into 60 mm plates. The next day cells were treated with 5μM of U0126 or 1μg/ml of doxorubicin (described in 2.1.4). After 48 hours of treatment cells were trypsinised and counted (described in 2.1.3), 1000 cells were placed in 60 mm plates (duplicates). Cells were placed in the 20% or 5% O_2 incubator and left to grow for 14-15 days. Media was changed every 5 days and extra 5μM U0126 was added.

2.3.1 Giemsa Staining

Plates were washed with 3 ml of 1× PBS and fixed with 2 ml of 10% neutral buffered formalin (SIGMA-ALDRICH™). Plates were incubated at room temperature for 30 min. Formalin was removed by aspiration and plates were washed twice with 1× PBS. Plates were allowed to completely air dry with the lids removed. 5 ml of Staining Reagent was added to the plates and they were incubated at room temperature for 5 hours. The stain was pour off and the plates were rinsed with ddH_2O. Plates were allowed to air dry and the number of colonies from each plate was counted and recorded.

Staining reagent: 6.4 ml of PO_4 buffer (67mM), 89.6 ml of dH_2O, 4 ml Giemsa stain (Fluka). Prepared fresh for each stain

1M PO_4 buffer: 1M Sodium Phosphate monobasic, 1M Sodium Phosphate dibasic mixed in a 2 (dibasic) to 1 (monobasic) ratio; pH to 7.0 with NaOH

2.4 Flow cytometry

Flow cytometry is a laser-based biophysical technology that allows, among other things, the detection of biomarkers. The principle of flow cytometry is the ability to measure the properties of individual particles, for this, it is important that particles or cells are passed through the laser beam one at a time. Through hydrodynamic focusing the flow cytometers are able to achieve a stream of individual cells, after this, each particle passess through one or more beams of laser light. Fluorescence measurements taken at different wavelengths can provide quantitative and qualitative data about fluorochrome-labelled molecules.

2.4.1 Propiduim Iodide

Propidium iodide (PI) is a fluorescent molecule that binds to nucleic acids. It intercalates in DNA and fluoresces red when excited with 488nm wavelength light. To assess percentage cell death, a PI staining followed by a FACS analysis was made. HCT116 cells were split into 6-well plates and left to grow for 24 hours before treating them with doxorubicin and/or U0126 (described in 2.1.4). All samples were made in duplicate. Media from each sample was collected in labelled 15 ml tubes. To wash the cells, 2 ml of PBS was added to the plates and kept in the same tube as the media. 1 ml of trypsin was added to the plates and cells were collected in the same tubes as the media and PBS. The tubes were centrifuged at 1100 rpm for 5 min and the pellet was

washed once with 1× PBS. To fix the cells, the pellet was resuspended in 1 ml of 70% ethanol and placed at -20 °C for at least 30 min.

Cells were taken out of the freezer and spun down for 5 min at 1100 rpm. The pellet was washed once with 1 ml of 1× PBS. Cells were resuspended in 500 µl of PI buffer and transferred to 3.5 ml polystyrene round-bottom tubes (VWR). The tubes were incubated for 30 min at 37 °C in the dark. 10,000 events were recorded for each sample using the Beckton Dickinson FACSCanto II and FACSDiva 6.0 software (Beckton Dickinson) for acquisition and analysis. The percentage of cells in sub-G1 phase was plotted for each sample.

PI Buffer: 50 µg/ml of Propidium Iodide, 10 µg/ml RNase A, 1 ×PBS

2.4.2 Annexin-V

One of the early changes in the cell during apoptosis is the translocation of phosphatidylserine (PS) from the inner side of the plasma membrane to the cell surface. Annexin-V is a protein that has strong binding affinity to PS and when it is fluorescently labelled, it allows the identification of apoptotic cells. To detect the percentage of apoptotic cells, HCT116 cells were split into 6-well plates and left to grow for 24 hours before treating them with doxorubicin and/or U0126. Medium was aspirated and cells were washed with 1× PBS, trypsinized and collected in 15 ml falcon tubes. The cells were spun down and the pellet was stained with annexin V-FLUOS

(Roche applied science) following the instructions provided by the manufacturer. 10,000 events were recorded for each sample using the Beckton Dickinson FACSCanto II and FACSDiva 6.0 software (Beckton Dickinson) for acquisition and analysis.

2.5 Protein Analysis

2.5.1 Protein lysates

Cells were split by trypsinization into 60 mm plates and the next day they were transfected (described in 2.2) and/or treated (described in 2.1.4) as desired. After 24 hours, plates were taken out of the incubator and placed immediately on ice. Medium was removed and plates were washed once with ice-cold 1x PBS. 500 µl of ProteoJET™ Mammalian Cell Lysis Reagent (Fermentas) was added to each plate. Cells were scraped and collected in a 1.5 ml microcentrifuge tube; 5 µl of Protease Inhibitor Cocktail Set III (Calbiochem) and 1µM Na_3VO_4 (SIGMA-ALDRICH™) were added to each sample. Tubes were centrifuged for 15 min at 12,000 rpm and the supernatant was transferred into a clean labelled tube and stored at -80°C until further use.

2.5.2 Protein Quantitation

Total protein concentration was quantified using Bradford reagent (Fermentas). The Bovine Serum albumin Standard Set (Fermentas) was used to create a Standard Curve for the Bradford protein quantification. The 0.5 mg/ml, 1.0 mg/ml, 1.5 mg/ml and 2.0 mg/ml aliquots were used to create the standard curve by plotting the absorbance vs. protein concentration of each protein standard. For the assay, 1 ml of Bradford reagent was pipetted into each cuvette and 20 µl of each pre-diluted standard or sample was added. The cuvettes were mixed well and read in a spectrophotometer set

at 595 nm, the protein concentration of unknown samples was determined by comparing their absorbance values against the standard curve.

2.5.3 SDS-Polyacrylamide gel Electrophoresis

Polyacrylamide gels were prepared using the kuroGEL Verti 1010 mini gel unit (VWR). The gel unit was assembled and a 10% resolving gel was prepared as follows: 4.8 ml of ddH_2O, 2.5 ml of 40% Acrylamide mix, 2.5 ml of 1.5M Tris (pH 8.8), 0.1 ml of 10% SDS, 0.1 ml of 10% Ammonium persulfate, 4 µl of TEMED. The mix was immediately poured into the mini gel unit leaving space for the stacking gel. When the gel was set, 3 ml of 5% stacking gel was prepared by mixing: 2.23 ml of ddH_2O, 380 µl of 40% Acrylamide mix, 380 µl of 1.0M Tris (pH 6.8), 30 µl of SDS, 30 µl of 10% ammonium persulfate, 3 µl of TEMED. The mix was poured on top of the resolving gel and the comb was immediately inserted, and the gel was left to set.

The 4× DualColor™ Protein Loading Buffer (Fermentas) was used for preparation of the protein samples for electrophoresis. Samples were prepared in 1.5 ml microcentrifuge tubes as follows: 20 µg of protein sample was mixed with 5 µl of Loading Buffer, 1 µl of 2M DTT and ddH_2O to a final volume of 20 µl. The samples were heated at 95-100°C for 5 min to denature them, spun down and loaded directly into the SDS-Polyacrylamide gel. Gel tank was connected to the power source and the gel was run at 160 V for approximately 1 hour and a half or until the proteins reached the bottom of the gel.

10× Running buffer: 0.25 M Tris, 1.92 M Glycine, 1% SDS

10× Transfer buffer: 0.25 M Tris, 1.92 Glycine. For 1× add 10% Methanol

Blocking solution: 3% Milk powder, 1× PBS, 0.1% Tween 20

Washing buffer: 1×PBS, 0.1% Tween 20

2.5.4 Western blotting

A piece of Immobilon-P membrane (Millipore) was cut to the dimensions of the gel and wet in 100% methanol for 30s. The membrane was then equilibrated in transfer buffer for 5 min. The assembly of the transfer stack was made in a tray with enough transfer buffer to cover it, one foam pad was placed on one side of the cassette holder and one sheet of filter paper was placed on top of the pad. The membrane was placed on top of the filter paper and the gel with the resolved proteins was placed on top of it. Another sheet of filter paper was placed on top of the gel and another foam pad on top. Then, the cassette holder was closed and placed into the transfer tank so that the side of the cassette with the gel was facing the cathode (-). The tank was filled with enough transfer buffer to cover the cassette holder and the system was turned on at 80 V for 1 hour.

Table 3. Primary Antibodies

Name	Source	Dilution	Molecular Weight	Supplier
Actin	Mouse	1:10,000	42 kDa	Abcam
Bax	Rabbit	1:1000	21 kDa	Abcam ab7977
Calnexin	Rabbit	1:2000	95 kDa	Cell Signalling #2433
Caspase 8	Mouse	1:1000	18, 43, 57 KDa	Abcam
HIF-1α	Mouse	1:1000	120 kDa	BD Transduction Laboratories #610958
MAPK	Rabbit	1:1000	42,44 kDa	Cell Signalling #9102
P- MAPK	Rabbit	1:1000	42,44 kDa	Cell Signalling #9101
p21	Rabbit	1:400	21 kDa	Santa Cruz sc-397
p53	Mouse	1:1000	53 kDa	Abcam ab28
PUMA	Rabbit	1:1000	18,23 kDa	Cell Signalling #4976
Stra6	Rabbit	1:200, 1:100	74 kDa	Abcam ab73490

Once the transfer was completed, the cassette holder was removed from the tank and the protein side of the membrane was marked. The membrane was placed in blocking solution and incubated for 1 hour at room temperature on a shaker. The primary antibody (Table 3) was diluted to the desired concentration in 2-3 ml of blocking solution and incubated overnight at 4 °C on a shaker.

Table 4. Secondary antibodies

Name	Dilution used	Label	Supplier
Mouse IgG	1:10,000	Horseradish peroxidase	Thermo Scientific #31430
Rabbit IgG	1:10,000	Horseradish peroxidase	Thermo Scientific #31460
Rabbit IgG	1:400	Alexa Fluor 488	Invitrogen A21441

The next day, the membrane was washed 3 times for 10 min each time with washing buffer and incubated with the corresponding secondary antibody (Table 4) for 1 hour at room temperature on a shaker. After the incubation time, membrane was washed 3 times for 10 min each time with washing buffer.

The detection of the proteins was made using Pierce ECL plus western blotting substrate (Thermo Scientific). Equal amounts of solution 1 and solution 2 were mixed and the membrane was incubated in it for 2 min. The excess of detection reagent was drained off and the membrane was wrapped in cling film and placed in a film cassette with the protein side up. In the dark room, a sheet of autoradiography film was placed on top of the membrane an exposed for the desired amount of time and then developed.

2.6 RNA isolation and qRT-PCR

2.6.1 RNA isolation

Cells were split by trypsinization and 24 hours later they were transfected or treated as desired. To isolate RNA from the cells, media was aspirated from the plates and the cells were washed once with ice-cold 1× PBS. One ml of TRIzol® Reagent (Invitrogen) was added to each 60 mm plate and cells were passed several times through the pipette to homogenize them. All the homogenate was transferred to a PGL 2 ml Heavy tube (5Prime) and incubated at room temperature for 5 min. After the incubation time, 200 µl of chloroform (Fisher Scientific) was added to each tube and they were shaken vigorously for a few seconds. The tubes were incubated for 2-3 min at room temperature and then centrifuged for 15 min at 12,000 ×g at 4 °C. The aqueous phase was transferred into a clean 1.5 ml microcentrifuge tube and 500 µl of Isopropyl alcohol was added to precipitate the RNA. Samples were incubated for 10 min at room temperature and then centrifuged at 12,000 ×g for 10 min at 4 °C. The supernatant was discarded and the pellet was washed once with 1 ml of 70% ethanol. The sample was mixed and then centrifuged at 7,500 × g for 5 min at 4°C. The supernatant was discarded and the pellet was briefly air-dried, RNA was resuspended in RNase-free water by passing the solution a few times through a pipette tip.

2.6.2 Reverse transcription

Total RNA was quantified using a Nanodrop ND8000 (Thermo Scientific). cDNA was prepared from 1 µg of RNA using the Precision *qScript*™ Reverse Transcription kit (Primerdesign). For each sample, the following was added to 0.2 ml PCR tubes: 1 µl of oligo-dT, 1 µg of RNA and RNase/DNase-free water up to a volume of 10 µl. The tubes were heated to 65°C for 5 min and then immediately cool on ice. For the RT reaction a 10 µl mix was made for each tube with the following reagents: qScript 10× Buffer, dNTP mix, DTT, RNase/DNase-free water and qScript enzyme. The mix was added to each of the tubes and they were incubated at 55°C for 20 min, followed by a heat inactivation of 15 min at 75°C. The samples were stored at -20°C until further use.

2.6.3 Quantitative Polymerase Chain Reaction (qPCR)

The primers used for the reaction were custom primers by PrimerDesign (Table 5). Primers for the reference genes Actin and GAPDH were used to normalize the samples (PrimerDesign Ltd). The reaction mix was made using 2× Precision™ Mastermix (PrimerDesign) as follows: 1 µl of resuspended primer mix (300nM), 10 µl of Mastermix and 4 µl of RNase/DNase free water. 15 µl of the mix were added to each well of a white LightCycler® 480 Multiwell Plate 96 (Roche). The cDNA was diluted 1:10 and 5 µl were used for the qPCR, each sample was put in triplicate. Reactions were carried out on a Roche Light Cycler 480 under the following conditions: enzyme activation for 10 min at 95°C, followed by 50 cycles of denaturation for 15s at 95°C and data collection for 60s at 60°C. A post PCR run melting curve was used to prove the specificity of the primers.

Table 5. Primers for qRT-PCR

Name	Forward	Reverse	Supplier
GLUT1	ACCTCACTCCTGTTACTTACCTA	ACCCCACTTACTTCTGTCTCA	Primerdesign Ltd
HIF-1α	TGCCACATCATCACCATATAGAG	TGACTCAAAGCGACAGATAACA	Primerdesign Ltd
PGK1	TGCCCATGCCTGACAAGTA	CTACACAGTCCTTCAAGAACAGA	Primerdesign Ltd
RARα	GGGCAAATACACTACGAACAAC	GGCGAACTCCACAGTCTTAAT	Primerdesign Ltd
RARβ	GCCTTACCCTAAATCGAACTCA	GCCTGTTTCTGTGTCATCCAT	Primerdesign Ltd
Stra6	TCCTGCCTACCATCCTCCT	AGACAGACCTCCACCCAAC	Primerdesign Ltd

2.7 Comet assay

The Comet assay, also known as single-cell electrophoresis, permits the detection of DNA strand breaks. In this thesis, an alkaline comet assay was used for specific detection of single strand breaks. The use of the enzyme formamidopyrimidine DNA-glycosylase (Fpg) allowed the detection of 8-OH guanine and other oxidatively damage purines. Cells were grown into 60 mm plates and treated with 0.4ug/ml of doxorubicin (described in 2.1.4). For the physiological oxygen part of the project, the cells were incubated at 20% or 5% O_2 for 24 hours.

2.7.1 H_2O_2 treatment

Treatment with Hydrogen peroxide (H_2O_2) was used as a positive control of single-strand breaks caused by oxidation. Media was aspirated and plates were washed once with ice-cold 1× PBS. 3 ml of serum-free media was added to the plates and also 3 µl of 0.1M H_2O_2 (final concentration 100µM). After 10 min, the media with H_2O_2 was aspirated and cells were washed once with 1× PBS.

Cells were trypzinized and counted (described in 2.1.3) and nine 1.5 ml microcentrifuge tubes with 40,000 cells each were used for each sample. Cells were spun down and the supernatant was aspirated. Slides previously coated with 1% agarose were labelled with the name of the sample and separated in three groups: Control, Buffer and Fpg. The cell pellet was resuspended in 170 µl of 0.6% low melting

point agarose (in PBS), two drops of 80 µl were put on each slide and coverslips were put on top of each of them. Slides were left to set on a cold metal tray. After the gels were set the coverslips were removed and the slides were incubated on lysis buffer overnight to expose the DNA in each cell.

Lysis Buffer: 2.5M NaCl, 0.1M Na_2EDTA, 10mM Tris-HCl, 1% Triton X-100 (add immediately before use), pH 10 with NaOH

2.7.2 Fpg treatment

Fpg enzyme was used to excise altered bases and nick the DNA backbone in places where oxidative damage had occurred. Buffer and Fpg slides were taken out of the lysis buffer and the excess of buffer was removed by gently blotting them on a paper towel. The slides were placed on a square plate and covered with ice-cold ddH_2O for 5 min. After this time, the ddH_2O was aspirated and three 5 min washes with ERB buffer were made. The slides were transferred into a dark cell culture plate containing a moistened tissue to prevent the slides from drying out during the enzyme treatment. The Fpg slides were treated with 50 µl of Fpg solution, 50 µl of ERB was added to the buffer slides. The slides were incubated at 37°C for 30 min. Control slides were taken out of the lysis buffer and washed once with ddH_2O. Fpg and buffer slides were taken out of the oven and placed in a square plate. All the slides were washed two times with ddH_2O, first wash 5 min and second wash 10 min.

Enzyme Reaction Buffer (ERB): 40mM HEPES, 0.02% BSA, 100mM KCl, 0.5mM Na_2EDTA, pH 8.0 with 1M KOH

Electrophoresis Buffer: 300mM NaOH, 1mM Na_2EDTA, pH 13

Neutralization Buffer: 0.4M Tris-HCl, pH 7.5

2.7.3 Electrophoresis and Staining

The slides were transferred to an electrophoresis tank set on ice and they were cover with ice-cold alkaline electrophoresis buffer. The slides were incubated for 20 min in the dark to allow the unwinding of the DNA. After the incubation time, the tank was switch on and set to exactly 30V 300mA and the slides were electrophoresed for 20 min. The slides were then transferred to a square plate and each slide was gently flooded with neutralization buffer for 20 min. Slides were rinsed with ddH_2O twice, first wash 5 min and second wash 10 min. The slides were transferred into a tray and put into the oven at 37°C to dry.

The next day, the slides were rehydrated for 30 min with ddH_2O and incubated with a 2.5 µg/ml propidium iodide solution for 20 min to stain the DNA. The slides were cover with ddH_2O for 30 min and then transferred into a tray and put in the oven to dry at 37°C.

Comet images were visualized using an Olympus fluorescence BHS microscope and were captured by an online charge-coupled device (CCD) camera and analysed using the Komet Analysis software (version 5.5) (Andor Technology). Fifty comets, randomly chosen, were analysed per gel and Percentage Tail DNA was recorded.

2.8 Luciferase assay

HCT116 cells were split into 24-well plates with 80,000 cells per well and left to grow for 24 hours. Cells were transfected by lipofection (described in 2.2.2) with the desired luciferase reporter plasmid (Table 2) and co-transfected with a β-galactosidase plasmid as a transfection control. For the physiological oxygen tensions experiments, cells were also treated with doxorubicin and U0126 and cultured at 5% or 20% O_2. For the retinoic acid pathway experiments, cells were treated with doxorubicin and ATRA. Each sample was made in duplicate.

5× lysis buffer: 6.25mM Tris pH 7.8, 10mM DTT, 10mM EDTA, 50% Glycerol, 5% Triton X-100, store 4 °C and dilute to 1× before use

β-Gal stock solution: 60mM Na_2HPO_4, 10mM KCl, 1mM $MgCl_2$, 40mM NaH_2PO_4

β-gal substrate: 10 ml of β-gal stock solution, 20 mg ONPG, 35 µl β-mercaptoethanol

24 hours after transfection, medium was removed from the wells and cells were washed once with 1× PBS. 140 µl of 1× lysis buffer was added to each well and the plates were incubated on the shaker for 2 hours at room temperature or for 30 min at -80 °C. For the β-galactosidase measurement, 80 µl of each cell lysate were transferred into a 96-well plate and 100 µl of β-gal substrate was added to each well and

incubated at 37 °C for 15 min. For the luciferase assay, 20 µl of each cell lysate were transferred into a white 96-well plate.

Plates were read using a VICTOR™ X5 multilabel reader (PerkinElmer). The β-galactosidase assay plate was placed in the plate reader and the absorbance at 405 nm was measured. The Luciferase Assay System (Promega E1500) was used for the luciferase assay. The white 96-well plate was placed in the plate reader and the dispenser was filled with the luciferase substrate and programmed to dispense 50 µl into each well. The light emission measurements were taken after 30 s of the addition of the substrate.

2.9 Caspase Assay

Caspases are the ultimate executioners of apoptosis. Caspase-Glo® 3/7 Assay (Promega) is a luminescent assay that measures the activity of caspase 3 and 7 that has a proluminescent caspase 3/7 substraate that is cleaved to release a substrate of luciferase. This assay was used to assess the activity of Caspases 3 and 7 at different oxygen concentrations. HCT116 cells were split into a white 96-well plate with 20,000 cells per well. Cells were treated with doxorubicin and cultured at 20% and 5% O_2. After 24 hours, 100 µl of caspase substrate was added to the media and the cells were incubated for 1 hour at 37 °C. Luminescence measurements were taken using a VICTOR™ X5 multilabel reader (PerkinElmer).

2.10 Chromatin Immunoprecipitation

A ChIP assay was used to analyse possible p53 binding sites in the promoter of Stra6. HCT116 and HCT116 p53-/- cells were split into two 100 mm plates each and one of the plates was treated the next day with doxorubicin (described in 2.1.4). Media was aspirated and the cells were washed once with 1× PBS. A small number of cells was scraped out of the plate and reserved for Western blot analysis. Cells were fixed using 1% Formaldehyde in PBS, 10 ml of the solution was added to each of the plates and they were incubated for 10 min at room temperature on the shaker. The reaction was stopped using a final concentration of 0.125M Glycine and incubating the plates for 10 min at room temperature on the shaker. After the incubation time, the solution was aspirated and the cells were washed twice with 1× PBS. The cells were scraped in 3 ml of PBS and collected in a 15 ml falcon tube. Cells were spun down at 1100 rpm and the pellet was stored at -80°C.

2.10.1 Cell extract preparation and sonication

To avoid proteases, PMSF was added to all the buffers immediately before use (1mM final concentration). Cell pellets were resuspended in 3 ml of Lysis Buffer 1 and incubated in the rotator for 15 min at 4°C. Nuclei were spun down at 2000 ×g for 10 min at 4°C. The supernatant was aspirated and the pellet of nuclei was resuspended in 3 ml of Lysis buffer 2 and incubated in the rotator for 15 min at 4°C. Chromatin was

spun down at 2000 ×g for 15 min at 4°C and the pellet was resuspendend in 600 µl of IP buffer.

Lysis Buffer 1: 0.25% Triton X-100, 10mM EDTA, 0.5mM EGTA, 10mM Tris-HCl pH 8.0

Lysis Buffer 2: 200mM NaCl, 10mM EDTA, 0.5mM EGTA, 10mM Tris-HCl pH 8.0

IP Buffer: 10mM Tris-HCl pH8.0, 100mM NaCl, 1mM EDTA, 0.5mM EGTA, 0.1% Na-deoxycholate, 0.5% N-lauroylsarcosine

Elution Buffer: 50mM Tris-HCl pH8.0, 10mM EDTA, 1% SDS

300 µl of chromatin extracts were transferred to polycarbonate tubes. The Diagenode Bioruptor 200 was used for sonicating the samples. The water bath on the bioruptor was pre-chilled with ice one hour before use. The Bioruptor was set to High and samples were sonicated for 30 min as follows: three 10 min sonication times with 15 min cooling down intervals. After the sonication time, samples were transfer to 1.5 ml microcentrifuge tubes and 30 µl of 10% Triton X-100 was added to each one. To pellet the debris, samples were spun down at 20,000 ×g for 10 min at 4°C. 50 µl of sonicated material was removed for Input DNA and stored at -20°C.

2.10.2 Immunoprecipitation

Dynabeads Protein A-conjugated were used for the IP, 20 µl of beads were used for each sample. The beads were washed 3 times with blocking solution (0.5% BSA in PBS) and then resuspended in 250 µl of blocking solution. 2 µg of p53 Ab6 antibody (Calbiochem #OP43) was added to the beads and they were incubated overnight in the rotator at 4°C.

The antibody-bead complex was washed 3 times in 1 ml of blocking solution and resuspended in 100 µl blocking solution. 300 µl of sonicated material was added to each of the tubes with the antibody-bead complex and incubated overnight at 4°C on the rotating wheel.

The following day, the samples were washed 3 times with 1 ml of RIPA Buffer and once with 1ml of TE containing 50mM NaCl. The tubes were spun down at 1000 ×g for 3 min at 4°C to remove any residual buffer. 210 µl of elution buffer was added to each tube and incubated at 65°C for 15 min; with brief vortexing to resuspend the beads every 2 min. The beads were spun down at 16,000 ×g for 1 min at room temperature. 200 µl of the supernantant were transferred to a new tube and the crosslinking was reversed by adding 8 µl of 5M NaCl and incubating overnight at 65°C. The Input samples were thawed and 150 µl of elution buffer were added to each one and mixed. 8 µl of 5M NaCl were added and the tubes were incubated overnight at 65°C.

The next day, 200 µl of TE were added to each tube to dilute the SDS in the elution buffer. 8 µl of 10mg/ml RNase A were added to each tube and they were incubated at 37°C for 2 hours. After the incubation time, 4 µl of 20mg/ml Proteinase K were added to the tubes and incubated at 55 °C for 2 hours. The DNA was purified using the PCR purification Kit (QIAGEN) and was eluted in 100 µl of RNase/DNase free water. The input samples were diluted 10-fold.

2.10.3 Analysis by quantitative PCR

All primers were ordered from Invitrogen and were designed on the region at the start of the transcription origin of Stra6 (Figure 2.1 and Table 6). Primers that recognize a p53 binding site on the promoter of the *p21* gene were used as a positive control for p53 binding, primers design on the promoter region of the *Actin* gene were used as negative controls. The primers were tested using input DNA to find the optimum conditions for amplification. The reaction mix was made using 2× Precision™ Mastermix (PrimerDesign), 2 µl of Input or IP sample were used for each reaction. Reactions were carried out on a Roche Light Cycler 480 under the following conditions: enzyme activation for 10 min at 95°C, followed by 50 cycles of denaturation for 15s at 95°C and data collection for 60s at 60°C. A post PCR run melting curve was used to prove the specificity of the primers.

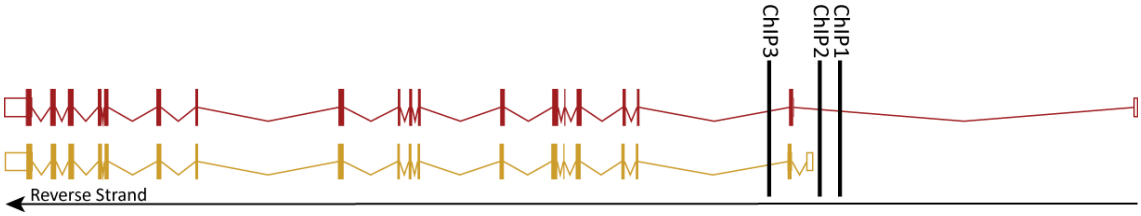

Figure 2.1 Localization of the primers used for ChIP assay in the Stra6 gene. Two representative Stra6 transcript variants (10 and 2) are shown in the picture. Boxes represent exons and lines represent introns. Vertical black lines represent approximate location of the primers.

Table 6. Primers for ChIP

Name	Forward	Reverse	Supplier
p21p53BS	GTGGCTCTGATTGGCTTTCTG	CTGAAAACAGGCAGCCCAAG	Invitrogen
Actin	TGGCTCAGCTTTTTGGATTC	GGGAGGATTGGAGAAGCAGT	Invitrogen
Stra6CHIP1	TCCCCTCTGGTGTTGTCTCCC	CCTTCCCCAGGCTGGTTTGGC	Invitrogen
Stra6CHIP2	GCTGGTGAACCTCAGGGCACA	AAAGCCATTGCTTGTTCTGGCGG	Invitrogen
Stra6CHIP3	CTGCCGGGCCCAGGTGTAAA	CACTCTGGTGCGTAGGGCAGC	Invitrogen

2.11 Immunofluorescence

HCT116 cells were split into 6-well plates containing sterile coverslips. Half of the cells were transfected with 4 µg of Stra6 plasmid (described in 2.2.2). After 24 hours the medium was aspirated from the wells and the cells were washed three times with 1× PBS. Cells were fixed using 1 ml of 4% Paraformaldehyde (PFA) for 30 min with gentle shaking. After fixing, cells were washed three times with 1× PBS and permeabilized with 1 ml of 0.1% Triton X-100 for 10 min. After the incubation time, cells were washed three times with 1× PBS and blocked with 1% BSA for 30 min. The coverslips were incubated with 100 µl of 1:100 Stra6 primary antibody (Table 3) overnight at 4°C.

The next day coverslips were washed three times with 1× PBS and incubated with 100 µl of secondary anti-rabbit antibody Alexa Fluor 488 (Table 4) for 45 min in the dark. After the incubation time, the coverslips were washed three times with 1× PBS and stained with DAPI for 10 min. Slides were labelled and the coverslips were mounted and sealed with transparent nail varnish. Slides were analysed using the Nokia TE300 semi-automatic microscope.

Chapter 3. Influence of physiological oxygen tensions on the cellular responses to damage

Atmospheric oxygen ranges between 20-21%, but the amount of O_2 that a cell in the human body receives depends on its proximity to the arterial blood supply and the rates of consumption by the cell and its neighbours. Although oxygenated arterial blood contains 10-12% O_2, healthy tissues normally have a lower oxygen pressure (between 2-9%). Most experiments done in laboratory conditions with cells in culture are performed at atmospheric O_2 tensions. The difference between the oxygen that healthy tissues receive and the conditions at which the experiments in laboratory conditions are performed is significant and an excess of oxygen could influence the cellular responses to DNA damage, as it has previously been observed that mouse embryonic fibroblasts proliferate for longer when cultured at physiological oxygen tensions (Parrinello et al., 2003).

3.1 Resistance to cell death at 5% O_2

The first experiment was to assess the response to DNA damage induced by doxorubicin at physiological oxygen tensions. 5% was the oxygen tension chosen to perform these experiments as it is within the range of oxygen that normal tissues

receive. To explore differences in cell death, HCT116 were treated with 0.4 μg/ml doxorubicin for 24 hours and percentage of cell death was determined by Propidium Iodide (PI) staining and flow cytometry (FACS) analysis. The results show that cells grown at physiological oxygen tensions (5% O_2) have a survival advantage when treated with Doxorubicin (Figure 3.1). In cells cultured at 20% O_2, up to twice as much cell death (46%) can be observed compared to cells at 5% O_2 (23%) (Figure 3.1A).

3.1.1 Resistance at 5% O_2 in other cell lines

HCT116 is a colorectal cancer cell line and as with most cell lines it has a variety of mutations and adaptations to growing in culture. The osteosarcoma cell line U2OS and the breast cancer cell line MCF-7 were used to investigate if our findings could be extended to other human cancer cell lines. Cells were cultured at 20% and 5% O_2 and treated with 0.4 μg/ml of doxorubicin. Percentage of cell death was assessed by PI DNA staining and analysed by FACS. As shown in figure 3.2, U2OS cells have a significant reduction in cell death at 5% O_2 (8%) compared to 20% O_2 (25%). In MCF-7 cells a similar result can be observed in which the percentage of doxorubicin-induced cell death is reduced from 30% to 11% when cells are cultured at physiological oxygen tensions (Figure 3.2, lower panel). These results suggest that cells, independently of the tissue of origin, are more resistant to doxorubicin-induced cell death when cultured at physiological oxygen tensions.

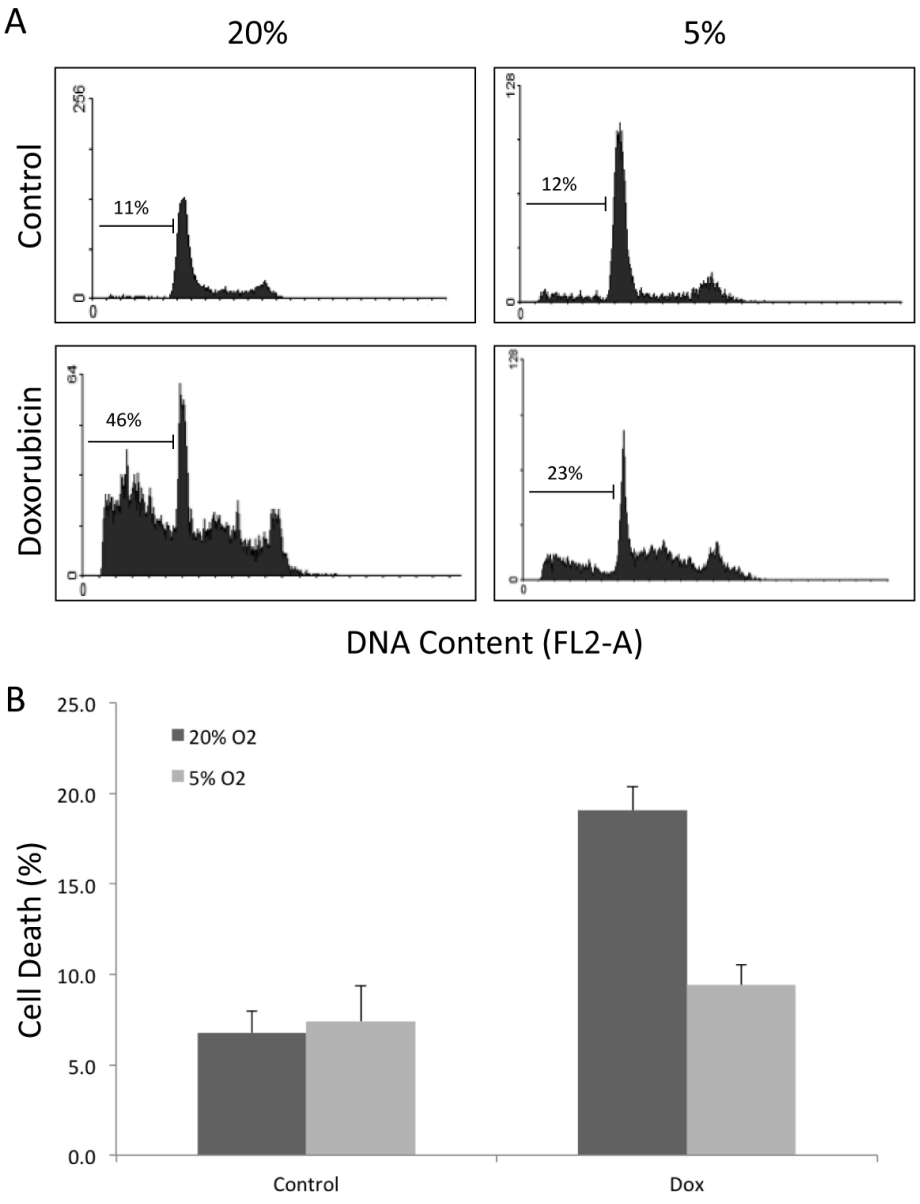

Figure 3.1 HCT116 cells resist to DNA damage-induced apoptosis at physiological oxygen tensions. A. Cells treated with doxorubicin (0.4µg/ml) for 24 hours and cultured at 20% and 5% O_2, stained with PI and analysed by FACS (representative experiment) show a reduction in cell death when cultured at 5% O_2. B. Summary of two FACS experiments with PI staining in HCT116 cells after treatment with doxorubicin (0.4µg/ml) showing a reduction in cell death in cells cultured at 5% O_2.

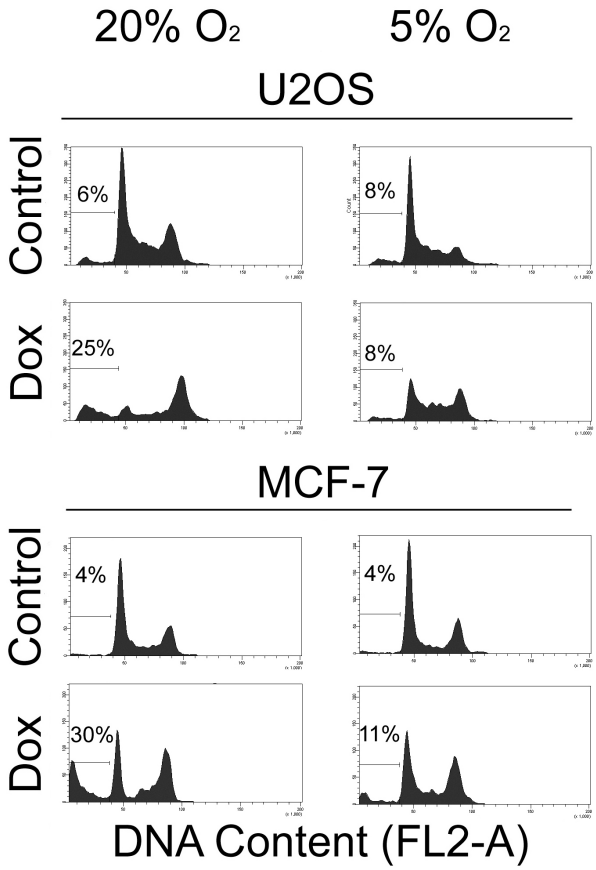

Figure 3.2 Resistance to cell death in U2OS and MCF-7 at 5% O_2. A reduced amount of cell death can be observed in U2OS (upper panel) and MCF-7 (lower panel) when 5% O_2 compared to 20% O_2 when treated with 0.4µg/ml of Doxorubicin. Assessed by PI staining followed by FACS analysis.

3.1.2 Different concentrations of doxorubicin

HCT116 cells were treated with different concentrations of doxorubicin for 48 hours to assess if the resistance to cell death observed was independent of the concentration used. Resistance to doxorubicin-induced cell death at 5% O_2 was observed at all the concentrations used (Figure 3.3). At higher concentrations of doxorubicin (1µg/ml) the

percentage of cell death at both oxygen concentrations appears to be very similar, this may be due to the high toxicity of this concentration.

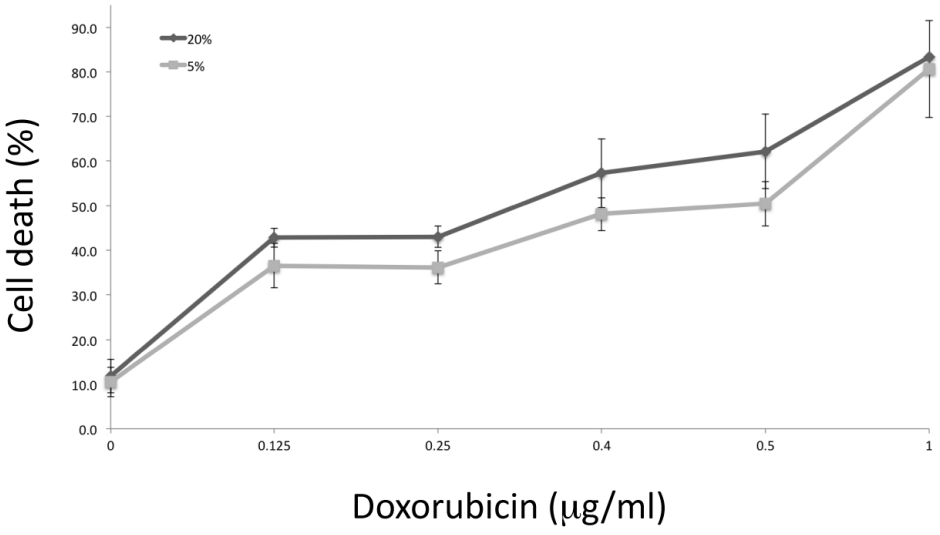

Figure 3.3 Resistance at 5% O_2 is observed regardless of the concentration of doxorubicin used. HCT116 were treated with 0.125, 0.25, 0.4, 0.5 and 1 μg/ml of doxorubicin and cultured at 20% and 5% O_2 for 48 hours. Percentage cell death was determined by PI staining and analysed by flow cytometry. A reduction in cell death can be observed in cells cultured at 5% O_2 (grey line) regardless of the concentration of doxorubicin used.

3.1.3 Cell survival at 5% O_2

To assess the cell survival at physiological oxygen tensions, a Colony formation assay was performed. It was observed that HCT116 cells cultured at 5% O_2 are able to form more colonies compared to cells cultured at 20% O_2 (Figure 3.4). When these cells were treated with doxorubicin a reduced number of colonies were formed in both conditions (as expected), but a larger amount of them could be observed at 5% O_2. These results confirm the pro-survival effect of physiological oxygen tensions observed by FACS. The colonies formed at 5% O_2 were on average, bigger in size, suggesting a

growth advantage at lower oxygen concentrations consistent with previous reports (Parrinello et al., 2003). Overall, this result suggests that cells at 5% O_2 are more likely to survive and replicate compared to cells at higher oxygen concentrations.

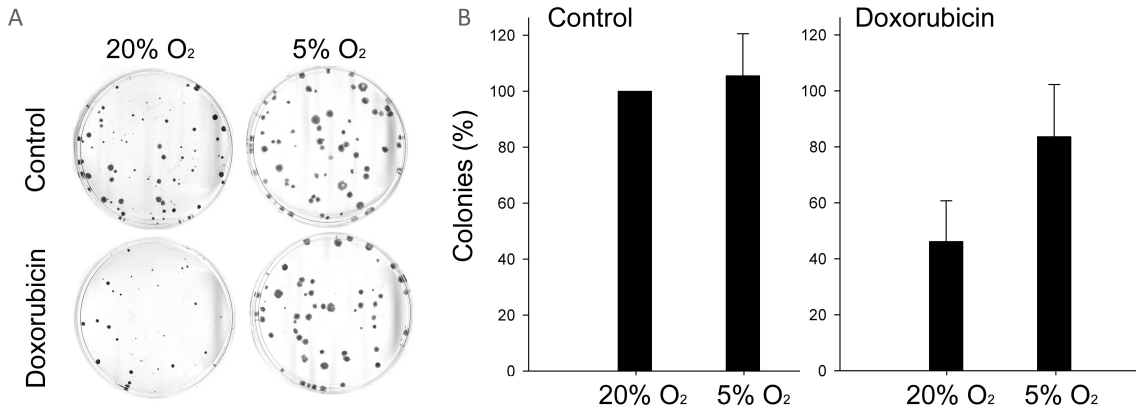

Figure 3.4 Increased number of colonies at 5% O_2. A. Representative colony formation experiment, 1000 cells were seeded in each plate and half of the plates were treated with 0.25 µg/ml of doxorubicin and cultured at 5% O_2 or 20% O_2 for 14 days. Colonies at 5% O_2 are bigger in size and number than those at 20% O_2. B. Graph of number of colonies from A, bars represent average of three independent experiments.

3.2 The role of p53 in the resistance to cell death at 5% O_2

Doxorubicin is a topoisomerase inhibitor that functions by intercalating with DNA and causing DNA damage. This triggers a cellular response leading to apoptosis or growth arrest. One of the principal executioners of DNA damage responses is p53. HCT116, U2OS and MCF-7 cells contain wild type p53. To explore if the resistance to cell death was dependent on p53, we used p53-null HCT116 cells and MEFs. p53 -/- MEFs were cultured at both oxygen concentrations and exposed to different concentrations of doxorubicin. PI staining followed by FACS analysis was used to assess percentage cell death. As shown in figure 3.5, no differences in cell death could be observed between the cells cultured at 5% and 20% O_2, regardless of the concentration of doxorubicin used (Figure 3.5).

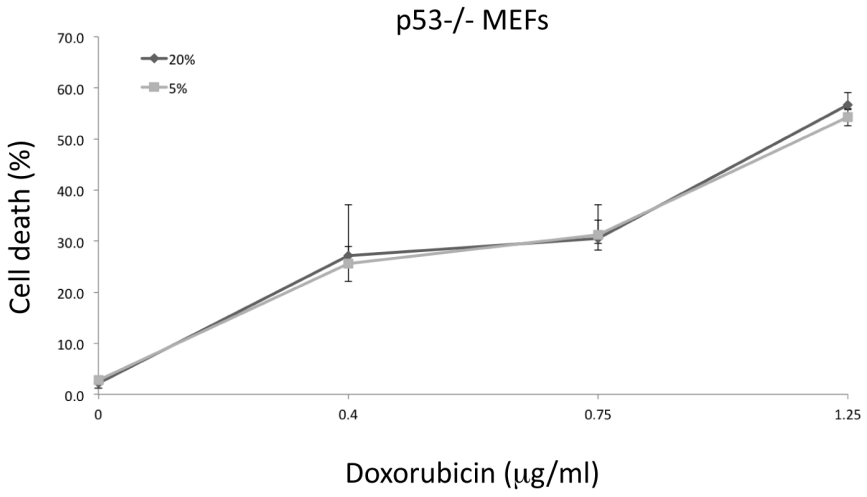

Figure 3.5 Resistance at 5% O_2 is not observed in p53-/- MEFs. Control cells and cells treated with doxorubicin were cultured at 20% and 5% O_2. No differences in cell death were observed for any of the concentrations used between the two oxygen tensions after PI staining and FACS analysis.

HCT116 cells with p53 knocked-out by homologous recombination were used to confirm the results observed with the MEFs. Cells were treated with 0.4 μg/ml of doxorubicin and cultured at both oxygen concentrations. As seen in figure 3.6, there is no difference between the percentages of cell death at physiological oxygen concentrations, compared with atmospheric oxygen concentrations. These results suggest that p53-independent cell death is not affected by changes in oxygen tensions.

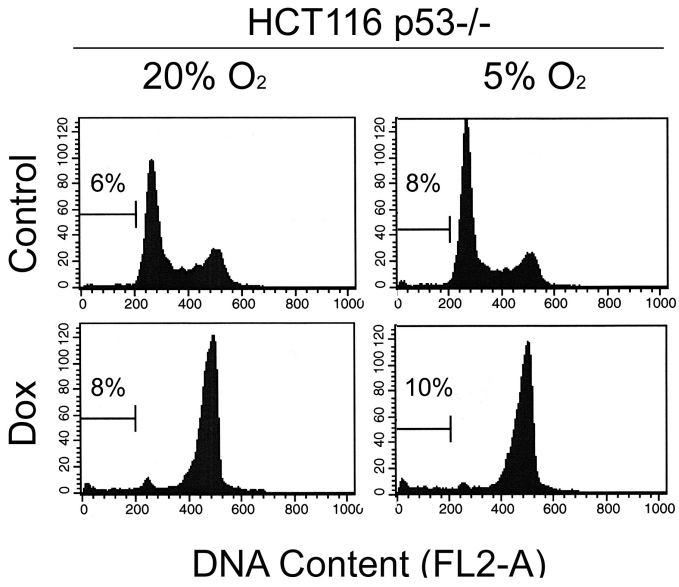

Figure 3.6 No difference in resistance in HCT116 p53 null cells at 5% O_2. HCT116 p53-/- cells were treated with 0.4 μg/ml doxorubicin and placed in the 20% or 5% O_2 incubator, percentage cell death was assessed by PI staining followed by FACS analysis. No differences can be observed in the percentage of cells in sub G1 phase between the two oxygen concentrations.

3.2.1 p53 expression

The resistance observed in cells cultured at physiological oxygen tensions appears to be p53-dependent. To explore the possibility that variations in p53 protein levels are responsible for the resistance at 5% O_2, lysates were obtained from HCT116 cells cultured at both oxygen concentrations and treated with doxorubicin. Results show that the protein levels of p53 increase after treatment with doxorubicin (as expected) but they were similar in cells cultured in both conditions (Figure 3.7).

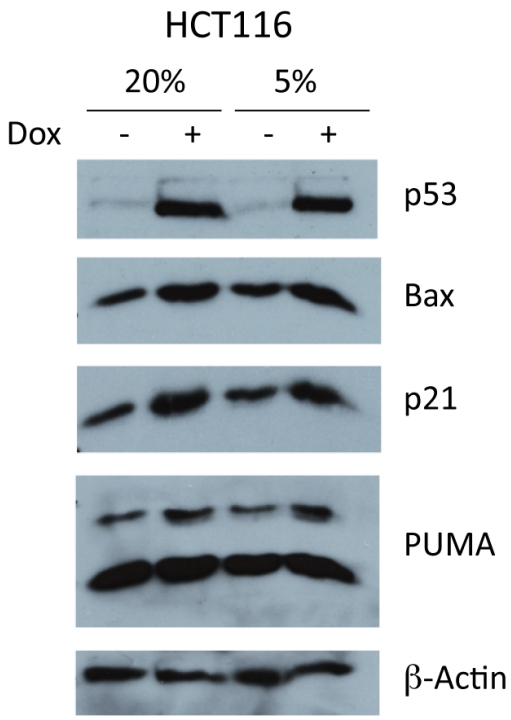

Figure 3.7 p53 protein levels are similar at physiological and atmospheric oxygen tensions. HCT116 cells were cultured at 20% and 5% O_2 and treated with (0.4μg/ml) or without doxorubicin. Western blot showing protein levels of p53 and p53 target genes (p21, Bax and PUMA), β-actin was used as a loading control. No difference can be observed in the levels of the proteins when comparing between the two oxygen concentrations.

Part of p53 function is activating the transcription of pro-apoptotic genes. To explore the possibility of changes in p53 activity at low oxygen concentrations, the protein levels of p53 target genes were assessed by western blotting. As seen in figure 3.7, the levels p21, Bax and PUMA rise after treatment with doxorubicin in a similar way at both oxygen concentrations. These results suggest that transcriptional activity of p53 is conserved at 5% O_2. Therefore, we conclude that the resistance to doxorubicin-induced apoptosis observed is not due to reduced p53 levels or transactivation activity at low oxygen concentrations.

3.3 Oxidative damage

It has been previously observed that MEFs proliferate for longer at physiological oxygen concentrations because they accumulate less oxidative damage than cells cultured at atmospheric oxygen tensions (Parrinello et al., 2003). Doxorubicin is a drug commonly used in chemotherapy that causes cell death partially by inducing ROS, which creates oxidative damage. In order to see if the difference in cell death observed between cells cultured at 5% O_2 compared to 20% O_2 was due to increased oxidative damage in response to doxorubicin at higher oxygen concentrations, we performed a comet assay. This assay, also known as single-cell electrophoresis, allows us to determine the DNA damage caused by oxidation.

Cells were grown at 20% and 5% O_2 and treated with 1μg/ml of doxorubicin, mixed with low melting point agarose and put on slides. They were lysated to expose their DNA and treated with Fpg to excise altered bases and nick the DNA backbone. Finally, electrophoresis was performed to separate the DNA. Damaged DNA, containing strand breaks migrates farther in the gel than intact DNA. As positive controls for oxidation damage, HCT116 cells treated with H_2O_2 that causes oxidative damage to the DNA of the cells and can be detected by the Fpg enzyme.

As show in figure 3.8, no difference was observed in oxidative DNA damage in cells cultured at 5% or 20% O_2. Cells treated with doxorubicin exhibited an increased

amount of oxidative damage compared to non-treated cells, as expected. The oxidative damage accumulated after treatment with doxorubicin was similar at both oxygen concentrations. This result suggests that the resistance to doxorubicin-induced cell death observed by FACS is not due to less oxidative damage in reduced oxygen conditions.

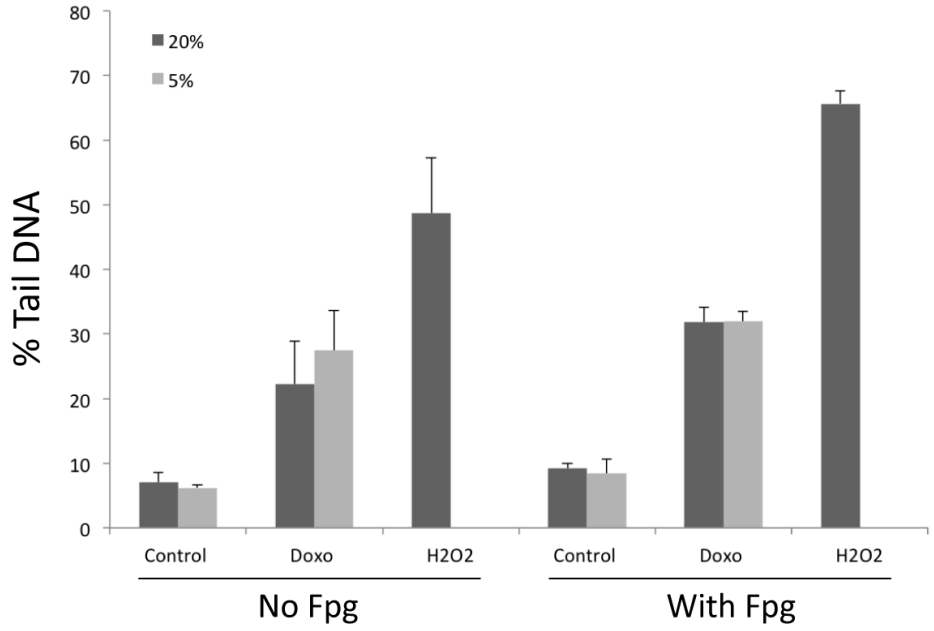

Figure 3.8 Levels of DNA damage caused by oxidation are similar at physiological and atmospheric oxygen tensions. Comet assay using HCT116 cells cultured at 20% and 5% O_2 and treated with doxorubicin (1μg/ml). Experiments were performed in the absence or presence of Fpg enzyme to determine DNA damage due to oxidation.

3.4 Caspase activity at 5% O_2

The ultimate effectors of apoptosis are the caspases, which orchestrate the dismantling and clearance of the apoptotic cell. To see if the activation of the caspases was affected by low oxygen concentrations, we performed a caspase assay. Caspase-3, caspase-6 and caspase-7 are effector caspases and they are responsible for carrying out the proteolysis seen during the demolition phase of apoptosis. The activity of caspase 3/7 was measured in HCT116 cells that were treated with doxorubicin and cultured at 20% and 5% O_2. As seen in figure 3.9, a decrease in caspase activity can be observed in cells cultured at physiological oxygen tensions compared to the ones cultured at atmospheric oxygen concentrations. This can be observed with all concentrations of doxorubicin used.

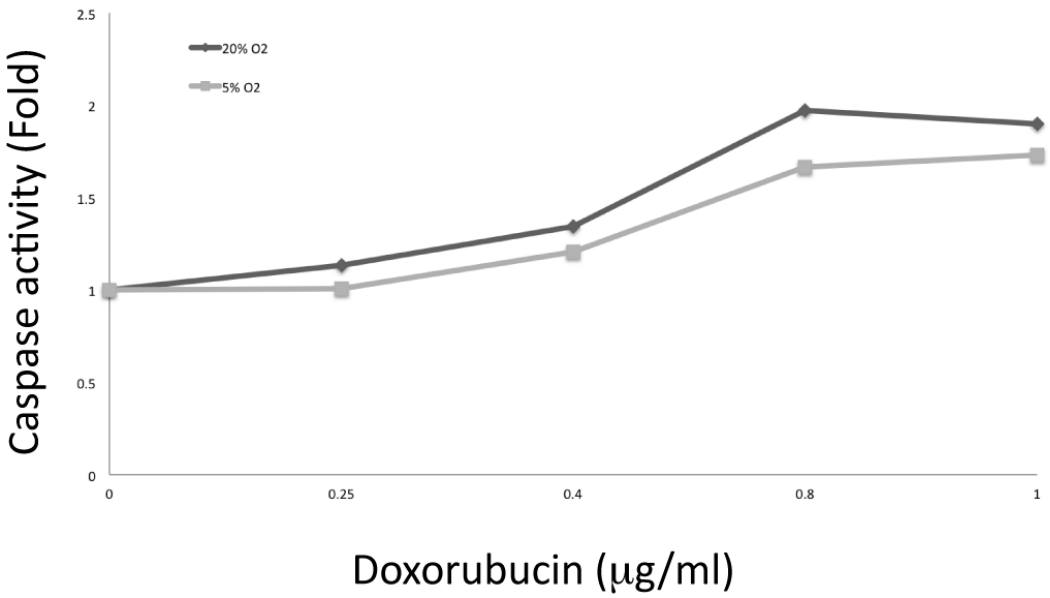

Figure 3.9 Caspase activation at physiological oxygen tensions. HCT116 were treated with 0, 0.25, 0.4, 0.8 and 1 µg/ml of doxorubicin and cultured at 20% or 5% O_2 for 24 hours. Caspase assay substrate was added to the cells and they were incubated for 1 hour at 37°C, light intensity was measured in a plate reader. Results show a small decrease of caspase activity at 5% O_2.

Caspase 8 is an initiator caspase that is part of the extrinsic pathway of apoptosis. Upon recruitment to the death-inducing signalling complex (DISC) it gets cleaved and activated. Activated caspase 8 cleaves and activates effector caspases 3/7. An antibody against caspase 8 was used to check if this caspase was also less active at physiological oxygen concentrations. HCT116 cells were treated with 0.4 µg/ml of doxorubicin and cultured at 20% and 5% O_2. A decrease in cleaved caspase 8 could be observed in cells cultured at physiological compared to atmospheric oxygen tensions after treatment with doxorubicin (Figure 3.10). These results suggest there is less caspase activity at physiological oxygen tensions, which would explain the resistance to apoptosis observed after doxorubicin treatment (Figure 3.1).

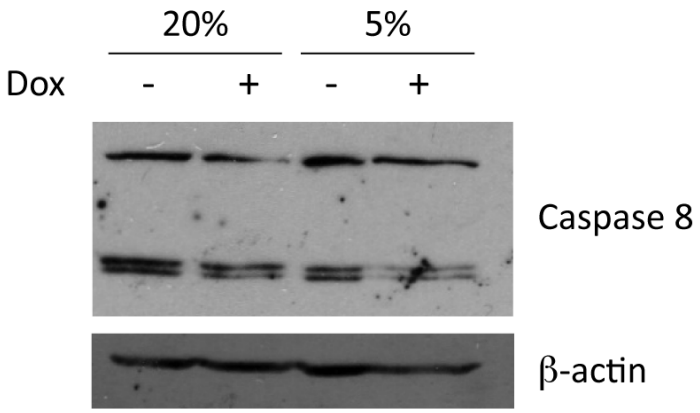

Figure 3.10 Variation of caspase 8 levels at 5% O_2. Western blot showing lysates from HCT116 cells treated with 0.4 μg/ml and cultured at 20% or 5% O_2. A small decrease could be observed in the cleavage of caspase 8 in cells at physiological oxygen concentrations compared to atmospheric oxygen tensions.

3.5 Activation of MAPK at physiological oxygen tensions

MAPK coordinates a wide variety of cellular activities; ERK1/2 promotes cell proliferation by up regulating genes involved in cell growth and down regulating anti-proliferative genes. Our colony formation assays (figure 3.4) showed that cells cultured at 5% O_2 were more likely to survive and proliferate, indicating a possible role for pro-survival pathways. An increase in the levels of phosphorylation of MAPK has been seen after treatment with γ radiation (Lee et al., 2000), suggesting activation of pro-survival pathways in response to DNA damage in the presence of p53. In this part of the project we wanted to explore the activation of MAPK after damage at physiological oxygen tensions. U0126 is a chemical inhibitor of MEK 1/2, which works by blocking its enzymatic activity and thus preventing the phosphorylation and activation of ERK 1/2 (Favata et al., 1998) and was used here to explore the role of MAPK in the cellular responses to damage at 5% O_2.

To investigate a possible increase in phosphorylation of ERK1/2 at physiological oxygen levels, HCT116 cells were cultured at 20% or 5% O_2 and treated with doxorubicin (0.4 μg/ml) and U0126 (1.75μM). Results show there is an increase in the phosphorylation levels of ERK1/2 when cells are cultured at physiological oxygen levels, even in the absence of damage (Figure 3.11). In cells treated with doxorubicin, an increase in phosphorylation can also be observed at both 5% and 20% O_2, as expected. The

increase in the phosphorylation in MAPK can be blocked with the use of the MEK inhibitor U0126, as expected.

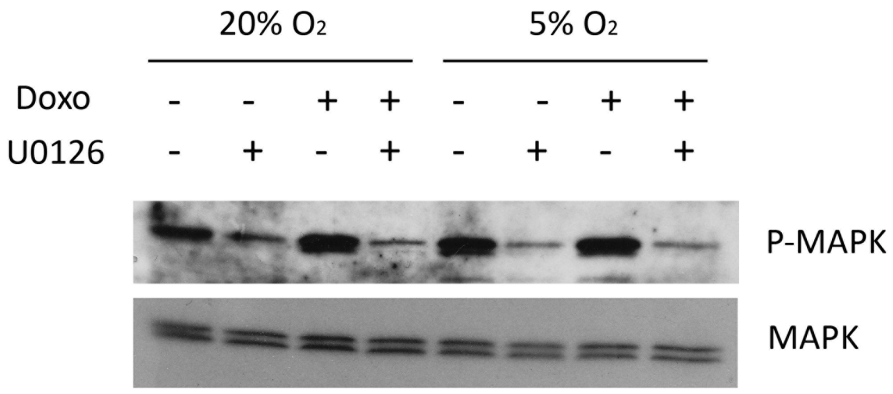

Figure 3.11 Increase in the phosphorylation levels of MAPK at physiological oxygen tensions. HCT116 cells cultured at 20% and 5% O_2 and treated with 0.4 μg/ml of Doxorubicin and 5μM of U0126. Western blot showing phosphorylated MAPK; the levels of endogenous MAPK were used as a loading control. Levels of phosphorylation increase in cells cultured at 5% O_2.

U2OS cells were used to confirm these observations in another cell line. U2OS cells were treated with 5μM of U0126 and 0.4 μg/ml of doxorubicin and cultured at 20% or 5% O_2. Similar results to the ones observed with HCT116 were observed in U2OS cells (Figure 3.12): the levels of phosphorylation of MAPK increase at 5% O_2 and in cells exposed to doxorubicin. It was also possible to block this activation with the use of U0126.

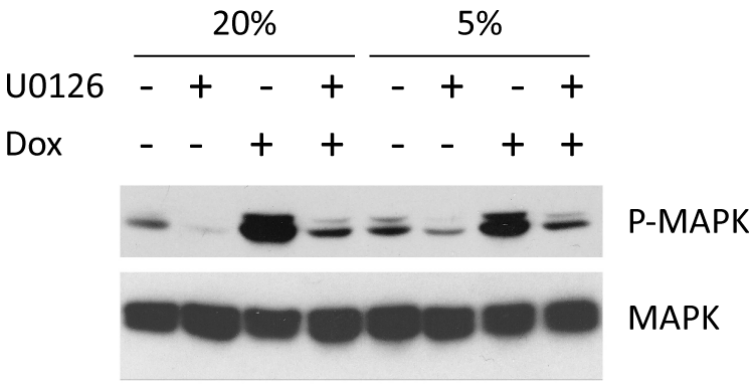

Figure 3.12 Increase in MAPK activation in U2OS cells at physiological oxygen tensions. Western blot showing an increase in MAPK phosphorylation in U2OS cells that were cultured at 5% and 20% O_2 and treated with doxorubicin (0.4µg/ml) and U0126 (5µM).

To check if the activation of MAPK was transient, HCT116 cells were cultured at 5% O_2 for up to a period of 5 days. As shown in figure 3.13, the phosphorylation of MAPK increases after 1 day of being cultured at 5% O_2, and it appears to be sustained over a period of at least 5 days.

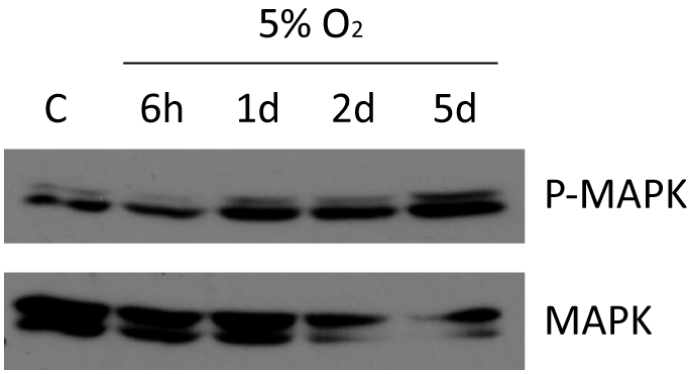

Figure 3.13 Sustained activation of MAPK at physiological O_2 tensions. Western blot showing protein lysates of HCT116 cells incubated at 5% O_2 for 6h, 1 day, 2 days and 5 days. First lane shows the control (C), lysate from cells cultured at 20% O_2. The levels of phosphorylation increase after day 1.

3.5.1 Role of MAPK in the survival at 5%

The results obtained by colony formation assay showed an increase in colony number in HCT116 cells cultured under physiological oxygen conditions (Figure 3.4). To explore the possibility that the activation of MAPK is responsible for making cells survive better at physiological oxygen tensions, HCT116 were treated with MEK inhibitor U0126 (1.25µM) and cultured at 20% and 5% O_2. As observed in figure 3.14, there is a reduction in colony number at 5% O_2 after the inhibition of MEK. A reduction in colony size was also observed after inhibition of MEK. These results suggest that the activation of the MAPK pathway at physiological oxygen tensions can have an effect on cell proliferation and survival.

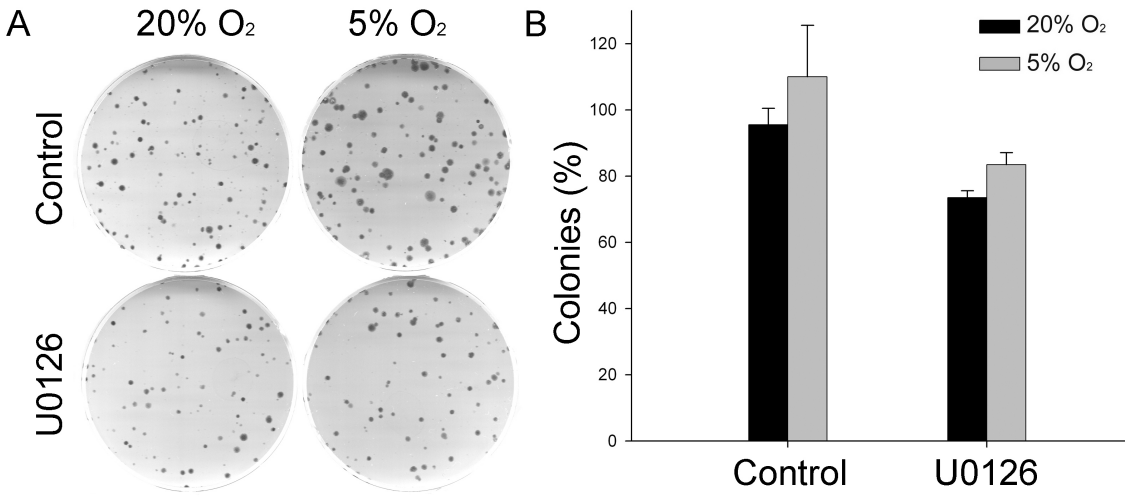

Figure 3.14 MAPK inhibition and colony formation. A. 1000 HCT116 cells were seeded in each plate and treated with 1.25 µM of U0126 and cultured at 5% O_2 or 20% O_2 for 14 days. After treatment with the MEK inhibitor U0126 the colonies formed by HCT116 cells cultured at 5% O_2 are similar in size and number to the ones at 20% O_2. B. Graph representing average number of colonies from three independent experiments in plates cultured at 20% (black bars) and 5% O_2 (grey bars) (as shown in A).

3.6 Effect of MAPK on the resistance to apoptosis

As an activation of MAPK signalling could be observed at 5% O_2, we wanted to explore the possibility that MAPK was responsible for the resistance to cell death observed. U0126 was used to inhibit the activation of ERK 1/2 at 5% O_2 and to explore the effect of this inhibition in the resistance to cell death. HCT116 cells were treated with 2.5µM of U0126 and 0.4 µg/ml of doxorubicin and cultured at 5% or 20% O_2. Percentage of cell death was determined by Annexin-V staining and FACS analysis. As shown previously, resistance could be observed in cells cultured at 5% O_2 and treated with doxorubicin with a 20% reduction in cell death under these conditions (Figure 3.15). No differences in percentage of cell death could be observed when cells were treated with U0126 only. As shown in figure 3.15, when HCT116 cells are treated with a combination of U0126 and doxorubicin, the resistance to apoptosis at 5% O_2 is lost and similar percentages of apoptosis could be observed with the two oxygen concentrations (63% vs. 60%). This result suggests that activation of MAPK is responsible for the resistance of HCT116 cells to apoptosis at 5% O_2.

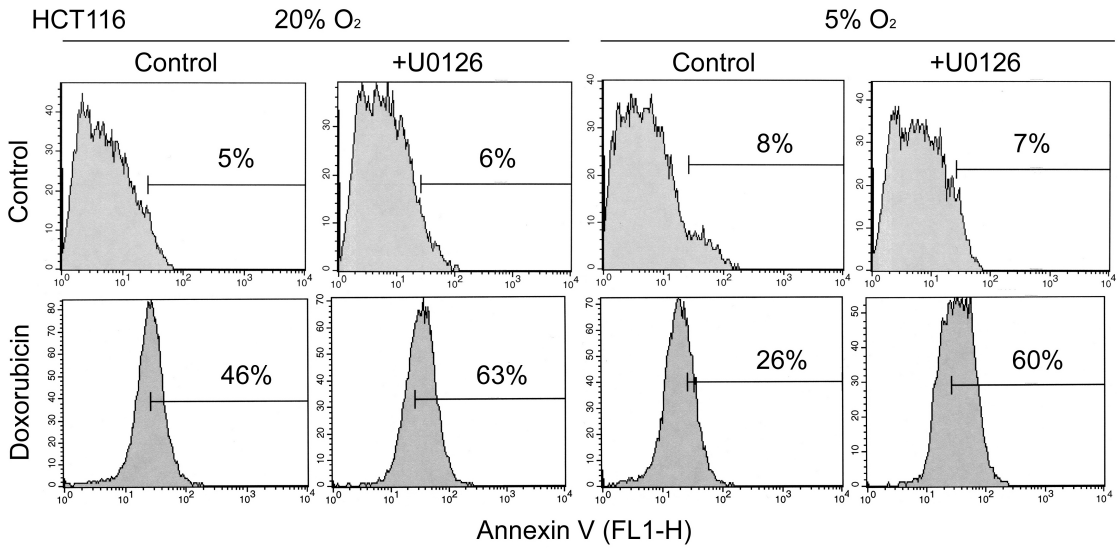

Figure 3.15 MAPK inhibition and resistance to apoptosis. HCT116 cells were culture at 20% and 5% O_2 and treated with 2.5µM U0126 and 0.4 µg/ml of doxorubicin for 48 hours before PI staining and FACS analysis. A reduction of the resistance to cell death could be observed in cells treated with doxorubicin and U0126 and cultured at 5% O_2 compared to the ones only treated with doxorubicin and cultured under the same conditions.

U2OS cells were used to confirm this results with another cell line. U2OS cells were treated with 0.25 µg/ml of doxorubicin and 5 µM U0126 and cultured at 20% or 5% O_2. The percentage of cell death was assessed by PI staining and FACS analysis. As seen in figure 3.16, inhibition of MAPK was not sufficient to restore cell death in U2OS cells cultured at 5% O_2. Although, a small increase in cell death can be observed after the treatment with U0126. This result suggests that the involvement of MAPK in the resistance to apoptosis may be tissue-specific, but further experiments are needed to elucidate this. These results could also be explained by an incomplete down-regulation of MAPK in U2OS cells (Figure 3.12).

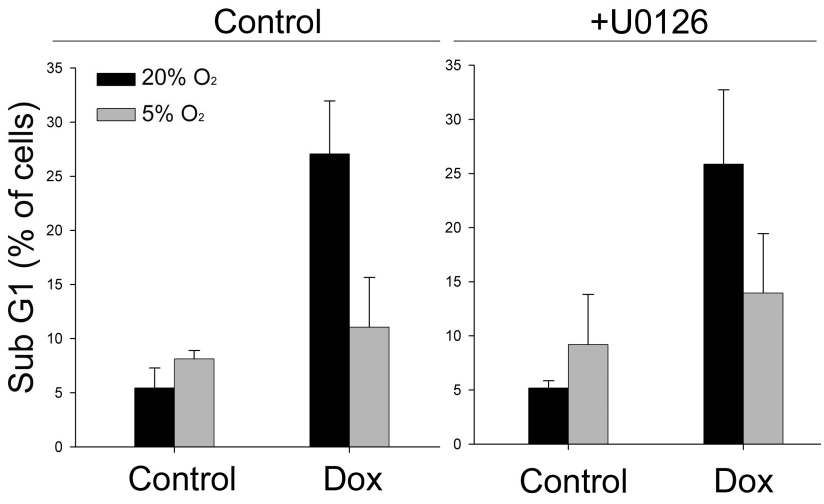

Figure 3.16 Inhibition of MAPK activation in U2OS cells. U2OS cells were cultured at 20% and 5% O_2 and treated with 0.25 µg/ml of Doxorubicin and 5µM U0126. Inhibition of MEK by U0126 does not restore the sensitivity of U2OS cells to doxorubicin-induced apoptosis at 5% O_2.

3.6.1 MEK 1/2 siRNA

As mentioned before, U0126 is a chemical compound that inhibits the enzymatic activity of MEK; another alternative for blocking MEK activity is the use of small interference RNA. A siRNA against MEK 1 and MEK 2 was used to corroborate that activation of MAPK was responsible for the resistance to apoptosis at physiological oxygen tensions.

The first experiment was to check that phosphorylation of MAPK could be inhibited by blocking MEK 1 and 2. HCT116 cells were transfected with 100nM of siRNA and treated with 0.25 µg/ml of doxorubicin. After 24 hours, protein lysates were collected and a western blot was run to confirm downregulation of ERK 1/2 phosphorylation. As

observed in figure 3.17, the siRNA was able to partially reduce the phosphorylation of MAPK in control cells and in cells treated with doxorubicin.

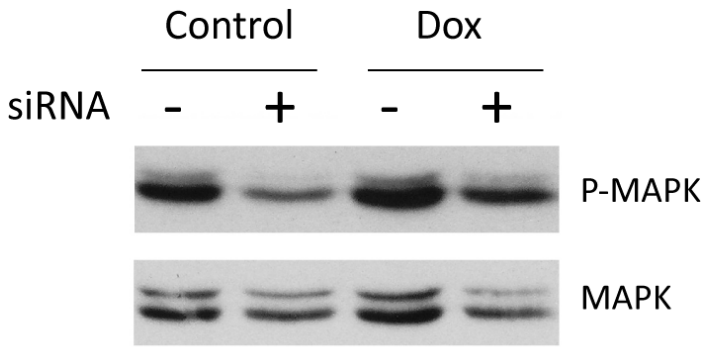

Figure 3.17 Inhibition of P-MAPK by siRNA. Western blot showing the levels of P-MAPK in HCT116 cells transfected with 100nM siRNA against MEK 1/2 and treated with doxorubicin (0.25 μg/ml). Levels of MAPK were used as a loading control. Partial reduction of the phosphorylation of MAPK can be observed.

The next step was to block MAPK activation with the use of the siRNA and test the effect on doxorubicin-induced apoptosis. HCT116 cells were transfected with siRNA against MEK 1/2 and cultured at 20% or 5% O_2. Cell death was assessed by PI staining and FACS analysis. It can be observed in figure 3.18 that HCT116 cultured at 5% O_2 show a reduction in cell death after being treated with doxorubicin, in accordance to our previous observations. In cells transfected with the siRNA, a slight increase in the levels of apoptosis can be observed. This may be due to the fact that MAPK activity influences survival and inhibiting it can increase apoptosis. When cells are transfected with MEK siRNA, a loss of the resistance to apoptosis at 5% O_2 after treatment with doxorubicin can be observed. The percentage of cell death at both oxygen concentrations is similar when MEK is knocked down. These results suggest that the

MAPK pathway is responsible for the resistance to doxorubicin-induced cell death observed at physiological oxygen concentrations.

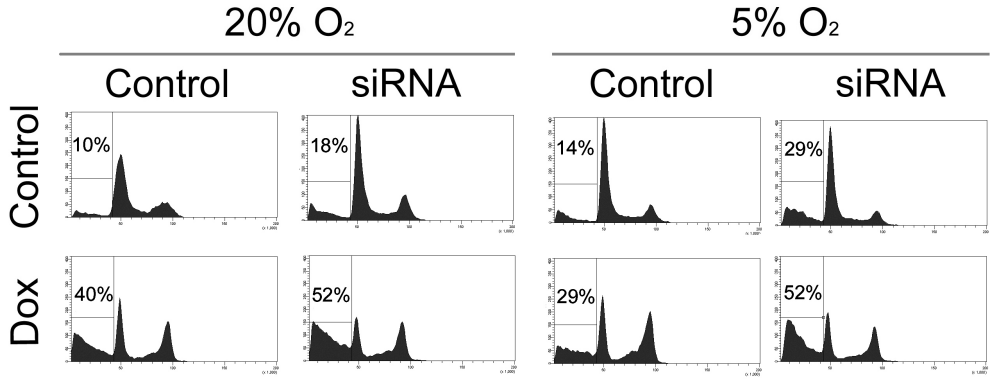

Figure 3.18 MEK siRNA and loss of the resistance to apoptosis. PI stain and FACS analysis of HCT116 cells (at 20% and 5% O_2) transfected with 100nM of MEK 1/2 siRNA and treated with 0.25 μg/ml of doxorubicin. It can be observed that the doxorubicin-induced cell death at 5% O_2 and 20% O_2 is similar after inhibition of MEK.

3.6.2 Inhibition of MAPK does not affect the levels of p53 protein

From the beginning our results showed that the resistance to apoptosis at physiological oxygen tensions was dependent on p53, as cells lacking p53 did not show differences in cell death between the two oxygen concentrations (Figures 3.5 and 3.6). We were not able to see any differences in the levels of p53 protein or its target genes that could explain the resistance to apoptosis (Figure 3.7). To make sure that the levels of p53 were not affected by the inhibition of MAPK, MCF-7 cells were treated with U0126 and doxorubicin and cultured at 20% or 5% O_2. Lysates were collected 24 hours after treatment and protein levels were assessed by western blotting. As shown in figure 3.19, levels of p53 rise after treatment with doxorubicin equally at both oxygen

concentrations, as observed before. No difference in p53 levels could be observed when these cells were treated with U0126. This result confirms that the inhibition of MAPK does not have an effect in the levels of p53 and that the loss of resistance to apoptosis is not due to an increase in p53.

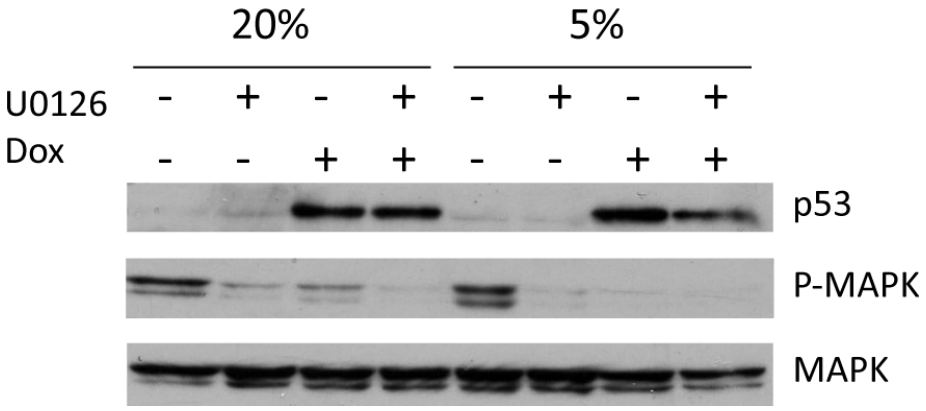

Figure 3.19 Levels of p53 after inhibition of MAPK. Western blot showing MCF-7 cells treated with 4μM U0126 and 0.4 μg/ml of doxorubicin and cultured at 20% or 5% O_2. Levels of p53 increase after treatment with doxorubicin in a similar way at both oxygen concentrations. Inhibition of MAPK does not affect the levels of p53.

Chapter 4. Involvement of HIF-1α in the effects of physiologic oxygen tensions on cell growth and DNA damage responses

HIF-1 is the main regulator of the responses to low oxygen concentrations in mammalian cells. The levels of HIF-1 protein are dependent on the availability of the HIF-1α subunit, which is mainly regulated by oxygen levels. This regulation is controlled by PDHs enzymes that hydroxylate the subunit when high oxygen levels are present, allowing it to be recognized by pVHL and target for degradation in the proteasome. PHD enzymes have a high Km for oxygen, which means that the enzyme needs high substrate concentrations in order to achieve maximum reaction velocity. Physiological oxygen concentrations are below the Km values of PHDs. This ensures that PHD activity is sensitive to small fluctuations in O_2 concentrations and suggests the possibility of HIF-1 being expressed at this condition (Ehrismann et al., 2007). It has been shown that subtle changes in the oxygen concentration can have a great effect on the levels of the protein (Jiang et al., 1996). The persistence of basal levels of HIF-1α protein, like the ones present at physiological oxygen tensions, may have important implications for normal physiological functions, but this possibility has not been extensively explored yet.

4.1 HIF-1α at physiological oxygen tensions

The first objective was to confirm if 5% O_2 was an oxygen concentration sufficiently low to prevent hydroxylation of HIF-1α and its further degradation. In order to see if HIF-1α was expressed at physiological oxygen concentrations, western blotting was used to assess the protein levels. HCT116 cells were treated with 0.4 μg/ml of doxorubicin and then cultured at 20% and 5% O_2 for 24 hours. Protein lysates were collected and a western blot was used to determine the levels of HIF-1α protein. As shown in figure 4.1, HIF-1α protein could be observed in cells cultured at 5% O_2 (Figure 4.1). This result suggests that 5% O_2 is sufficiently low to allow the expression of HIF-1α, although the levels are lower compared to those observed in hypoxia consistent with previous reports (Jiang et al., 1996).

In the cells treated with doxorubicin a reduction in the levels of HIF-1α can be observed. It has been previously observed that doxorubicin (and other anthracycline antibiotics) can interfere with the activity of HIF-1 by interfering with its binding to DNA (Lee et al., 2009). However, we also observe a decrease in the protein levels suggesting that doxorubicin may also be affecting the stability of the protein at physiological oxygen tensions.

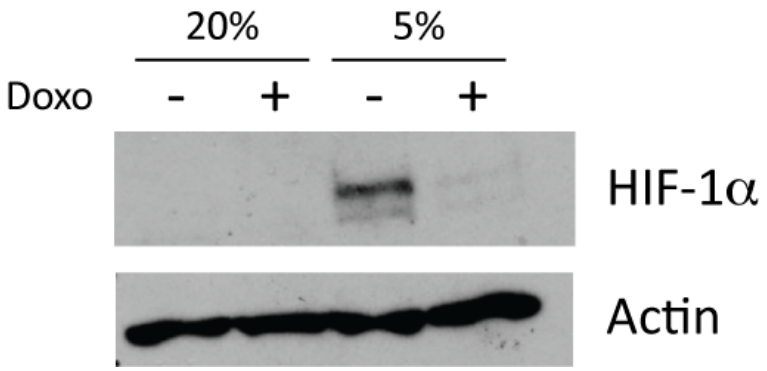

Figure 4.1 Physiological oxygen tensions are sufficient for an increase in HIF-1α protein levels. Western blot showing the levels of HIF-1α and Actin (loading control), HCT116 cells were treated with 0.4 μg/ml of doxorubicin and cultured at 20% or 5% O_2 for 24 hours. An increase in the levels of HIF-1α could be observed at 5% O_2.

4.1.1 HIF-1α and p53

HIF-1α has been shown to interact with p53 (An et al., 1998), although there is still a great controversy in the nature of the association between HIF-1 and p53 (Ravi et al., 2000; Blagosklonny et al., 1998). HCT116 cells lacking p53 was used to investigate if p53 was required for the expression of HIF-1α at physiological oxygen tensions. HCT116 p53 -/- cells were treated with 0.4 μg/ml of doxorubicin and cultured at 20% or 5% O_2. Protein lysates were collected and the levels of HIF-1α were assessed by western blot. As seen on figure 4.2, the levels of HIF-1α increase in cells lacking p53 and being cultured at physiological oxygen levels. From this experiment we can conclude that p53 is not necessary for stabilizing HIF-1α at 5% O_2.

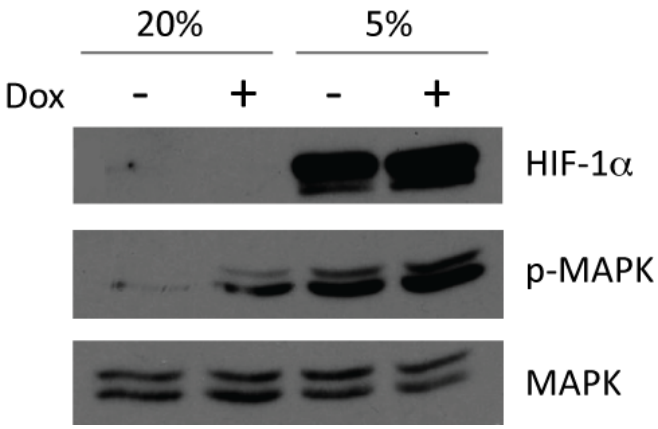

Figure 4.2 HIF-1α is present at 5% O_2 in cells lacking p53. HCT116 p53 -/- cells were treated with doxorubicin and cultured at 20% or 5% O_2. The presence of HIF-1α can be observed in the cells cultured at physiological oxygen tensions, regardless of lack of p53.

4.2 HIF-1 activity at physiological oxygen tensions

HIF-1 binds to specific sequences within target genes, known as hypoxia responsive elements (HREs). HIF-1 functions as a DNA-binding transcription factor that activates at least 100-200 genes that promote adaptation and survival under low O_2 concentrations; these include the erythropoietin (EPO) gene (Jiang et al., 1996a), the vascular endothelial growth factor (VEGF) genes (Carmeliet et al., 1998), and also other genes encoding glycolytic enzymes. The activation of these genes by HIF-1 can have major implications for growing tumours, because they can lead to survival and proliferation by mediating angiogenesis (Liao et al., 2007; Hiraga et al., 2007) and promoting an aggressive tumour phenotype (Hockel et al., 1996; Generali et al., 2006).

To test if HIF-1α was active at 5% O_2 and the protein levels observed were sufficient to activate HREs we used a PGK-1 reporter plasmid that contains trimers of the HREs of the PGK-1 gene in the pGL3 Promoter vector which contains the SV40 promoter (without the SV40 enhancer) upstream of the firefly LUC gene (Ameri et al., 2002). HCT116 cells were cultured at 20% and 5% O_2 and transfected with the reporter plasmid and a β-galactosidase plasmid as a control for transfection. Cells were treated with doxorubicin (0.4 μg/ml) and the luciferase activity was measured in a plate reader. Luciferase activity was normalized to β-galactosidase activity. As seen in figure 4.3, there is an increase in the activity of the vector at 5% O_2. In cells treated with doxorubicin, a reduction could be observed in the activity of the reporter at 5% O_2

compared to the control (Figure 4.3); this correlates with a reduction in the protein levels after doxorubicin treatment observed by western blotting (Figure 4.1). We can conclude that the levels of HIF-1α present at physiological oxygen tensions are sufficient to activate the reporter, suggesting that HIF-1 transactivation function is present at these conditions.

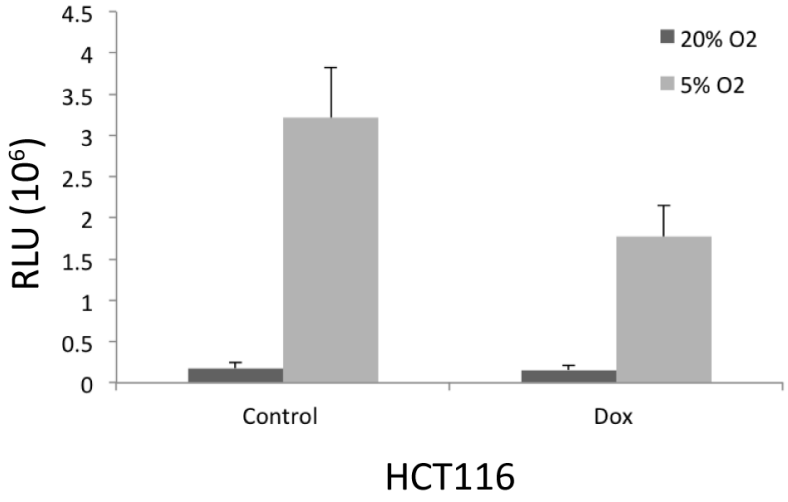

Figure 4.3 HIF-1 activity at physiological oxygen tensions. HCT116 were transfected with the PGK-1 luciferase reporter plasmid and the β-galactosidase plasmid. Cells were treated with 0.4 μg/ml of doxorubicin and cultured at 20% or 5% O_2 for 24 hours. β-galactosidase activity was used to normalize luciferase activity. An increase in the reporter activity can be observed in cells cultured at 5% O_2, there is only a moderate increase in activity in cells treated with doxorubicin at physiological oxygen tensions.

The levels of mRNA of HIF-1 targets genes were assessed to confirm the results observed with the luciferase assay. HCT116 cells were cultured at 20% or 5% O_2 for 24 hours and total RNA was isolated. RNA isolated from HCT116 cells treated with Deferoxamine (DFX), an iron chelator, was used as a positive control for HIF-1 activation. cDNA was prepared from the RNA and levels of mRNA of PGK-1 and Glut-1

were assessed by qPCR. As observed in figure 4.4, there is a 2-fold increase in the levels of PGK-1 and a 3-fold increase in the levels of Glut-1 in cells cultured at physiological oxygen tensions. This result suggests that the levels of HIF-1 at physiological oxygen tensions are sufficient to activate transcription of its target genes and confirms the results observed with the luciferase reporter.

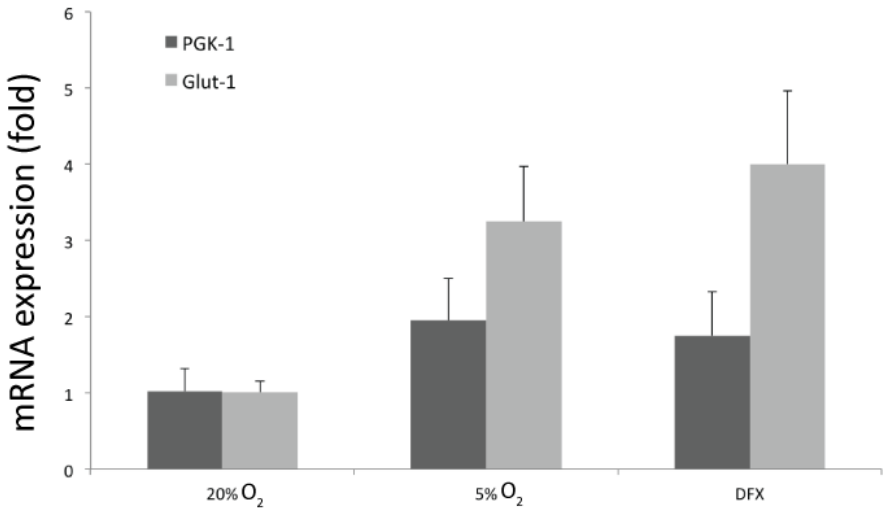

Figure 4.4 mRNA levels of HIF-1 target genes increase at 5% O_2. qRT-PCR showing mRNA levels of PGK-1 and Glut-1 from HCT116 cells cultured at 20% and 5% O_2 for 24 hours. RNA from HCT116 cells treated with DFX for 24 hours was used as a positive control. An increase in the levels of both mRNAs can be observed in cells cultured at physiological oxygen tensions.

4.3 HIF-1 and MAPK

A link between the MAPK and HIF-1 pathways has been suggested. ERK1/2 is able to phosphorylate HIF-1α (Richard et al., 1999) and it has been shown that it enhances HIF-1 activity without affecting HIF-1α expression (Sutton et al., 2007). MAPK may have an effect on the interaction of HIF-1α with p300, an interaction that is required for the transactivation activity of HIF-1 (Sang et al., 2003). MAPK as well as HIF-1 are proteins that activate a series of pro-survival signals. As previous observations (chapter 3) had shown an increase in the activation of MAPK at physiological oxygen tensions, we wanted to explore the effect that these two proteins have on each other.

4.3.1 Effect of HIF-1 on MAPK expression

It has been previously reported that HIF-1 may have an effect on the induction of MAPK during hypoxia and after stimulation with growth factors (Ren et al., 2010). The chemical inhibitor of HIF-1α, YC-1 (Yeo et al., 2003), was used to block the levels of HIF-1α. YC-1 was used to explore the possibility that HIF-1 is responsible for the activation of MAPK at physiological oxygen tensions. HCT116 cells were treated with 40μM of YC-1 and 0.4 μg/ml of doxorubicin and cultured at 20% or 5% O_2. HCT116 cells treated with 500μM of $CoCl_2$ were used as a positive control for HIF-1α. As observed in figure 4.5, YC-1 is able to effectively reduce the levels of HIF-1α. The inhibition of HIF-1α by YC-1 does not have an effect on the levels of phosphorylation of MAPK at physiological oxygen tensions.

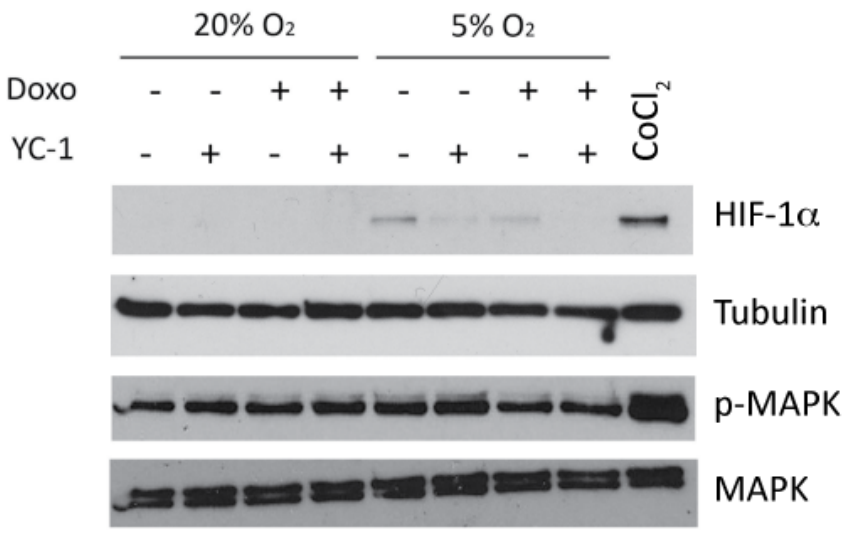

Figure 4.5 Chemical inhibition of HIF-1α does not have an effect on the phosphorylation of MAPK. HCT116 cells were treated with 40μM YC-1 and 0.4 μg/ml of doxorubicin and cultured at 20% or 5% O_2. Cells treated with $CoCl_2$ were used as a positive control for HIF-1α. Lysates were collected and a western blot was run to assess the protein levels of HIF-1α, tubulin, p-MAPK and MAPK. The results show that inhibition of HIF-1α does not have an effect on the phosphorylation levels of MAPK.

An siRNA against HIF-1α was used to confirm the results observed with YC-1. The siRNA was used to explore the influence of HIF-1 on the levels of p-MAPK. HCT116 cells were transfected with 200pmol of siRNA, treated with 0.4 μg/ml of doxorubicin and cultured at 20% or 5% O_2. Protein lysates were collected and a western blot was run to assess the levels of HIF-1α, p53, p-MAPK and MAPK. A reduction in the protein levels of HIF-1α can be observed when the siRNA was used (Figure 4.6). The levels of p53 and p-MAPK seem unaffected by the inhibition of HIF-1α. This suggests that, although HIF-1 is expressed at 5% O_2, it is not responsible for the activation of the MAPK pathway at physiological oxygen concentrations.

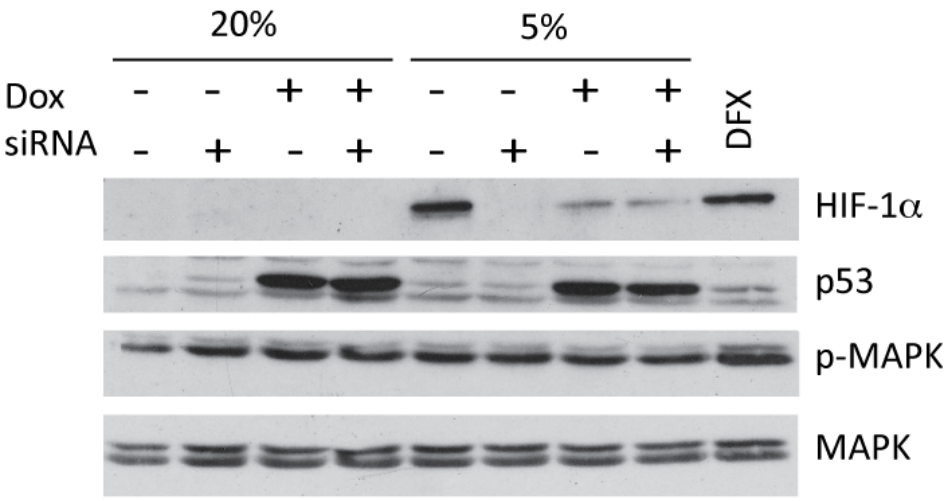

Figure 4.6 Inhibition of HIF-1α has no effect on the phosphorylation of MAPK. Western blot showing the levels of HIF-1α, p53, P-MAPK and MAPK in HCT116 cells transfected with 200pmol of siRNA against HIF-1α and treated with doxorubicin (0.4μg/ml). A reduction in the protein levels of HIF-1α can be observed after the use of the siRNA but this has no effect on the levels of p-MAPK.

To corroborate that the siRNA was able to reduce the levels of HIF-1 activity, the PGK-1 luciferase reporter was used. HCT116 cells were transfected with 50pmol of HIF-1α siRNA or treated with 0.4 μg/ml of doxorubicin and cultured at 20% or 5% O_2. As previously observed in figure 4.3, the levels of the reporter increase when cells are cultured at 5% O_2. The increase of the reporter activity at physiological oxygen tension is inhibited by HIF-1α siRNA (figure 4.7). It can be seen that the activity of the reporter is decreasing when cells are treated with doxorubicin and the levels look similar to the levels of the knock down. This suggests that doxorubicin is interfering with HIF-1.

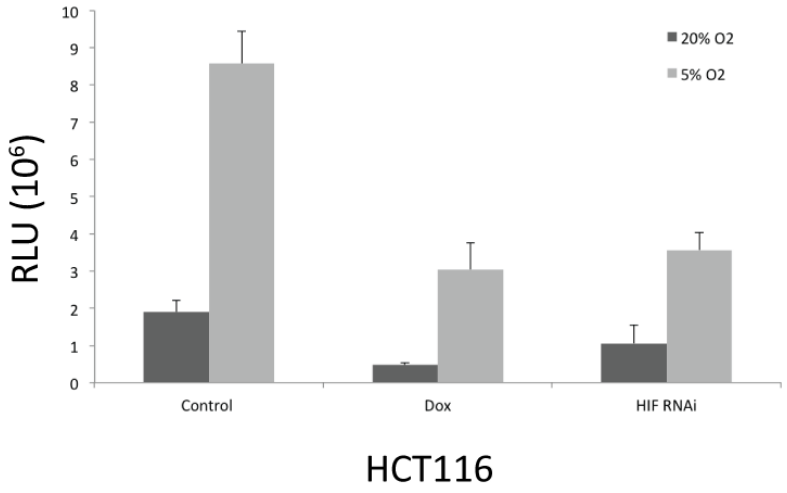

Figure 4.7 Inhibiton of HIF-1α by siRNA. Luciferase assay showing the activity of a PGK-1 reporter in HCT116 cells transfected with 50pmol of HIF-1α siRNA and treated with 0.4 μg/ml of doxorubicin. Cells were cultured at 20% or 5% O_2 for 24 hours. An inhibition of the reporter activity can be observed with the use of the siRNA.

4.3.2 Effect of MAPK on HIF expression/activity

Previous reports suggest that MAPK can phosphorylate HIF-1α and activate HIF-1 promoting its transcriptional activity (Richard et al., 1999). Inhibition of MAPK has a negative effect in the activity of HIF-1 during hypoxia, without affecting its expression, localization or capacity of binding to HIF-1β (Sutton et al., 2007).

HCT116 cells were used to assess if the inhibition of MAPK also had an effect on the levels of HIF-1α at physiological oxygen levels. HCT116 cells were treated with 1.25μM of U0126 and 0.4 μg/ml of doxorubicin and cultured at 20% or 5% O_2. Protein lysates were collected and the protein levels were assessed with the use of western blotting. As observed in figure 4.8, the levels of HIF-1α protein decreased after MEK inhibition by U0126. Results also show that the combination of doxorubicin and U0126 has an

effect on the levels of HIF-1α at physiological oxygen levels, reducing them to similar levels as the ones observed for atmospheric oxygen concentrations. This result suggests that MAPK is upstream of HIF-1 and it is responsible for the stabilization of HIF-1α at physiological oxygen tensions.

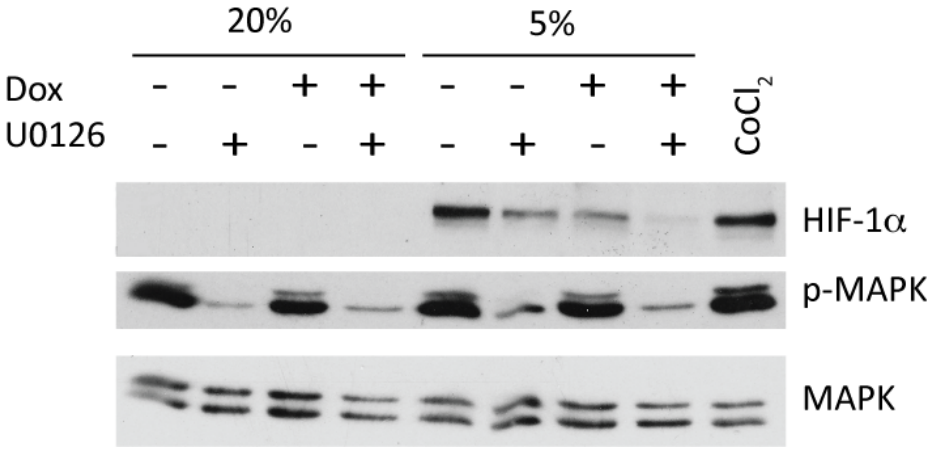

Figure 4.8 Inhibition of MAPK causes a decrease in HIF-1α protein. HCT116 cells were treated with 1.25μM U0126 and 0.4 μg/ml of doxorubicin and cultured at 20% or 5% O_2. Lysates were collected and a western blot was run. A decrease in the levels of HIF-1α can be observed after the inhibition of MAPK.

To corroborate that the effect of MAPK over HIF-1α was sustained after a period of time, HCT116 cells were treated with 1.25μM of U0126. Cells were cultured at 20% or 5% and lysates were collected 12, 24, 32 or 48 hours after the treatment with U0126. As seen in figure 4.9, the levels of HIF-1α decrease after 12 hours of treatment with U0126 and remain low as long as MAPK is repressed by U0126.

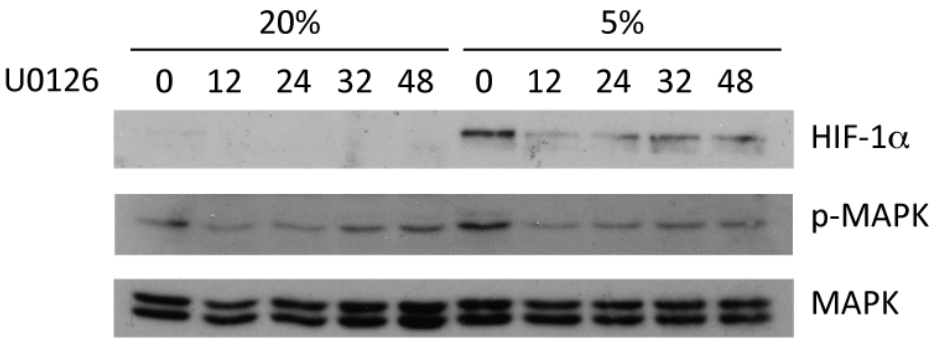

Figure 4.9 Inhibition of MAPK at different time points has an effect on HIF-1α. HCT116 were treated with 1.25μM of U0126 and cultured at 20% or 5% O_2. Protein lysates were collected 12, 24, 32 and 48 hours after treatment. Lysates at time 0 correspond to untreated controls. A reduction on the levels of HIF-1α compared to the control can be observed at al time points.

We previously observed that the expression of HIF-1α at physiological oxygen tensions was independent of p53. To check if the effect of MAPK over HIF-1α was also independent of p53, HCT116 p53 -/- cells were treated with 1.25μM of U0126 and 0.4 μg/ml of doxorubicin and cultured at 20% or 5% O_2. Western blotting was used to assess the protein levels of HIF-1α, p-MAPK and MAPK. As observed in figure 4.10, the levels of MAPK phosphorylation decrease after treatment with U0126, as expected. It can also be observed that the levels of HIF-1α decrease after MEK is inhibited. This result suggests that the stabilization of HIF-1α by MAPK is independent of the p53 status of the cell.

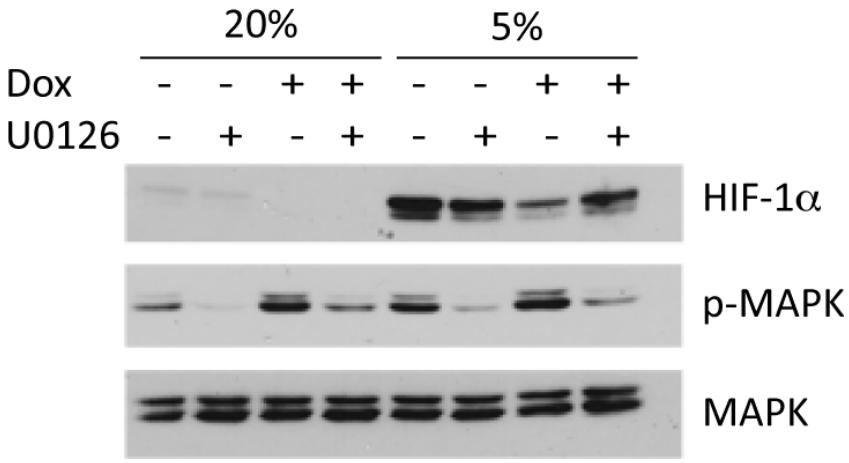

Figure 4.10 Effect of MAPK on HIF-1α is independent of p53. HCT116 p53 -/- cells were treated with 1.25μM of U0126 and 0.4 μg/ml of doxorubicin and cultured at 20% or 5% O_2 for 24 hours. Western blotting was used to assess protein levels of HIF-1α, p-MAPK and MAPK. Results show a decrease in the levels of HIF-1α after treatment with U0126 even in the absence of p53.

4.4 HIF-1 and the resistance to apoptosis

Our results showed that MAPK is at least partially responsible for the resistance to doxorubicin-induced apoptosis observed at physiological oxygen tensions. It was also observed that MAPK was responsible for stabilizing HIF-1α at physiological oxygen tensions.

To assess if MAPK was helping cell survival by stabilizing HIF-1α at physiological oxygen tension, HIF-1α was inhibited with the use of siRNA and cell death was assessed by FACS. HCT116 cell were transfected with 50pmol siRNA and treated with 0.4 μg/ml of doxorubicin. Cells were cultured at 20% or 5% O_2 for 24 hours prior to PI staining and FACS analysis. As observed previously, cells cultured at 5% O_2 and treated with doxorubicin are more resistant to cell death compared to cells cultured at 20% O_2 (Figure 4.11). It can be observed that inhibition of HIF-1α does not sensitize HCT116 cells to apoptosis at physiological oxygen tensions. This result suggests that MAPK is promoting cell survival through a mechanism that is independent of its stabilization of HIF-1 at physiological oxygen tensions.

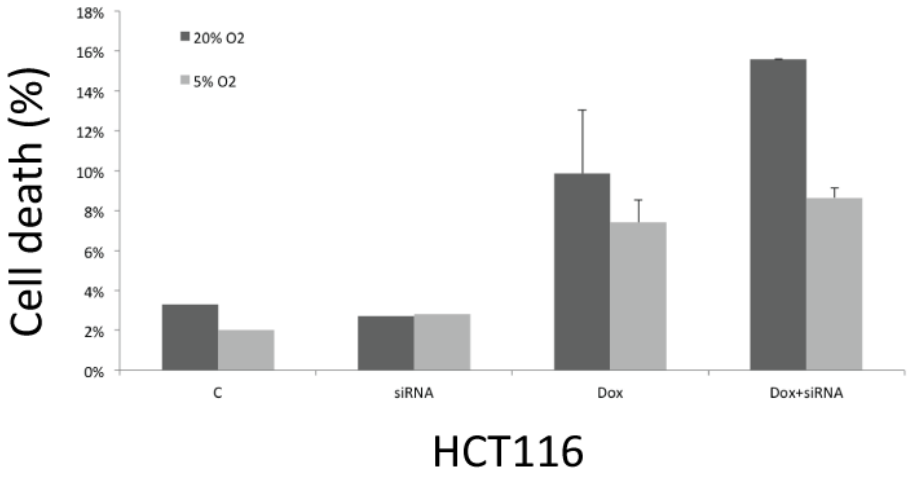

Figure 4.11 HIF-1α is not responsible for the resistance to doxorubicin induced apoptosis at 5% O_2. HCT116 cells were transfected with 50pmol of siRNA against HIF-1α and treated with 0.4 μg/ml of doxorubicin. Cells were cultured at 20% or 5% O_2 for 24 hours and cell death was assessed by PI staining and FACS analysis. It can be observed that even after inhibition of HIF-1α the cells cultured at 5% O_2 are more resistant to doxorubicin-induced apoptosis.

Chapter 5. Stra6 and the cellular responses to damage

Stra6 is the cellular receptor for retinol bound to RBP4 and it mediates the cellular uptake of retinol. Stra6 has important functions in development and mutations in this protein cause severe phenotypes in humans that are associated with deficiency of cellular vitamin A uptake. Due to the fact that mutations in RBP4 are associated with milder phenotypes in mammals, it has been suggested that Stra6 may have different functions besides the intake of retinol or may be involved in an additional unknown process (Blaner, 2007).

5.1 Induction of Stra6 by p53

Previous results in our laboratory have suggested that p53 was able to increase the expression of STRA6 (Figure 5.1). EJp53 cells are a human bladder cancer cell line that contains a tet-off inducible system that induces the expression of p53 upon removal of tetracycline (Sugrue et al., 1997). These cells were used to investigate the induction of Stra6 by p53. It can be observed in figure 5.1 that after p53 induction there is an increase in the mRNA levels of Stra6. A more physiological way of increasing p53 expression is by inducing DNA damage. HCT116 cells and the human fibroblasts IMR90 were treated with 0.8 μg/ml of doxorubicin and the levels of Stra6 mRNA were assessed by RT-qPCR. It can be observed that the amount of Stra6 mRNA also increases

after treatment with doxorubicin. This response is only present in cells that have wild-type p53 as we can observe that levels of Stra6 mRNA remain the same in HCT116 p53 -/- cells after treatment with doxorubicin. This suggests that p53 has an effect on the levels of Stra6.

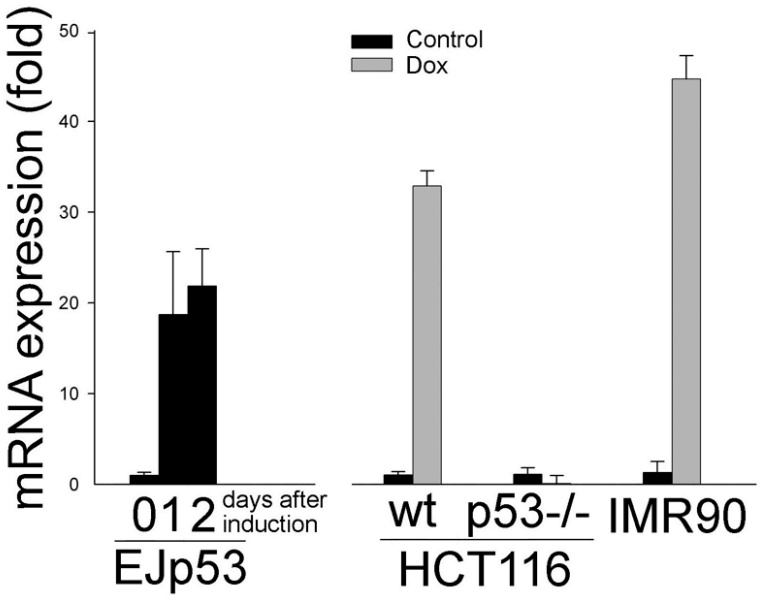

Figure 5.1 p53 induces Stra6 expression. The levels of Stra6 mRNA were assessed by qRT-PCR in EJp53, HCT116 and IMR90 cells. EJp53 were cultured without tetracycline for 0, 1 and 2 days. HCT116, HCT116 p53 -/- and IMR90 cells were treated with 0.8 µg/ml of doxorubicin. Expression was normalized to TBP. An increase in Stra6 expression can be observed after induction of p53, no increase can be observed in HCT116 p53 -/- cells as expected (Carrera, et al., 2012 submitted for publication)

A western blot was performed to explore if the protein levels of Stra6 also increased after p53 induction. EJp53 cells were cultured without tetracycline for 0, 1 and 2 days and total protein lysate was isolated. As observed in figure 5.2A, the levels of p53 increase after removal of tetracycline for 1 and 2 days as expected. There can be

observed an increase in the protein levels of Stra6 that correlate with the induction of p53.

To corroborate this result with DNA damage, HCT116 cells were treated with 0.4 µg/ml of doxorubicin for 24 hours. Protein lysates were collected and Stra6 levels were assessed by western blot. It can be observed in figure 5.2B that levels of Stra6 increase after treatment with doxorubicin. It can be observed that the levels of Stra6 are not very intense; we believe this is due to the sensitivity of the antibody. These results show that p53 increases the expression of Stra6 at the mRNA and protein levels.

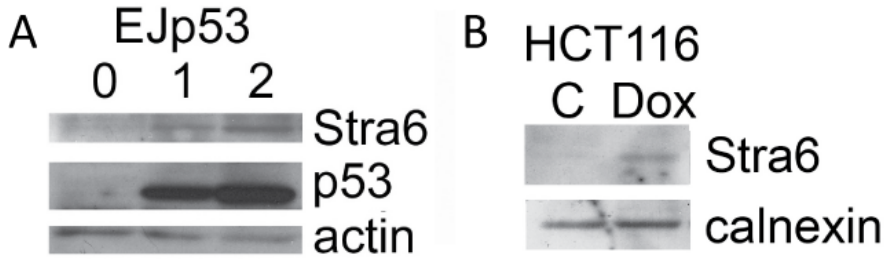

Figure 5.2 Stra6 protein levels increase after p53 induction. A. p53 was induced in EJp53 cells by removal of tetracycline for 0, 1 and 2 days. Protein levels of Stra6 and p53 were assessed by western blot, Actin was used as a loading control. Levels of p53 increase after 1 day and 2 days induction, the levels of Stra6 increase accordingly. **B.** HCT116 were treated with 0.4 µg/ml of doxorubicin (Dox) for 24 hours and levels of Stra6 protein were assessed by western blot. Antibody against calnexin was used as a loading control. An increase in the levels of Stra6 could be observed after doxorubicin treatment.

5.2 p53 binding to the Stra6 gene

Our results suggest that p53 is able to induce Stra6. To investigate if Stra6 is a direct target gene of p53 we performed a ChIP assay. As the promoter of the Stra6 gene has not been identified the region proximal to exon 2 was used to identify possible p53 binding sites (Figure 2.1). The online program ConSite was used to search for possible p53 binding sites in the Stra6 gene (Sandelin et al., 2004). Primers that include these regions were designed (Table 6) and tested to optimize them to the best conditions.

HCT116 cells and HCT116 p53 -/- were treated with 0.4 μg/ml of doxorubicin for 24 hours and the process was continued as explained in section 2.10. Once the DNA for each sample was isolated a qRT-PCR was performed and the Ct values were recorded. For each primer a melting curve was produced to ensure the specificity of the primers. All the Ct values for the IP samples were normalized to their correspondent Ct value for the INPUT sample. The normalized ChIP Ct values (HCT116 cells) were adjusted for the normalized background Ct values (HCT116 p53 -/- cells) to obtain the ΔΔCt. From this value the IP fold enrichment was calculated.

Primers designed for a p53-binding site in the promoter of the p21 gene were used as a positive control for p53 binding. Primers designed in the promoter region of the actin gene were used as a negative control. As observed in figure 5.3, p53 is able to bind to

the promoter of the p21 gene, as expected. There were no indications that p53 was able to bind to any of the three putative p53 binding sites (ChIP 1, 2 and 3) in the region of Stra6 explored. These results indicate that p53 does not bind to this region of Stra6, however it is possible that p53 could be binding to a different region or to different sites near this region. More possible p53 binding sites need to be explored in order to be able to determine if Stra6 is a direct target for p53.

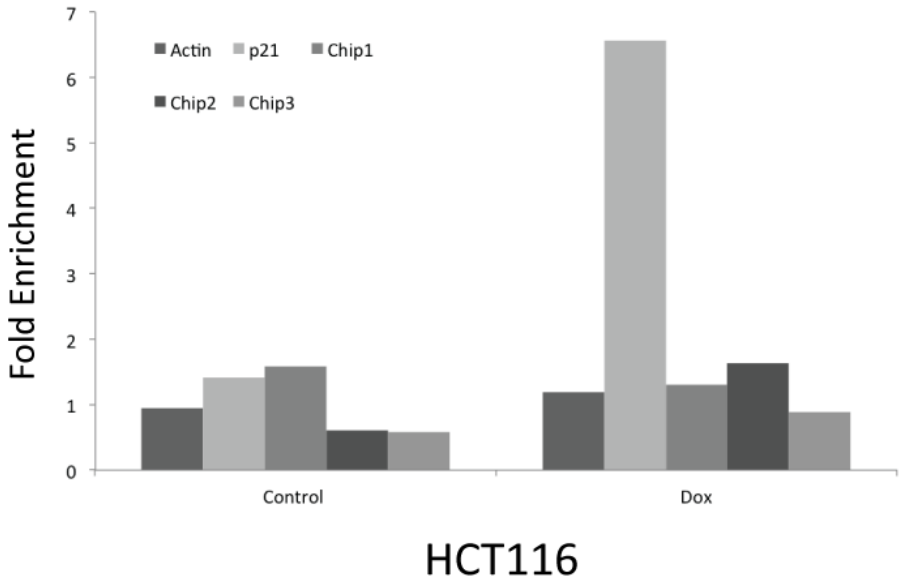

Figure 5.3 p53 binding to Stra6 gene. ChIP assay performed with HCT116 and HCT116 p53 -/- cells treated with 0.4 µg/ml of doxorubicin. p53 binding to three possible binding sites in the start of Stra6 gene was explored using the ChIP 1, 2 and 3 primers. Primers for a p53-binding site in the promoter of the p21 was used as a positive control, primers for the actin gene were used as a negative control. Results show and increase in the control, but not in any of the sites in Stra6 gene explored.

5.3 Stra6 and the response to apoptosis

Our results suggested that Stra6 could be induced by p53 after DNA damage; therefore, we wanted to explore the role of Stra6 in the p53 pathway. The Stra6 transcript variant 2 cloned into the pCMV6-XL4 plasmid (OriGene) was used to overexpress the protein and explore its effect on cell physiology (Table 2). To test the efficiency of the plasmid on the expression of Stra6, HCT116 cells were transfected and the levels of Stra6 mRNA and protein were assessed.

HCT116 cells were transfected with 4μg of Stra6 plasmid or treated with 0.4 μg/ml of doxorubicin. Total RNA was isolated and cDNA was obtained by reverse transcription, followed by qPCR using primers for the Stra6 mRNA. As observed in figure 5.4A, the levels of Stra6 increase after treatment with doxorubicin as previously shown. An increase in the levels of Stra6 mRNA can be observed after transfection with the Stra6 plasmid, as expected.

To test if Stra6 protein levels also increased after DNA damage, HCT116 cells were transfected with 4μg of Stra6 plasmid and total protein lysates were collected. A Western blot was run to assess the levels of Stra6 protein; actin was used as a loading control. As seen in figure 5.4B, the levels of Stra6 increase after transfection with the

Stra6 plasmid. The levels of expression of Stra6 after transfection are much higher than the physiological levels of Stra6 induced by doxorubicin.

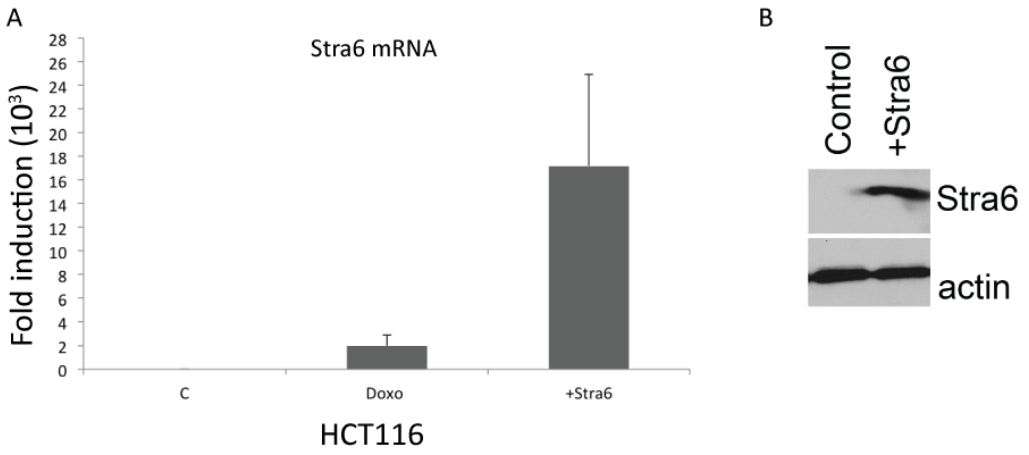

Figure 5.4 Overexpression of Stra6. A Stra6 plasmid containing the Stra6 transcript variant 2 was used to overexpress Stra6 (OriGene). **A.** Graph showing the increase in Stra6 mRNA induction in HCT116 samples after treatment with 0.4 μg/ml of doxorubicin or transfected with Stra6 plasmid. **B.** Western blot showing the increase in the levels of Stra6 protein after transection with the Stra6 plasmid. Actin was used as a loading control.

Once the induction of Stra6 by transfection of the plasmid was corroborated, the effect of Stra6 overexpression was explored by FACS analysis by other members of my group. IMR90, HCT116 and the two ovarian cancer cell lines PA-1 and A1847 were transfected with 4μg of Stra6 plasmid and/or treated with 0.8 μg/ml of doxorubicin. Cell death was assessed by Annexin V staining and FACS analysis. Results show that after induction of Stra6 there is a moderate increase in the amount of cell death in IMR90 and HCT116 cells, but a more significant increase could be observed in the PA-1 (32%) and A1847 (84%) cells (Figure 5.5). It was also observed that the combination of doxorubicin and Stra6 had an additive effect on cell death in all the cell lines studied.

These results suggest that Stra6 has pro-apoptotic activity and that p53 could be inducing Stra6 to enhance its cell death response.

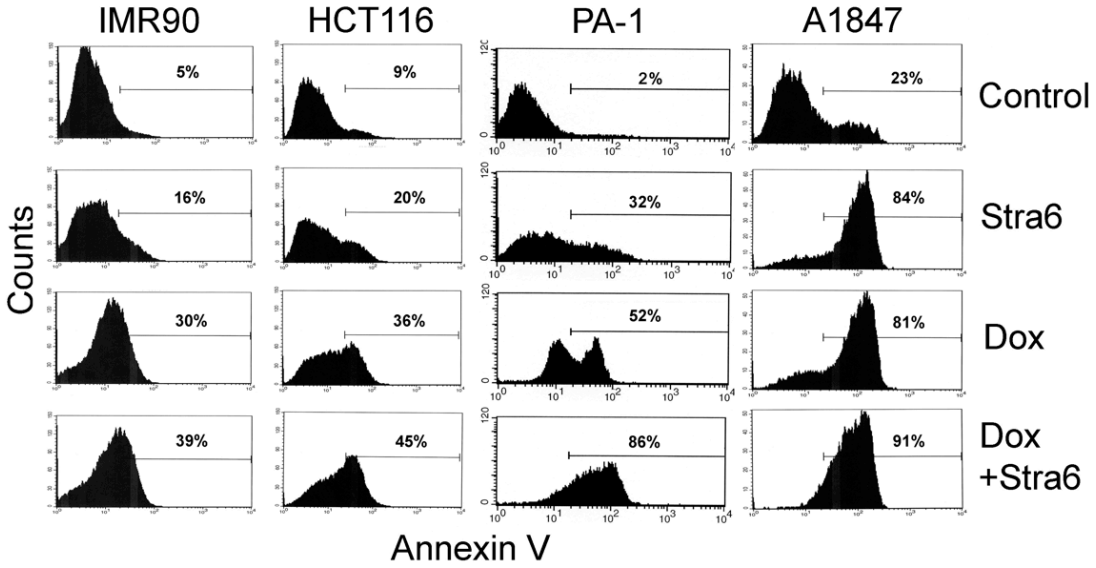

Figure 5.5 Stra6 contributes to p53-induced apoptosis. FACS analysis of Annexin V stained IMR90, HCT116, PA-1 and A1847 cells transfected with 4µg of Stra6 plasmid (Stra6 and Dox+Stra6) and treated with 0.8 µg/ml of doxorubicin (Dox and Dox+Stra6). Percentages indicate Annexin-V positive cells. An increase in apoptosis can be observed in all cell lines after transfection with Stra6; combination of doxorubicin and Stra6 had an additive effect on apoptosis. (Carrera, et al., 2012 submitted for publication)

5.3.1 Effect of the lack of Stra6 on cell death

To better explore the physiological relevance of our findings, HCT116 cells stably expressing shRNA against Stra6 were generated in our laboratory. HCT116 cells stably transfected with an shRNA against the luciferase gene were used as a control. To corroborate that the shRNA was able to silence Stra6 gene expression, HCT116 shStra6 cells and HCT116 shLuci cells were treated with 2µM ATRA for 24 hours. RNA was isolated from these samples and cDNA was prepared, levels of Stra6 mRNA were

assessed by qPCR. As observed in figure 5.6, the levels of Stra6 mRNA increase in HCT116 shLuci cells after treatment with ATRA. There was no increase in the levels of Stra6 mRNA in HCT116 shStra6 cells suggesting that the shRNA was able to successfully knockdown Stra6 in these cells.

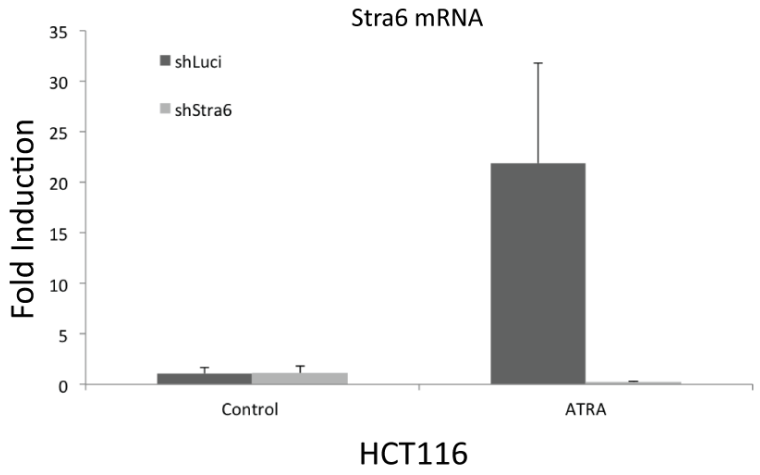

Figure 5.6 mRNA levels of Stra6 are knocked-down with the use of shRNA. RNA was isolated from HCT116 shStra6 and shLuci cells treated with 2µM ATRA for 24 hours. qRT-PCR showing that levels of Stra6 mRNA increase after treatment of HCT116 shLuci cells with ATRA, but not in shStra6 cells.

Once the effectiveness of the shRNA was tested, we wanted to see the effect of Stra6 absence in the responses to genotoxic stress. HCT116 shLuci cells and HCT116 shStra6 cells were treated with 0.8 µg/ml of doxorubicin for 48 hours. Cell death was assessed by PI and Annexin V staining and FACS analysis. Results with PI staining shown that cells lacking Stra6 are more resistant to doxorubicin-induced apoptosis compared to the controls cells, with only 25% of cells dying after treatment with doxorubicin, against 40% in cells with Stra6 (Figure 5.7, left column). Similar results were observed

when assessing apoptosis by Annexin V staining with 23% of cells lacking Stra6 undergoing apoptosis after treatment with doxorubicin compared to 45% of control cells (Figure 5.7, right column). These results suggested that the absence of Stra6 impaired apoptosis after genotoxic stress, with less than half the amount of cell death being induced after exposure to doxorubicin when measured by either PI or Annexin V staining.

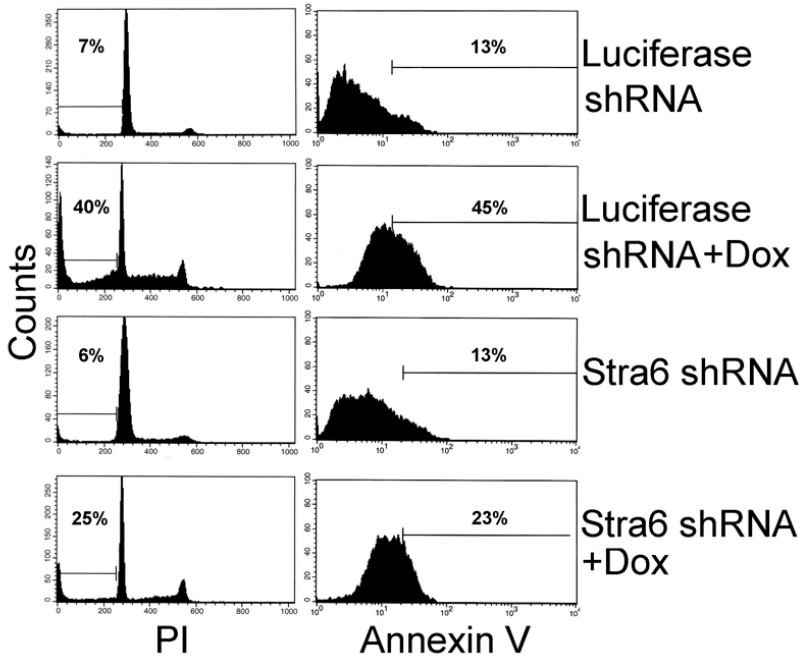

Figure 5.7 Cells are resistant to apoptosis in the absence of Stra6. HCT116 shLuci and HCT116 shStra6 cells were treated with 0.8 µg/ml of doxorubicin for 24 hours. Apoptosis was assessed by PI (left column) and Annexin V (right column) staining and FACS analysis. Percentages indicate Sub-G1 cells (PI) and Annexin V positive cells. A reduction in doxorubicin-induced cell death could be observed in cells lacking Stra6 compared to control cells.

5.4 Role of Stra6 in oxidative damage accumulation

To explore the possibility that the increase in apoptosis after DNA damage observed in cells containing Stra6 was due to an accumulation of oxidative damage, a comet assay was performed. Taking advantage of the cells with the shRNA against Stra6, our objective was to see if the resistance to doxorubicin induced apoptosis was due to this cells accumulating less oxidative damage after genotoxic stress. HCT116 and HCT116 shStra6 cells were cultured and treated with 0.4 μg/ml of doxorubicin. HCT116 cells treated with H_2O_2 were used as a positive control for oxidative damage. The enzyme Fpg was used to detect DNA damage caused by oxidation. As observed in figure 5.8, cells that express wild-type Stra6 accumulate more oxidative damage compared to cells lacking Stra6. This result suggests that the resistance to apoptosis observed in cells lacking Stra6 is due to less oxidative damage after exposure to doxorubicin and suggests that Stra6 may be enhancing the production of ROS in response to damage.

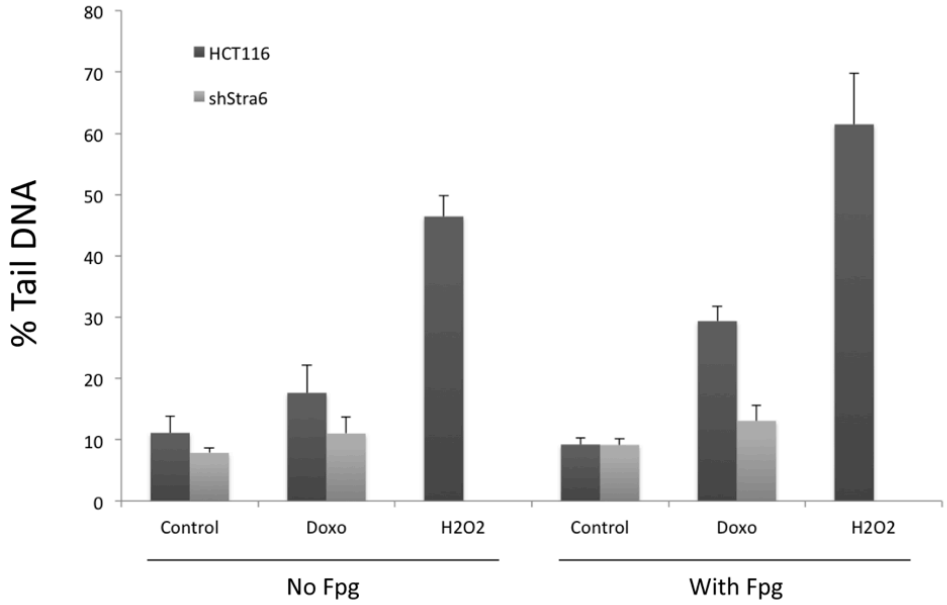

Figure 5.8 Cells with Stra6 accumulate more oxidative damage. HCT116 and HCT116shStra6 cells were treated with 0.4 µg/ml of doxorubicin and cultured for 24 hours. HCT116 cells treated with 100 µM of H_2O_2 for 10 minutes were used as positive control. HCT116 cells accumulate more oxidative damage after treatment with doxorubicin compared to cells that lack Stra6.

5.5 Retinoic acid pathway in the response mediated by Stra6

As Stra6 is part of the retinoic acid pathway we wanted to explore if the responses to DNA damage observed were dependent on RA signalling, since the RA pathway has been shown to be involved in apoptosis (Altucci et al., 2007). RXRs and RARs bind to DNA-response elements termed RA response elements (RAREs). To check if the retinoic acid pathway was being activated as a consequence of p53 induction of Stra6, we used a vector that contains five consensus RAREs in the pGL2 Promoter vector upstream the firefly LUC gene (Table 2) (Bartholin et al., 2006). HCT116 cells were transfected with the reporter and a β-galactosidase plasmid as a control of transfection. Cells were treated with doxorubicin (0.4 μg/ml), ATRA (2μM) or transfected with Stra6 plasmid (0.4 μg) and activity of the reporter was measured in a plate reader. Luciferase activity was normalized to β-galactosidase activity. Treatment with ATRA was used as a positive control. An increase in the activity of the vector could be observed after treatment with ATRA, as expected. The activity of the reporter vector did not increase when Stra6 was overexpressed or when cells were treated with doxorubicin (Figure 5.9). This suggests that overexpression of Stra6 or DNA damage induction by doxorubicin is not sufficient to activate the retinoic acid pathway.

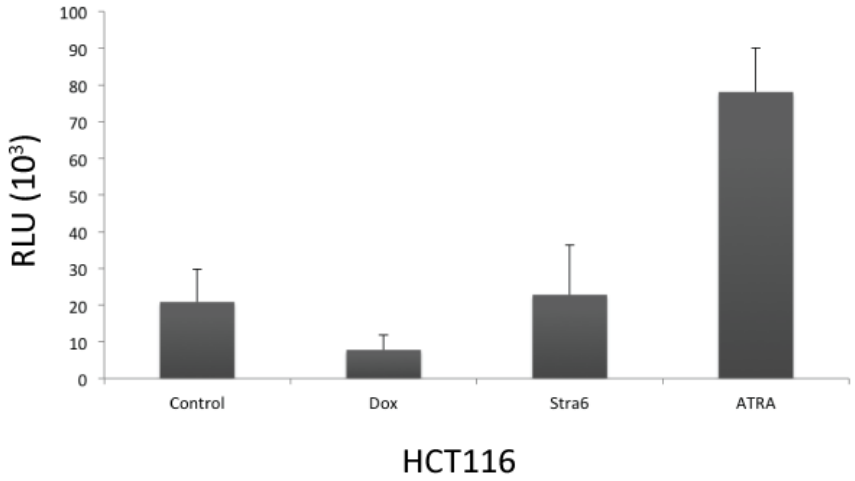

Figure 5.9 Effect of p53 induction of Stra6 on the retinoic acid pathway. HCT116 were transfected with the Stra6LUC luciferase reporter plasmid and the β-galactosidase plasmid. Cells were treated with 0.4 µg/ml of doxorubicin (Dox), 2µM of ATRA or transfected with 0.4 µg of Stra6. β-galactosidase activity was used to normalize luciferase activity. An increase in the reporter activity can be observed after treatment with ATRA, but not with doxorubicin or Stra6 overexpression.

To confirm that the retinoic acid pathway was not involved in Stra6 mediated responses to doxorubicin-induced cell death, EJp53 cells were used to overexpress p53 and see its effect on the expression of RA responsive genes. EJp53 cells were cultured and p53 expression was induced by removal of tetracycline from the media. RNA was isolated from the cells after 0, 1 day and 2 days of p53 induction. The mRNA levels of Stra6, RARα and RARβ were assessed by qRT-PCR. As previously observed in figure 5.1, a 6-fold induction of Stra6 mRNA was observed after only 1 day of p53 overexpression; the expression increased further after day 2 (8-fold) (Figure 5.10). The levels of RARα and RARβ mRNA were unaffected by the overexpression of p53. This suggests that although p53 is able to induce Stra6 expression, it has no effect on the expression of other genes that are part of the RA pathway. These results suggest that Stra6 may

have novel functions independent of the RA pathway that contribute to p53-mediated DNA damage responses.

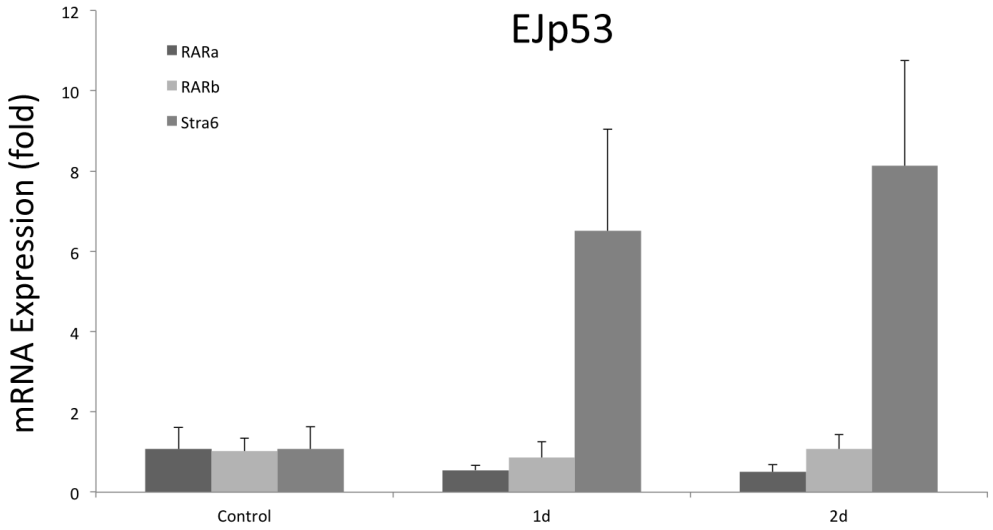

Figure 5.10 Induction of Stra6 mRNA by p53. RNA was isolated from EJp53 cells after p53 induction by removal of tetracycline for 1 day (1d) or 2 days (2d). An increase in the levels of Stra6 mRNA could be observed after expression of p53.

5.6 Cellular localization of Stra6

Stra6 is the cell surface receptor for retinol, but previous results in our laboratory suggested a change in cellular localization of the protein upon DNA damage (Figure 5.11). HCT116 cells were grown in coverslips and treated with 0.4 μg/ml for 24 hours. Cells were fixed, permeabilized and incubated with the antibody against Stra6. DAPI was used to stain the nucleus. It can be observed in figure 5.11 that the endogenous levels of Stra6 are low and almost no signal is visible (upper middle panel). When cells are treated with doxorubicin an increase in the levels of Stra6 can be observed (lower middle panel). Of note, on the merged image it can be observed that Stra6 can be localized to the nucleus after DNA damage.

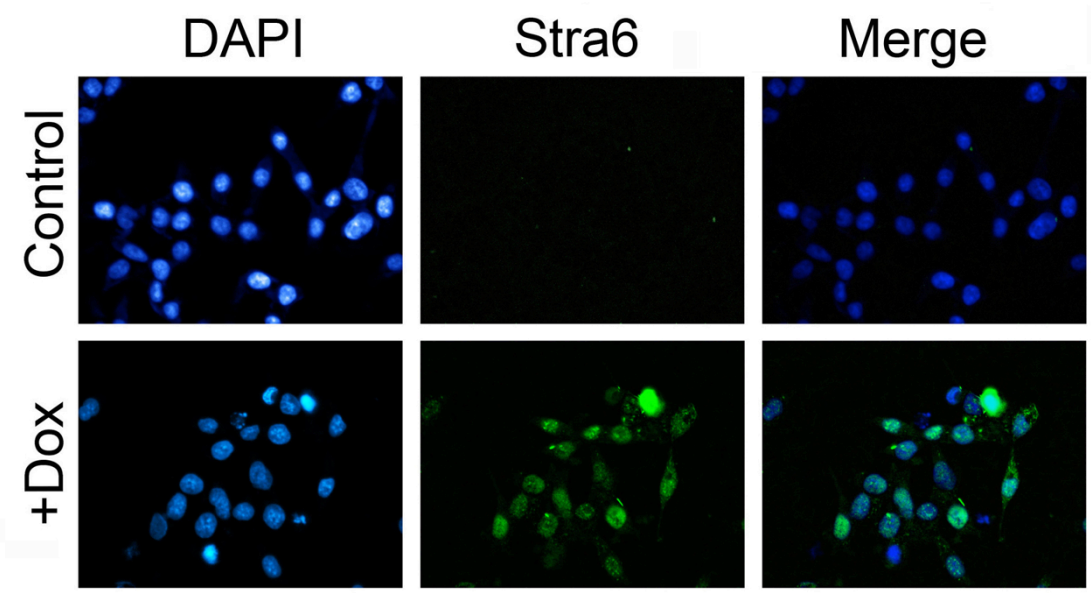

Figure 5.11 Localization of Stra6 after DNA damage. Immunofluorescence with antibody against Stra6 (green) in cells treated with 0.4 µg/ml of doxorubicin (+Dox). Nucleus stained with DAPI (blue). Stra6 is induced after treatment of the cells with doxorubicin and it can be observed that the protein is mainly localized to the nucleus after DNA damage. (Carrera, et al. 2012 manuscript submitted for publication)

As observed in figure 5.11, endogenous Stra6 is expressed in very low quantities. To have a better idea of Stra6 localization, we overexpressed Stra6 to confirm the results obtained in the previous figure. HCT116 cells were transfected with 0.4µg of Stra6 plasmid and after 24 hours of transfection the cells were treated with 0.4 µg/ml of doxorubicin, 2µM ATRA or 6µM H_2O_2. Cells were fixed, permeabilized and incubated with the antibody against Stra6. As observed in figure 5.12, in cells transfected with the Stra6 plasmid the protein localizes mainly at the cell membrane with small amounts accumulating in the cytoplasm. When cells are treated with ATRA, the protein can be seen localized to the membrane, as expected. Upon DNA damage, in cells treated with doxorubicin or H_2O_2, the amount of Stra6 increases and appears to be accumulated all around the cell. This result suggests an accumulation of Stra6 upon

DNA damage that correlates with our results that show an increase in the protein and mRNA levels after treatment with doxorubicin or overexpression of p53. From this particular experiment it is not possible to determine the exact location of Stra6 after DNA damage and further studies are needed to elucidate the nature of Stra6 translocation under these conditions.

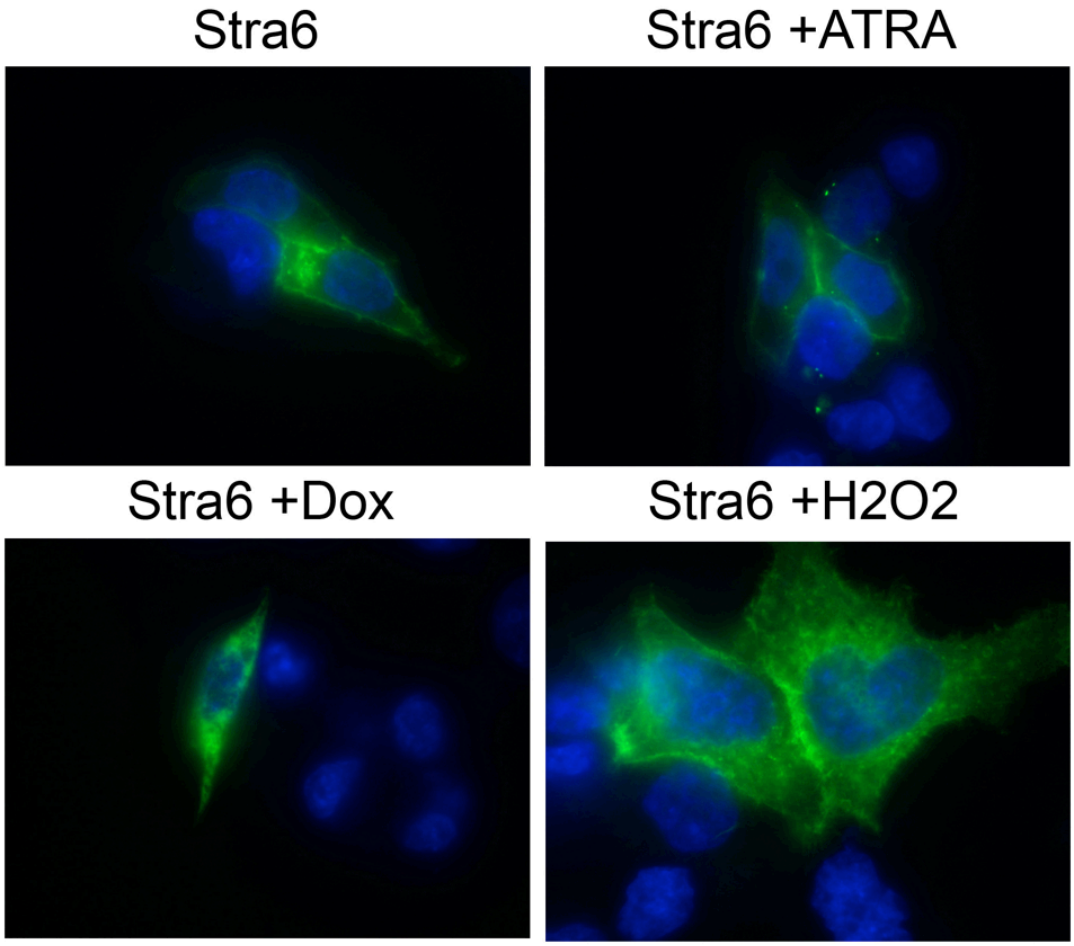

Figure 5.12 Stra6 accumulates in the membrane, cytoplasm and nucleus of the cell after DNA damage. Immunofluorescence showing the expression of Stra6 (green) in HCT116 cells after transfection with 0.4µg of Stra6 plasmid. Nulceus are stained with DAPI (blue). Cells were treated with 0.4 µg/ml of doxorubicin (Dox), 2µM ATRA or 6nM H_2O_2. Stra6 localizes mainly in the membrane, but upon DNA damage it appears to accumulate in different areas of the cell.

Chapter 6. Discussion

6.1 Resistance to apoptosis at physiological oxygen tensions

The role of physiological oxygen tensions on the cellular responses to DNA damage has not been extensively explored before. Most mammalian cell culture performed in laboratories around the world is carried out at atmospheric oxygen tensions (20% O_2); this level of oxygen is higher than the one normally found in tissues. It has been previously demonstrated that cells cultured at physiological oxygen tensions behave differently to the ones cultured at atmospheric oxygen tensions. Mouse embryonic fibroblasts (MEFs), human fibroblasts and human mesenchymal stem cells (hMSC) have all been shown to proliferate for longer and have increased growth rates when cultured at physiological oxygen tensions (Parrinello et al., 2003; Estrada et al., 2012). In accordance to this, our results show that HCT116 cells cultured at 5% O_2 form a higher number of colonies and they are bigger in size compared to the ones from cells cultured at atmospheric oxygen tensions (20% O_2) (Figure 3.4). This suggests that cells at 5% O_2 have an advantage for growth and proliferation compared to their 20% O_2 counterparts. We also observed an increase in number and size of the colonies formed at 5% O_2 when treated with doxorubicin. This leads us to the idea that the proliferation and growth observed at 5% O_2, could have an effect on the cellular responses after DNA damage.

We show that cell lines cultured at physiological oxygen tensions are more resistant to doxorubicin-induced apoptosis than cells at 20% O_2. This resistance was observed in different normal and cancer cell lines and at different concentrations of doxorubicin used, although the difference in the percentage of cell death varied slightly from experiment to experiment. We believe this is due to the innate variability associated with tissue culture and small differences in culture times. Even though cells grow better at physiological oxygen tensions this does not completely explain why cells resist more to apoptosis induced by DNA damaging agents and we wanted to investigate this point further.

6.1.1 Resistance to apoptosis is p53-dependent

Most of the responses to DNA damage are executed through p53. We first explored if the resistance to apoptosis at physiological oxygen tensions was also observed in p53 null-cells. Doxorubicin mostly induces apoptosis in cells *via* p53, thus the cells lacking p53 show only a minor increase in apoptosis after treatment with doxorubicin. We did not observe a further decrease in apoptosis at 5% O_2 in these cells. However, results in our laboratory have shown that the response to physiological oxygen tensions is p53-dependent, as p53 -/- cells radiated with UV shown there is no difference in the percentage of apoptosis at 5% O_2 compared to atmospheric oxygen tensions (Carrera et al., 2010).

Although the response was p53-dependent, we did not observed differences in the levels of p53 or its target genes in cells cultured at physiological oxygen tensions. This suggests that the resistance to apoptosis observed is not due to a difference on p53 expression or transcriptional activity at lower oxygen levels. This does not rule out the possibility that other p53 functions may differ at lower oxygen concentrations. The possibility of changes in p53 cytoplasmic activity had not been explored in this project, but it would be interesting to know if there are changes in non-transcriptional p53 activity that could justify the dependence of the resistance at 5% O_2 on p53 and its effect on survival.

Doxorubicin partially induces apoptosis by inducing ROS and causing DNA damage. Also, higher concentrations of oxygen cause an increase in the amount of ROS in the cells and this could lead to more DNA damage. We hypothesize that these two factors could be leading to the accumulation of DNA damage at higher oxygen concentrations (20% O_2), and thus sensitizing the cells to apoptosis. We found that HCT116 cells cultured at 5% O_2 did not accumulate less oxidative damage that the ones cultured at atmospheric oxygen tensions. In contrast to our results, it had been previously shown that cells cultured at physiological oxygen tensions accumulate less oxidative damage and DNA DSBs than the ones cultured at atmospheric oxygen (Parrinello et al., 2003; Estrada et al., 2012). The difference may be explained because of the type of cells used. In contrast to the experiments from Parrinello, *et al.* (2003) and Estrada, *et al.* (2012) our experiments were performed using immortalized cancer cell lines and they used MEFs and hMSCs. We observed resistance to apoptosis in IMR90 fibroblast

cultured at physiological oxygen tensions, but we did not explore the differences in oxidative DNA damage. We do not have reasons to suspect that there will be any difference, since when Parrinello *et al.* (2003) assessed the amount of oxidative damage in human fibroblasts cultured at atmospheric O_2 by comet assay they did not observe more DNA damage at higher oxygen concentrations.

6.1.2 MAPK is activated at 5% O_2

In cells, there is a balance between death signals and survival signals that would determine the fate of the cell after a cellular stress. Our previous results had shown there is no apparent difference in the cell death pathways between cells cultured at atmospheric or physiological oxygen tensions. If cells at this concentration of oxygen have an advantage for survival, some of the pro-survival pathways in the cell may be involved in the response. It has also been suggested that MAPK can be activated in cells cultured at physiological oxygen tensions (Conrad et al., 1999). We decided to explore the role of the MAPK pathway on the cellular responses to DNA damage at physiological oxygen tensions. There is an increase in the levels of MAPK phosphorylation when cells are cultured at physiological oxygen tensions. Similar results were obtained by Conrad *et al.* (1999) when they cultured PC12 cells at 5% O_2. This does not appear to be the case in cells exposed to hypoxia (≤1% O_2) as it has been shown that there is not an increase in MAPK phosphorylation under these conditions (Richard et al., 1999; Sang et al., 2003).

6.1.3 MAPK is partially responsible for the resistance at 5% O_2

MAPK is phosphorylated at physiological oxygen tension, but what effect does this has on the cellular responses to damage? We show that inhibition of MAPK at physiological oxygen tensions has a negative effect on the number and size of cell colonies formed (Figure 3.14). This suggest that MAPK confers an advantage to cells for growth and proliferation at 5% O_2, It would be interesting to assess differences in cell growth rates between the two oxygen concentrations to confirm the results with the colony formation.

We also observed that the activation of MAPK at 5% O_2 was responsible for the resistance to apoptosis in HCT116 cells, as inhibition of this pathway restores sensitivity to apoptosis in these cells (Figure 3.15). MAPK is helping HCT116 cells survive better after doxorubicin treatment when the cells are cultured at physiological oxygen tensions. Although resistance to doxorubicin-induced apoptosis and activation of MAPK at 5% O_2 was also observed in U2OS cells, we did not observe a loss of resistance when the cells were treated with U0126. The use of other cell lines from different origins is necessary to elucidate if MAPK is responsible for the resistance to apoptosis at physiological oxygen tensions in a wide variety of tissues. We do not discard the possibility that the role of MAPK in the resistance at 5% O_2 could be a cell-specific response, as HCT116 have an activating mutation on Ras that could determine its dependence on MAPK for survival. More experiments are needed to fully elucidate the role of MAPK signalling at physiological oxygen tensions and its effect on resistance to apoptosis.

The exact mechanism by which MAPK blocks apoptosis at physiological oxygen tensions remains to be elucidated. Our results showed a small difference in the activity of caspase-3, caspase-7 (Figure 3.9) and caspase-8 (Figure 3.10) when cells are cultured at physiological oxygen tension. Less activity of caspases explains the resistance to apoptosis under these conditions. It has been previously suggested that MAPK can inhibit the processing and activation of caspase-9, and in consequence inhibit caspase-3 (Allan et al., 2003). Although the difference in the activity is not huge, this result suggests that MAPK could be interfering with the caspase activity and making cells more resistant to apoptosis at this oxygen tensions. We have not checked if the inhibition of MAPK at 5% O_2 restores the activity of caspase-3 but it would be interesting to determine if this is the case.

Overall, in this part of the thesis we showed that cells cultured at physiological oxygen tensions are more resistant to apoptosis than cells cultured at atmospheric oxygen tensions. MAPK is activated at 5% O_2 and its activation has a positive effect on the growth and proliferation of cells. Also, the inhibition of MAPK in HCT116 cells restores its sensitivity to apoptosis suggesting that MAPK activation has an important role on cell survival under physiological oxygen conditions.

6.2 HIF-1α at physiological oxygen tensions and the response to DNA damage

HIF-1 is an important regulator of the responses to low oxygen concentrations. The O_2 concentrations of mammalian tissues under normoxic conditions ranges from 2-9% (10-30μM) and they are so low that the activities of both the PHDs and FIH may be limited under this conditions *in vivo* (Koivunen et al., 2003). It has been suggested that the amount of oxygen that the enzymes required for activation is around 100μM (Ehrismann et al., 2007). This would suggest that their enzymatic activity could be limited at physiological oxygen concentrations, preventing hydroxylation of HIF-1α and binding of the pVHL protein. The protein levels of HIF-1α increase with decreasing oxygen concentrations, and it has been shown to be present at a range of physiological O_2 tensions (Jiang et al., 1996). Our results have shown an increase survival in response to DNA damage at physiological oxygen tensions, HIF-1 is the principal factor responsible for the adaptation of cells to lower oxygen concentrations therefore we hypothesize that HIF-1 might be involved in the resistance to apoptosis at 5% O_2.

6.2.1 HIF-1α is expressed and active at 5% O_2

We confirmed that HIF-1α is expressed at physiological oxygen tensions (5% O_2). The levels of the protein increased after cells were cultured at 5% O_2 (Figure 4.1), although these levels were lower than the positive control, cells treated with the hypoxia mimicking agent $CoCl_2$. It has been shown that the levels of HIF-1α increase

proportionally as the levels of O_2 decrease (Jiang et al., 1996). This suggests that some of the protein is still being degraded at 5% O_2 but that the levels are low enough to allow an accumulation of the protein. The expression of HIF-1α under physiological oxygen concentrations is independent of p53 as cells that are p53-null still showed an increase in the levels of HIF-1α (Figure 4.2).

The accumulation of the protein at physiological oxygen tensions does not necessarily mean that the protein is active. With the use of a luciferase reporter plasmid containing the HREs of the *PGK1* gene we showed that HIF-1 is active at physiological oxygen tensions (Figure 4.3). Confirming this result, we also saw an increase in the mRNA expression of HIF-1 target genes (PGK-1 and Glut1) in these conditions (Figure 4.4). This correlates with the data found through a microarray in hMSC in which several HIF-1 target genes were up regulated in cells cultured at physiological oxygen tensions (Estrada et al., 2012). Analysing cells grown at 3% and 20% O_2, Estrada *et al.* (2012) found that the majority of genes with altered expression were those involved in carbohydrate metabolism, especially glycolysis. The authors think this is due to an increase in the activity of HIF-1 at physiological oxygen tensions although the presence of HIF-1α was not tested.

We think that the presence of HIF-1 activity at physiological oxygen concentrations may have an important role for normal physiology. FIH has lower Km values for O_2 than PHDs enzymes; this indicates that a minor decrease in O_2 concentrations from

those present in the air is likely to influence the activities of PHDs but a higher decrease is needed to inactivate FIH. This will lead to rapid stabilization and accumulation of HIF-1α, but a larger decrease in O_2 concentration is needed to inhibit FIH and allow the binding of p300, achieving HIF-1 maximal transcription activity (Dayan et al., 2006). It has been shown that not all HIF-1 target genes are equally sensitive to inhibition of CAD by FIH (Dayan et al., 2006; Lando et al., 2002). This can lead to some genes being activated at more physiological levels of oxygen than others that will require hypoxic conditions for their activation. It would be interesting to assess which HIF-1 target genes are being activated during physiological oxygen conditions and if indeed there is a differential expression of genes in a range of oxygen tensions.

Doxorubicin was used throughout this project to induce DNA damage and apoptosis. We found that treatment of cells with doxorubicin inhibits HIF-1α protein expression and activity. It has been previously suggested that doxorubicin can interfere with HIF-1 activity through an increase in the levels of p53; the mechanism suggested involves the binding of p53 to p300 (Blagosklonny et al., 1998). Also, it has been suggested that p53 could decrease HIF-1α protein levels as well as its activity (Ravi et al., 2000). We do not think that, in this case, p53 is responsible for the decrease in the levels of HIF-1α protein, as the levels decrease after treatment with doxorubicin even in the absence of p53. Also, we did not observed differences in the amount of HIF-1α being expressed in HCT116 p53-/- cells compared to cells containing p53.

Another possibility is that doxorubicin is directly interfering with HIF-1α. It has been shown previously that anthracyclin drugs, like doxorubicin, inhibit HIF-1 activity. Lee, *et al.* (2009) showed that the mRNA of HIF-1 target genes decrease after treatment with these drugs. The authors suggested that anthracyclines directly interfere with the binding of HIF-1 to DNA. Anthracyclines bind DNA at 5'-(A/T)CG-3' and 5'-(A/T)GC-3', HIF-1 binds to HRE elements that are 5'-(A/G)CGTG-3' overlapping with the preferable binding site for these drugs. Besides interfering with HIF-1 activity, we also found that doxorubicin decreases the levels of HIF-1α protein at physiological oxygen tensions. We did not test if other drugs also have a negative effect on the expression and activity of HIF-1α. It would also be interesting to elucidate if this is a direct effect of doxorubicin on HIF-1α protein or if doxorubicin is acting on another factor that regulates HIF-1α. We did not analyse if the levels of HIF-1α mRNA were affected by doxorubicin treatment which would suggest an effect on the transcriptional regulation, and not on the protein.

6.2.2 HIF-1 and MAPK

We had shown that MAPK signalling is activated at physiological oxygen tensions (Figure 3.11), but the mechanism responsible for this activation is not evident. It has been previously suggested that MAPK can be activated during hypoxia (Conrad et al., 1999; Minet et al., 2000) but the involvement of HIF-1 in this activation has not been explored. We wanted to investigate the possibility that HIF-1 was responsible for the

activation of MAPK. Our results showed that the knocking-down of HIF-1α by siRNA did not have any effect on the activation of MAPK at physiological oxygen tensions (Figure 4.5 and 4.6).

On the other hand, it has been previously reported that MAPK could have an effect on HIF-1α stabilization (Richard et al., 1999; Sang et al., 2003; Sutton et al., 2007). Our results show that inhibition of MAPK causes a decline on the protein levels of HIF-1α and has an effect on its activity (Figure 4.8). It has been reported previously that the inhibition of MAPK with the MEK inhibitor PD98059 blocks HIF-1 transcriptional activity (Richard et al., 1999). This was suggested to be a consequence of a decrease in the phosphorylation of HIF-1 by MAPK, causing a reduction on the transcriptional activity of HIF-1. Besides a decrease in HIF-1 activity, we also find a decrease in the protein levels; contrary to previous findings that MAPK is not involved in the stabilization, localization or capacity to bind to HIF-1β (Richard et al., 1999; Sang et al., 2003; Chen et al., 2001). The exact nature of the effect of MAPK in HIF-1α expression at physiological oxygen tensions remains to be elucidated.

6.2.3 HIF-1α is not responsible for the resistance to apoptosis at 5% O_2

We have shown that the activation of MAPK is responsible for the resistance to apoptosis at physiological oxygen tensions (Chapter 3) and that it is also contributes to HIF-1α stabilization at these oxygen levels (Figure 4.8). We explored the possibility that MAPK was promoting survival at 5% O_2 through activation of HIF-1α. We found that

the inhibition HIF-1α has no effect on the resistance to doxorubicin-induced apoptosis at physiological oxygen tensions or MAPK activation (Figure 4.11). MAPK is promoting survival of cells to apoptosis at physiological oxygen tensions independently of its role on the activation of HIF-1.

HIF-1 is an important mediator of the responses and adaptations to hypoxia and acts by regulating pathways involved in angiogenesis and glycolytic metabolism, among others. We explored the involvement of HIF-1α on the resistance to apoptosis at physiological oxygen tensions. Our results show that although HIF-1α is expressed and active at 5% O_2 it is not involved in the responses to DNA damage. We also showed that MAPK is necessary for the stabilization of HIF-1α under physiological oxygen tensions. The function of HIF-1α at physiological oxygen concentrations has not been extensively explored, our results show that HIF-1α is expressed and active at this condition and we believe that this may have important implications for normal physiology. Most of the cell culture in laboratories is performed at atmospheric oxygen tensions, according to our results cells behave differently under oxygen tensions more similar to the ones found *in vivo*. It would be necessary to perform more experiments to further elucidate the role of HIF-1 at physiological oxygen tensions.

6.3 Stra6 is involved in p53-mediated apoptosis

Stra6 is the cellular receptor for retinol bound to RBP4. Mutations in Stra6 are associated with severe phenotypes (Pasutto et al., 2007; Golzio et al., 2007; Isken et al., 2008). On the other hand, only two mutations in RBP4 have been identified in humans and they are not associated with severe phenotypes (Seeliger et al., 1999). RBP -/- mice have impaired retinol function during the first few months of life, but are otherwise healthy (Quadro et al., 1999). Normal vision can be restored in these animals if their diet is supplemented with vitamin A. Deficiencies in RBP do not cause severe phenotypes, compared to deficiencies in Stra6. This discrepancy between the phenotypes of Stra6 and RBP4 mutations suggests that Stra6 is involved in an additional unknown processes.

We have shown that p53 has an effect on the levels of Stra6 (Figure 5.1). An increase in Stra6 mRNA and protein were observed after p53 was induced artificially with the use of a tet-off system, the same effect was observed when p53 was induced by DNA damaging agents (Figure 5.1 and 5.2).

The principal function of p53 is as a transcription factor and the increase in Stra6 mRNA gives the possibility that it could be a p53 target gene. Previous efforts have been made to identify the promoter region of Stra6, but the 1.4kb genomic sequence

located upstream of exon 1 did not display features of eukaryotic gene promoters (Bouillet et al., 1997). The authors cloned fragments of the 4.5kb region upstream exon 1 into a reporter plasmid, but it did not yield any sign of promoter activity in this region. We performed a search for possible p53 binding sites in the area between exon 1 and 2 of the *Stra6* gene. None of the sites identified showed p53 binding after a ChIP assay was performed (Figure 5.3). This does not rule out the possibility that p53 is binding to a different region on the start of the gene and further experiments are required to elucidate if p53 is able to bind directly to the Stra6 promoter.

As Stra6 was induced after DNA damage, we explored its role in p53-induced apoptosis. We found that overexpression of Stra6 induces apoptosis in different cell lines. Of note, some cell lines (PA-1 and A1847) were more sensitive to apoptosis after overexpression of Stra6 and this correlated with its sensitivity to doxorubicin-induced apoptosis (Figure 5.5). Combination of Stra6 overexpression and DNA damage had an additive effect on the percentage of apoptotic cells observed.

When Stra6 was knocked-down by shRNA (Figure 5.6), cells became more resistant to doxorubicin-induced apoptosis (Figure 5.7). In correlation with our results, Chen *et al.* (2012) showed that siRNA against Stra6 attenuated the levels of active Caspase 3. The authors suggest that Stra6 does this through a mechanism involving STAT5 and JAK2 (Chen et al., 2012). It has also been shown that Stra6 binds to STAT5 and JAK2, and that this binding is induced upon stimulation with retinol-RBP (Berry et al., 2011). They

suggest that RBP4 enhances JAK2 and STAT5 through Stra6, this increases c-AMP production leading to apoptosis through suppression of CRBP-1 and RARα and activation of JNK1 and p38. More experiments are needed to elucidate the downstream mechanism by which p53, in combination with Stra6, is inducing apoptosis.

As mentioned before, doxorubicin induces apoptosis partially by increasing the levels of ROS. We found that HCT116 cells that lack Stra6 accumulate less oxidative damage than their wild-type counterparts after treatment with doxorubicin (Figure 5.8). This suggests that Stra6 is important for the accumulation of DNA damage after treatment of cells with DNA damaging agents.

Stra6 principal function is as the cellular receptor for retinol/RBP so it is evident to think that the RA pathway may be involved in the response to p53. We explored this possibility, but we found that the RA pathway is not involved in the induction of apoptosis after induction of Stra6. There was no increase in the activity of a luciferase reporter plasmid containing RAREs after overexpression of Stra6 or treatment of cells with doxorubicin (Figure 5.9). Also, the mRNA levels of RA responsive genes, RARα and RARβ, were not affected by the induction of p53 (Figure 5.10). Stra6, besides its function as a retinol transporter, has also been suggested to function as a surface signalling receptor; Berry *et al*. (2011) also found that RA did not enhance STAT5 expression suggesting its independence from RA pathway.

It is becoming more evident that Stra6 may have additional functions to its role as cell membrane receptor for retinol. We explored the cellular localization of Stra6 after induction of DNA damage. Our results showed that Stra6 is mainly localized to the plasma membrane under normal conditions, but when cells are treated with doxorubicin it appears to be accumulated in the cell (Figure 5.11 and 5.12). More experiments are needed to elucidate the exact localization of Stra6 on the cell after DNA damage and the implications that this may have on the induction of apoptosis. The change in localization of the protein after induction of DNA damage would suggest that Stra6 might be implicated in a different pathway, besides its role as a cellular receptor for retinol/RBP4.

Stra6 has been observed to be overexpressed in human colorectal tumours (Szeto et al., 2001). On the basis of their ability to promote cell-cycle arrest and induce apoptosis, retinoids could be useful for the treatment of diverse cancers. Differentiation therapy with retinoic acid is being used in combination with chemotherapy for treatment of acute promyelocytic leukaemia (Huang et al., 1988).

Overall, our results suggest that p53 controls the expression of Stra6 and that it can be induced after genotoxic stress in a p53-dependent manner. Moreover, we have shown that Stra6 is an important contributor to p53-induced apoptosis. Since Stra6 is a RA-responsive gene and its expression can be induced by treatment with retinoids, this

provides a rationale to further explore the potential of Vitamin A as an adjuvant in chemotherapy, which could induce the expression of Stra6 and contribute to p53 tumour suppressor functions.

6.4 Concluding remarks

We have shown here that the extracellular factors can have a significant effect on the responses to DNA damage. First, physiological oxygen availability in normal and cancer cells can make cells more resistant to cancer therapy. We believe that the amount of oxygen at which cells are cultured in the laboratory should be taken into account when investigating the responses to DNA damage and other cellular stresses. It could be of interest to see if other processes in the DNA damage repair pathway, besides p53-induced apoptosis, are also affected by culturing the cells at physiological oxygen tensions. Also, it still needs to be elucidated the mechanism by which MAPK interferes with apoptosis at physiological oxygen tensions and the way p53 participates in this response.

We have corroborated that HIF-1α is expressed and active at physiological oxygen tension and that MAPK is important for its expression and activity under these conditions. Although we found that HIF-1α does not have a role on the resistance to apoptosis at physiological oxygen tension, the presence of the protein and its activity at this higher oxygen tensions may have other implications for normal physiology. As far as we are aware, the physiological role of HIF-1α has not been extensively explored and it would be interesting to know its role in cellular homeostasis.

On the other hand, we have shown that Stra6 is activated in response to p53 and that this activation may have an important role in the induction of p53-mediated apoptosis. The link between p53 pathway and the retinoic acid pathway has been suggested in the past, and could be an interesting area of research with the potential of designing adjuvant therapies for cancer. Also, there is a great amount of research still to come on Stra6 as it is a relatively newly characterized protein, and with the recent description of its role as a signalling molecule there is a lot of questions to be answered about its biological roles. It is yet to be determined if the apoptotic functions of Stra6 that we describe in this thesis are linked with its role in signalling and insulin resistance described by others. Although we have shown an increase in the ROS levels and DNA damage caused by oxidation after overexpression of Stra6, the exact mechanism by which Stra6 is involved in p53-mediated apoptosis is still to be elucidated.

Carrera S, de Verdier PJ, Khan Z, Zhao B, Mahale A, Bowman KJ, Zainol M, Jones GD, Lee SW, Aaronson SA, Macip S. Protection of cells in physiological oxygen tensions against DNA damage-induced apoptosis. J Biol Chem. 2010 Apr 30;285(18):13658-65

http://dx.doi.org/10.1074/jbc.M109.062562

References

Alarcón, R. et al., 1999. Hypoxia induces p53 accumulation through MDM2 down-regulation and inhibition of E6-mediated degradation. *Cancer Research*, 59(24), pp.6046-51.

Allan, L.A. et al., 2003. Inhibition of caspase-9 through phosphorylation at Thr 125 by ERK MAPK. *Nature Cell Biology*, 5(7), pp.647-54.

Altucci, L. et al., 2007. RAR and RXR modulation in cancer and metabolic disease. *Nature Reviews Drug Discovery*, 6(10), pp.793-810.

Ameri, K., Burke, B., Lewis, C.E. & Harris, A.L., 2002. Regulation of a rat VL30 element in human breast cancer cells in hypoxia and anoxia: role of HIF-1. *British Journal of Cancer*, 87(10), pp.1173-81.

An, W.G. et al., 1998. Stabilization of wild-type p53 by hypoxia-inducible factor 1alpha. *Nature*, 392(6674), pp.405-8.

Balmer, J.E. & Blomhoff, R., 2005. A robust characterization of retinoic acid response elements based on a comparison of sites in three species. *The Journal of steroid biochemistry and molecular biology*, 96(5), pp.347-54.

Bardos, J.I. & Ashcroft, M., 2004. Hypoxia-inducible factor-1 and oncogenic signalling. *BioEssays*, 26(3), pp.262-69.

Bartholin, L. et al., 2006. TGIF Inhibits Retinoid Signaling. *Molecular and cellular biology*, 26(3), pp.990-1001.

Berry, D.C., Jin, H., Majumdar, A. & Noy, N., 2011. Signaling by vitamin A and retinol-binding protein regulates gene expression to inhibit insulin responses. *Proceedings of the National Academy of Sciences of the United States of America*, 108(11), pp.4340-5.

Blagosklonny, M.V. et al., 1998. p53 inhibits hypoxia-inducible factor-stimulated transcription. *The Journal of biological chemistry*, 273(20), pp.11995-8.

Blaner, W.S., 2007. STRA6, a cell-surface receptor for retinol-binding protein: the plot thickens. *Cell metabolism*, 5(3), pp.164-6.

Bonni, A. et al., 1999. Cell Survival Promoted by the Ras-MAPK Signaling Pathway by Transcription-Dependent and -Independent Mechanisms. *Science*, 286(5443), pp.1358-62.

Bouillet, P. et al., 1997. Developmental expression pattern of Stra6, a retinoic acid-responsive gene encoding a new type of membrane protein. *Mechanisms of development*, 63(2), pp.173-86.

Braun, R.D., Lanzen, J.L., Snyder, S.A. & Dewhirst, M.W., 2001. Comparison of tumor and normal tissue oxygen tension measurements using OxyLite or microelectrodes in rodents. *American journal of physiology Heart and circulatory physiology*, 280(6), pp.H2533-44.

Campisi, J., 2003. Cancer and ageing: rival demons? *Nature Reviews Cancer*, 3(5), pp.339-49.

Carmeliet, P. et al., 1998. Role of HIF-1alpha in hypoxia-mediated apoptosis, cell proliferation and tumour angiogenesis. *Nature*, 394(6692), pp.485-90.

Carrera, S. et al., 2010. Protection of Cells in Physiological Oxygen Tensions against DNA Damage-induced Apoptosis. *Journal of Biological Chemistry*, 285(18), pp.13658-65.

Chambon, P., 1996. A decade of molecular biology of retinoic acid receptors. *FASEB journal : official publication of the Federation of American Societies for Experimental Biology*, 10(9), pp.940-54.

Chen, Q. et al., 1995. Oxidative DNA damage and senescence of human diploid fibroblast cells. *Proceedings of the National Academy of Sciences of the United States of America*, 92(10), pp.4337-41.

Chen, C.-H. et al., 2012. Increased Unbound Retinol-binding Protein 4 Concentration Induces Apoptosis through Receptor-mediated Signaling. *Journal of Biological Chemistry*, 287(13), pp.9694-707.

Chen, C. et al., 2001. Regulation of glut1 mRNA by Hypoxia-inducible Factor-1. INTERACTION BETWEEN H-ras AND HYPOXIA. *Journal of Biological Chemistry*, 276(12), pp.9519-25.

Cho, Y., Gorina, S., Jeffrey, P.D. & Pavletich, N.P., 1994. Crystal structure of a p53 tumor suppressor-DNA complex: understanding tumorigenic mutations. *Science*, 265(5170), pp.346-55.

Conrad, P.W. et al., 1999. Selective activation of p38alpha and p38gamma by hypoxia. Role in regulation of cyclin D1 by hypoxia in PC12 cells. *The Journal of biological chemistry*, 274(33), pp.23570-6.

Dayan, F. et al., 2006. The oxygen sensor factor-inhibiting hypoxia-inducible factor-1 controls expression of distinct genes through the bifunctional transcriptional character of hypoxia-inducible factor-1alpha. *Cancer research*, 66(7), pp.3688-98.

Dhillon, A.S., Hagan, S., Rath, O. & Kolch, W., 2007. MAP kinase signalling pathways in cancer. *Oncogene*, 26(22), pp.3279-90.

Duester, G., 2008. Retinoic acid synthesis and signaling during early organogenesis. *Cell*, 134(6), pp.921-31.

Ehrismann, D. et al., 2007. Studies on the activity of the hypoxia-inducible-factor hydroxylases using an oxygen consumption assay. *The Biochemical journal*, 401(1), pp.227-34.

Epstein, A.C. et al., 2001. C. elegans EGL-9 and mammalian homologs define a family of dioxygenases that regulate HIF by prolyl hydroxylation. *Cell*, 107(1), pp.43-54.

Erhardt, P., Schremser, E.J. & Cooper, G.M., 1999. B-Raf inhibits programmed cell death downstream of cytochrome c release from mitochondria by activating the MEK/Erk pathway. *Molecular and Cellular Biology*, 19(8), pp.5308-15.

Estrada, J.C. et al., 2012. Culture of human mesenchymal stem cells at low oxygen tension improves growth and genetic stability by activating glycolysis. *Cell death and differentiation*, 19(5), pp.743-55.

Favata, M.F. et al., 1998. Identification of a novel inhibitor of mitogen-activated protein kinase kinase. *The Journal of biological chemistry*, 273(29), pp.18623-32.

Feng, Z., Zhang, H., Levine, A.J. & Jin, S., 2005. The coordinate regulation of the p53 and mTOR pathways in cells. *Proceedings of the National Academy of Sciences of the United States of America*, 102(23), pp.8204-9.

Fong, G.-H., 2009. Regulation of angiogenesis by oxygen sensing mechanisms. *Journal of Molecular Medicine*, 87(6), pp.549-60.

Fornari, F.A. et al., 1994. Interference by doxorubicin with DNA unwinding in MCF-7 breast tumor cells. *Molecular pharmacology*, 45(4), pp.649-56.

Fukuda, R. et al., 2002. Insulin-like Growth Factor 1 Induces Hypoxia-inducible Factor 1-mediated Vascular Endothelial Growth Factor Expression, Which is Dependent on MAP Kinase and Phosphatidylinositol 3-Kinase Signaling in Colon Cancer Cells. *Journal of Biological Chemistry*, 277(41), pp.38205-11.

Generali, D. et al., 2006. Hypoxia-inducible factor-1alpha expression predicts a poor response to primary chemoendocrine therapy and disease-free survival in primary

human breast cancer. *Clinical cancer research : an official journal of the American Association for Cancer Research*, 12(15), pp.4562-8.

Gewirtz, D.A., Holt, S.E. & Grant, S., 2007. *Apoptosis, Senescence and Cancer*. 2nd ed. New Jersey: Humana Press.

Giguere, V., Ong, E.S., Segui, P. & Evans, R.M., 1987. Identification of a receptor for the morphogen retinoic acid. *Nature*, 330(6149), pp.624-9.

Golzio, C. et al., 2007. Matthew-Wood syndrome is caused by truncating mutations in the retinol-binding protein receptor gene STRA6. *American journal of human genetics*, 80(6), pp.1179-87.

Graeber, T.G. et al., 1994. Hypoxia induces accumulation of p53 protein, but activation of a G1-phase checkpoint by low-oxygen conditions is independent of p53 status. *Molecular and Cellular Biology*, 14(9), pp.6264-77.

Greenblatt, M.S., Bennett, W.P., Hollstein, M. & Harris, C.C., 1994. Mutations in the p53 tumor suppressor gene: clues to cancer etiology and molecular pathogenesis. *Cancer research*, 54(18), pp.4855-78.

Green, D.R. & Kroemer, G., 2009. Cytoplasmic functions of the tumour suppressor p53. *Nature*, 458(7242), pp.1127-30.

Héron-Milhavet, L. et al., 2001. Insulin-like growth factor-I (IGF-I) receptor activation rescues UV-damaged cells through a p38 signaling pathway. Potential role of the IGF-I receptor in DNA repair. *The Journal of biological chemistry*, 276(21), pp.18185-92.

Hammond, E.M. et al., 2006. Genome-wide analysis of p53 under hypoxic conditions. *Molecular and cellular biology*, 26(9), pp.3492-504.

Haupt, Y., Maya, R., Kazaz, A. & Oren, M., 1997. Mdm2 promotes the rapid degradation of p53. *Nature*, 387(6630), pp.296-9.

Haupt, Y. et al., 1995. Induction of apoptosis in HeLa cells by trans-activation-deficient p53. *Genes & development*, 9(17), pp.2170-83.

Heery, D.M., Kalkhoven, E., Hoare, S. & Parker, M.G., 1997. A signature motif in transcriptional co-activators mediates binding to nuclear receptors. *Nature*, 387(6634), pp.733-6.

Hiraga, T. et al., 2007. Hypoxia and hypoxia-inducible factor-1 expression enhance osteolytic bone metastases of breast cancer. *Cancer research*, 67(9), pp.4157-63.

Hirsilä, M. et al., 2003. Characterization of the human prolyl 4-hydroxylases that modify the hypoxia-inducible factor. *The Journal of biological chemistry*, 278(33), pp.30772-80.

Hockel, M. et al., 1996. Association between tumor hypoxia and malignant progression in advanced cancer of the uterine cervix. *Cancer research*, 56(19), pp.4509-15.

Honda, R. & Yasuda, H., 2000. Activity of MDM2, a ubiquitin ligase, toward p53 or itself is dependent on the RING finger domain of the ligase. *Oncogene*, 19(11), pp.1473-6.

Huang, M.E. et al., 1988. Use of all-trans retinoic acid in the treatment of acute promyelocytic leukemia. *Blood*, 72(2), pp.567-72.

Isken, A. et al., 2008. RBP4 disrupts vitamin A uptake homeostasis in a STRA6-deficient animal model for Matthew-Wood syndrome. *Cell metabolism*, 7(3), pp.258-68.

Jiang, B.H. et al., 2001. Phosphatidylinositol 3-kinase signaling controls levels of hypoxia-inducible factor 1. *Cell growth & differentiation : the molecular biology journal of the American Association for Cancer Research*, 12(7), pp.363-9.

Jiang, B.H. et al., 1996a. Dimerization, DNA binding and transactivation properties of Hipoxia-inducible factor 1. *The Journal of Biological Chemistry*, 271(July 26), pp.17771-78.

Jiang, B.H., Semenza, G.L., Bauer, C. & Marti, H.H., 1996. Hypoxia-inducible factor 1 levels vary exponentially over a physiologically relevant range of O2 tension. *The American journal of physiology*, 271(4 Pt 1), pp.C1172-80.

Kakudo, Y. et al., 2005. Lack of correlation between p53-dependent transcriptional activity and the ability to induce apoptosis among 179 mutant p53s. *Cancer research*, 65(6), pp.2108-14.

Kawaguchi, R. et al., 2007. A Membrane Receptor for Retinol Binding Protein Mediates Cellular Uptake of Vitamin A. *Science*, 315(5813), pp.820-25.

Kawaguchi, R. et al., 2008. An essential ligand-binding domain in the membrane receptor for retinol-binding protein revealed by large-scale mutagenesis and a human polymorphism. *The Journal of biological chemistry*, 283(22), pp.15160-8.

Kawaguchi, R. et al., 2008. Mapping the membrane topology and extracellular ligand binding domains of the retinol binding protein receptor. *Biochemistry*, 47(19), pp.5387-95.

Khandrika, L. et al., 2009. Hypoxia-associated p38 mitogen-activated protein kinase-mediated androgen receptor activation and increased HIF-1α levels contribute to

emergence of an aggressive phenotype in prostate cancer. *Oncogene*, 28(9), pp.1248-60.

Kikuchi, H. et al., 2009. Oncogenic KRAS and BRAF Differentially Regulate Hypoxia-Inducible Factor-1 and -2 in Colon Cancer. *Cancer Research*, 69(21), pp.8499-506.

Kim, G.-Y. et al., 2002. The stress-activated protein kinases p38 alpha and JNK1 stabilize p21(Cip1) by phosphorylation. *The Journal of biological chemistry*, 277(33), pp.29792-802.

Koivunen, P. et al., 2003. Catalytic Properties of the Asparaginyl Hydroxylase (FIH) in the Oxygen Sensing Pathway Are Distinct from Those of Its Prolyl 4-Hydroxylases. *Journal of Biological Chemistry*, 279(11), pp.9899-904.

Koumenis, C. et al., 2001. Regulation of p53 by hypoxia: dissociation of transcriptional repression and apoptosis from p53-dependent transactivation. *Molecular and cellular biology*, 21(4), pp.1297-310.

Krishna, M. & Narang, H., 2008. The complexity of mitogen-activated protein kinases (MAPKs) made simple. *Cellular and Molecular Life Sciences*, 65(22), pp.3525-44.

Kubbutat, M.H., Jones, S.N. & Vousden, K.H., 1997. Regulation of p53 stability by Mdm2. *Nature*, 387(6630), pp.299-303.

Lando, D. et al., 2002. FIH-1 is an asparaginyl hydroxylase enzyme that regulates the transcriptional activity of hypoxia-inducible factor. *Genes & development*, 16(12), pp.1466-71.

Lee, S.W. et al., 2000. Sustained activation of Ras/Raf/mitogen-activated protein kinase cascade by the tumor suppressor p53. *Proceedings of the National Academy of Sciences of the United States of America*, 97(15), pp.8302-5.

Lee, K. et al., 2009. Anthracycline chemotherapy inhibits HIF-1 transcriptional activity and tumor-induced mobilization of circulating angiogenic cells. *Proceedings of the National Academy of Sciences of the United States of America*, 106(7), pp.2353-8.

Liao, D., Corle, C., Seagroves, T.N. & Johnson, R.S., 2007. Hypoxia-inducible factor-1alpha is a key regulator of metastasis in a transgenic model of cancer initiation and progression. *Cancer research*, 67(2), pp.563-72.

Liu, X., Yue, P., Khuri, F.R. & Sun, S.-Y., 2004. p53 upregulates death receptor 4 expression through an intronic p53 binding site. *Cancer research*, 64(15), pp.5078-83.

Müller, M. et al., 1998. p53 activates the CD95 (APO-1/Fas) gene in response to DNA damage by anticancer drugs. *The Journal of experimental medicine*, 188(11), pp.2033-45.

Manalo, D.J. et al., 2005. Transcriptional regulation of vascular endothelial cell responses to hypoxia by HIF-1. *Blood*, 105(2), pp.659-69.

Maxwell, P.H. et al., 1999. The tumour suppressor protein VHL targets hypoxia-inducible factors for oxygen-dependent proteolysis. *Nature*, 399(6733), pp.271-5.

Meek, D.W., 2009. Tumour suppression by p53: a role for the DNA damage response? *Nature Reviews Cancer*, 9(10), pp.714-23.

Mihara, M. et al., 2003. p53 has a direct apoptogenic role at the mitochondria. *Molecular Cell*, 11(3), pp.577-90.

Milne, D.M., Campbell, D.G., Caudwell, F.B. & Meek, D.W., 1994. Phosphorylation of the tumor suppressor protein p53 by mitogen-activated protein kinases. *The Journal of biological chemistry*, 269(12), pp.9253-60.

Minet, E. et al., 2000. ERK activation upon hypoxia: involvement in HIF-1 activation. *FEBS letters*, 468(1), pp.53-8.

Minet, E. et al., 2001. Transduction pathways involved in Hypoxia-Inducible Factor-1 phosphorylation and activation. *Free radical biology & medicine*, 31(7), pp.847-55.

Morton, S., Davis, R.J., McLaren, A. & Cohen, P., 2003. A reinvestigation of the multisite phosphorylation of the transcription factor c-Jun. *The EMBO journal*, 22(15), pp.3876-86.

Murphy, L.O. et al., 2002. Molecular interpretation of ERK signal duration by immediate early gene products. *Nature Publishing Group*, 4(8), pp.556-64.

Murray, T.V.A. et al., 2008. A non-apoptotic role for caspase-9 in muscle differentiation. *Journal of cell science*, 121(Pt 22), pp.3786-93.

Nam, S.Y. & Sabapathy, K., 2011. p53 promotes cellular survival in a context-dependent manner by directly inducing the expression of haeme-oxygenase-1. *Oncogene*, 30(44), pp.4476-86.

Nardinocchi, L., Puca, R. & D'Orazi, G., 2011. HIF-1α antagonizes p53-mediated apoptosis by triggering HIPK2 degradation. *Aging*, 3(1), pp.33-43.

Naylor, H.M. & Newcomer, M.E., 1999. The structure of human retinol-binding protein (RBP) with its carrier protein transthyretin reveals an interaction with the carboxy terminus of RBP. *Biochemistry*, 38(9), pp.2647-53.

Olivier, M., Hollstein, M. & Hainaut, P., 2010. TP53 mutations in human cancers: origins, consequences, and clinical use. *Cold Spring Harbor perspectives in biology*, 2(1), p.a001008.

Olsson, M. & Zhivotovsky, B., 2011. Caspases and cancer. *Cell Death and Differentiation*, 18(9), pp.1441-49.

Palmer, L.A., Semenza, G.L., Stoler, M.H. & Johns, R.A., 1998. Hypoxia induces type II NOS gene expression in pulmonary artery endothelial cells via HIF-1. *The American journal of physiology*, 274(2 Pt 1), pp.L212-9.

Parrinello, S. et al., 2003. Oxygen sensitivity severely limits the replicative lifespan of murine fibroblasts. *Nature Publishing Group*, 5(8), pp.741-7.

Pasutto, F. et al., 2007. Mutations in STRA6 cause a broad spectrum of malformations including anophthalmia, congenital heart defects, diaphragmatic hernia, alveolar capillary dysplasia, lung hypoplasia, and mental retardation. *American journal of human genetics*, 80(3), pp.550-60.

Perissi, V. et al., 1999. Molecular determinants of nuclear receptor-corepressor interaction. *Genes & Development*, 13(24), pp.3198-208.

Petkovich, M., Brand, N.J., Krust, A. & Chambon, P., 1987. A human retinoic acid receptor which belongs to the family of nuclear receptors. *Nature*, 330(6147), pp.444-50.

Potts, P.R. et al., 2003. Critical function of endogenous XIAP in regulating caspase activation during sympathetic neuronal apoptosis. *The Journal of cell biology*, 163(4), pp.789-99.

Prives, C. & Hall, P.A., 1999. The p53 pathway. *The Journal of Pathology*, 187(1), pp.112-26.

Quadro, L. et al., 1999. Impaired retinal function and vitamin A availability in mice lacking retinol-binding protein. *The EMBO journal*, 18(17), pp.4633-44.

Ravi, D. et al., 2011. 14-3-3 σ Expression Effects G2/M Response to Oxygen and Correlates with Ovarian Cancer Metastasis. *PLoS ONE*, 6(1), p.e15864.

Ravi, R. et al., 2000. Regulation of tumor angiogenesis by p53-induced degradation of hypoxia-inducible factor 1alpha. *Genes & development*, 14(1), pp.34-44.

Ren, H., Accili, D. & Duan, C., 2010. Hypoxia converts the myogenic action of insulin-like growth factors into mitogenic action by differentially regulating multiple signaling pathways. *Proceedings of the National Academy of Sciences*, 107(13), pp.5857-62.

Richard, D.E. et al., 1999. p42/p44 mitogen-activated protein kinases phosphorylate hypoxia-inducible factor 1alpha (HIF-1alpha) and enhance the transcriptional activity of HIF-1. *The Journal of biological chemistry*, 274(46), pp.32631-7.

Riley, T., Sontag, E., Chen, P. & Levine, A., 2008. Transcriptional control of human p53-regulated genes. *Nature Reviews Molecular Cell Biology*, 9(5), pp.402-12.

Sandelin, A., Wasserman, W.W. & Lenhard, B., 2004. ConSite: web-based prediction of regulatory elements using cross-species comparison. *Nucleic acids research*, 32(Web Server issue), pp.W249-52.

Sang, N. et al., 2003. MAPK Signaling Up-regulates the Activity of Hypoxia-inducible Factors by Its Effects on p300. *Journal of Biological Chemistry*, 278(16), pp.14013-19.

Schofield, C.J. & Ratcliffe, P.J., 2004. Oxygen sensing by HIF hydroxylases. *Nature reviews Molecular cell biology*, 5(5), pp.343-54.

Seeliger, M.W. et al., 1999. Phenotype in retinol deficiency due to a hereditary defect in retinol binding protein synthesis. *Investigative ophthalmology & visual science*, 40(1), pp.3-11.

Semenza, G.L., 1999. Regulation of mammalian O2 homeostasis by hypoxia-inducible factor 1. *Annual review of cell and developmental biology*, 15, pp.551-78.

Stommel, J.M. & Wahl, G.M., 2004. Accelerated MDM2 auto-degradation induced by DNA-damage kinases is required for p53 activation. *The EMBO journal*, 23(7), pp.1547-56.

Sueoka, N. et al., 1999. Posttranslational mechanisms contribute to the suppression of specific cyclin:CDK complexes by all-trans retinoic acid in human bronchial epithelial cells. *Cancer research*, 59(15), pp.3838-44.

Sugrue, M.M., Shin, D.Y., Lee, S.W. & Aaronson, S.A., 1997. Wild-type p53 triggers a rapid senescence program in human tumor cells lacking functional p53. *Proceedings of the National Academy of Sciences of the United States of America*, 94(18), pp.9648-53.

Sun, H., Charles, C.H., Lau, L.F. & Tonks, N.K., 1993. MKP-1 (3CH134), an immediate early gene product, is a dual specificity phosphatase that dephosphorylates MAP kinase in vivo. *Cell*, 75(3), pp.487-93.

Sutton, K.M. et al., 2007. Selective inhibition of MEK1/2 reveals a differential requirement for ERK1/2 signalling in the regulation of HIF-1 in response to hypoxia and IGF-1. *Oncogene*, 26(27), pp.3920-29.

Szeto, W. et al., 2001. Overexpression of the retinoic acid-responsive gene Stra6 in human cancers and its synergistic induction by Wnt-1 and retinoic acid. *Cancer research*, 61(10), pp.4197-205.

Tait, S.W.G. & Green, D.R., 2010. Mitochondria and cell death: outer membrane permeabilization and beyond. *Nature Reviews Molecular Cell Biology*, 11(9), pp.621-32.

Tang, X.-H. & Gudas, L.J., 2011. Retinoids, Retinoic Acid Receptors, and Cancer. *Annual Review of Pathology: Mechanisms of Disease*, 6(1), pp.345-64.

Tasdemir, E. et al., 2008. Regulation of autophagy by cytoplasmic p53. *Nature cell biology*, 10(6), pp.676-87.

Vousden, K.H., 2000. p53: death star. *Cell*, 103(5), pp.691-4.

Vousden, K.H. & Prives, C., 2009. Blinded by the Light: The Growing Complexity of p53. *Cell*, 137(3), pp.413-31.

Walsh, S. et al., 2009. Hypoxia increases normal prostate epithelial cell resistance to receptor-mediated apoptosis viaAKT activation. *International Journal of Cancer*, 124(8), pp.1871-78.

Wang, G.L., Jiang, B.H., Rue, E.A. & Semenza, G.L., 1995. Hypoxia-inducible factor 1 is a basic-helix-loop-helix-PAS heterodimer regulated by cellular O2 tension. *Proceedings of the National Academy of Sciences of the United States of America*, 92(12), pp.5510-4.

Wei, M.C., 2001. Proapoptotic BAX and BAK: A Requisite Gateway to Mitochondrial Dysfunction and Death. *Science*, 292(5517), pp.727-30.

Xiu, M. et al., 2003. The transcriptional repressor HBP1 is a target of the p38 mitogen-activated protein kinase pathway in cell cycle regulation. *Molecular and cellular biology*, 23(23), pp.8890-901.

Yamamoto, T. et al., 2006. Continuous ERK activation downregulates antiproliferative genes throughout G1 phase to allow cell-cycle progression. *Current biology : CB*, 16(12), pp.1171-82.

Yang, Q. et al., 2005. Serum retinol binding protein 4 contributes to insulin resistance in obesity and type 2 diabetes. *Nature*, 436(7049), pp.356-62.

Yeo, E.-J. et al., 2003. YC-1: a potential anticancer drug targeting hypoxia-inducible factor 1. *Journal of the National Cancer Institute*, 95(7), pp.516-25.

Zhang, L. & Hill, R.P., 2004. Hypoxia enhances metastatic efficiency by up-regulating Mdm2 in KHT cells and increasing resistance to apoptosis. *Cancer research*, 64(12), pp.4180-9.

Zhong, H. et al., 2000. Modulation of hypoxia-inducible factor 1alpha expression by the epidermal growth factor/phosphatidylinositol 3-kinase/PTEN/AKT/FRAP pathway in human prostate cancer cells: implications for tumor angiogenesis and therapeutics. *Cancer Research*, 60(6), pp.1541-5.

Zhong, H. et al., 1999. Overexpression of hypoxia-inducible factor 1alpha in common human cancers and their metastases. *Cancer research*, 59(22), pp.5830-5.

Zundel, W. et al., 2000. Loss of PTEN facilitates HIF-1-mediated gene expression. *Genes & development*, 14(4), pp.391-6.